

DESIGN AND DEVELOPMENT OF A CYLINDER EXPANSION TEST SETUP
FOR DETERMINATION OF EQUATION OF STATE PARAMETERS OF
VARIOUS EXPLOSIVES

A THESIS SUBMITTED TO
THE GRADUATE SCHOOL OF NATURAL AND APPLIED SCIENCES
OF
MIDDLE EAST TECHNICAL UNIVERSITY

BY

EMİR TOPKARAOĞLU

IN PARTIAL FULFILLMENT OF THE REQUIREMENTS
FOR
THE DEGREE OF MASTER OF SCIENCE
IN
MECHANICAL ENGINEERING

DECEMBER 2014

Approval of the Thesis:

**DESIGN AND DEVELOPMENT OF A CYLINDER EXPANSION TEST
SETUP FOR DETERMINATION OF EQUATION OF STATE
PARAMETERS OF VARIOUS EXPLOSIVES**

submitted by **EMİR TOPKARAOĞLU** in partial fulfillment of the requirements
for the degree of **Master of Science in Mechanical Engineering Department,
Middle East Technical University** by,

Prof. Dr. Gülbin Dural Ünver
Dean, Graduate School of **Natural and Applied Sciences**

Prof. Dr. Tuna Balkan
Head of Department, **Mechanical Engineering**

Prof. Dr. Abdullah Ulaş
Supervisor, **Mechanical Engineering Department, METU**

Examining Committee Members:

Prof. Dr. Hüseyin Vural
Mechanical Engineering Dept., METU

Prof. Dr. Abdullah Ulaş
Mechanical Engineering Dept., METU

Assoc. Prof. Dr. Mehmet Metin Yavuz
Mechanical Engineering Dept., METU

Asst. Prof. Dr. Feyza Kazanç
Mechanical Engineering Dept., METU

Dr. Mehmet Ali Ak
Roketsan Missiles Industries, Ankara

Date: 01.12.2014

I hereby declare that all information in this document has been obtained and presented in accordance with academic rules and ethical conduct. I also declare that, as required by these rules and conduct, I have fully cited and referenced all material and results that are not original to this work.

Name, Last name : Emir TOPKARAOĞLU

Signature :

ABSTRACT

DESIGN AND DEVELOPMENT OF A CYLINDER EXPANSION TEST SETUP FOR DETERMINATION OF EQUATION OF STATE PARAMETERS OF VARIOUS EXPLOSIVES

Topkaraođlu, Emir

M.S., Department of Mechanical Engineering

Supervisor: Prof. Dr. Abdullah Ulař

December 2014, 155 pages

Explosives are energetic materials which are used for various military or civilian purposes. Several computer programs are used for predicting the behaviour of systems containing explosives. During modeling of various explosives in simulation software, Jones-Wilkins-Lee equation of state is widely used. However, the parameters used in JWL equation of state are not available for some of the explosives in open sources. A method called cylinder expansion test is used in order to determine these parameters. In this thesis study, a cylinder expansion test setup was designed and developed. Cylinder expansion tests were performed for four different types of explosives employing the designed setup and JWL equation of state parameters were obtained for these explosive compositions using the data gathered from the tests. Two tests were performed for each explosive. Two of the explosives selected were conventional explosive compositions with equation of state parameters available in the literature. Pressure versus specific volume ratio curves for these explosives were obtained using the JWL equations determined via the tests. The curves obtained via the tests results were compared with the curves based on the literature data and it was concluded that the results were close enough.

The other two explosives used in the tests were newly developed compositions with no JWL equation data available in the literature. JWL equation of state parameters for these explosives were also obtained successfully.

Keywords: Cylinder Expansion Test, Explosive Materials, JWL Equation of State, Velocity of Detonation.

ÖZ

ÇEŞİTLİ PATLAYICILARIN HAL DENKLEM PARAMETRELERİNİN BULUNMASI İÇİN KULLANILACAK BİR SİLİNDİR GENLEŞME TEST DÜZENEGİNİN TASARIMI VE GELİŞTİRİLMESİ

Topkaraoğlu, Emir

Yüksek Lisans, Makina Mühendisliği Bölümü

Tez Yöneticisi: Prof. Dr. Abdullah Ulaş

Aralık 2014, 155 sayfa

Patlayıcılar, çeşitli askeri ya da sivil amaçlı çalışmalarda kullanılan enerjik malzemelerdir. Patlayıcı içeren sistemlerin davranışını öngörmek amacıyla bazı bilgisayar programları kullanılmaktadır. Çeşitli patlayıcıların, benzetim yazılımlarında modellenmesi aşamasında Jones-Wilkins-Lee hal denklemi sıklıkla kullanılmaktadır. Ancak JWL hal denkleminde kullanılan parametreler bazı patlayıcı çeşitleri için açık kaynaklarda mevcut değildir. Bu parametrelerin bulunması için silindir genleşme testi adlı yöntem kullanılmaktadır. Bu tez çalışmasında, bir silindir genleşme test düzeneği tasarlanmış ve geliştirilmiştir. Tasarlanan düzeneğe kullanılarak dört farklı patlayıcı için silindir genleşme testleri gerçekleştirilmiş ve testlerden elde edilen veriler kullanılarak bu patlayıcı kompozisyonları için JWL hal denklem parametreleri elde edilmiştir. Her patlayıcı için ikişer test gerçekleştirilmiştir. Testlerde kullanılan patlayıcılardan ikisi, literatürde hal denklem parametreleri bulunan konvansiyonel patlayıcı kompozisyonlarından seçilmiştir. Bu patlayıcılar için, elde edilen JWL hal denklemi parametreleri kullanılarak basınç - özgül hacim oranı eğrileri elde edilmiştir. Testler vasıtasıyla elde edilen eğriler, literatür verisine dayanan eğriler

ile karşılaştırılmış ve sonuçların yeterince yakın olduğu değerlendirilmiştir. Testlerde kullanılan diğer iki patlayıcı, literatürde JWL denklemi verisi bulunmayan yeni geliştirilmiş bir patlayıcıdır. Bu patlayıcı kompozisyonları için de JWL hal denklemi parametreleri başarılı bir şekilde elde edilmiştir.

Anahtar Kelimeler: Silindir Genleşme Testi, Patlayıcı Malzemeler, JWL Hal Denklemi, Detonasyon Hızı.

To My Family

ACKNOWLEDGEMENTS

First, I would like to express my appreciation to my thesis supervisor, Prof. Dr. Abdullah Ulaş for his guidance, support and help for this thesis study.

I acknowledge ROKETSAN MISSILES INDUSTRIES INC. for supporting this study. I would like to thank to my superiors and colleagues, especially Mr. Tuğberk İncekürk, from Roketsan, for their patience, encouragement and technical support. I would also express my thanks to Rocket Test Department personnel for their work and support during the tests. MKEK (Mechanical and Chemical Industry Corporation) is also acknowledged for providing the testing area.

Finally, I would like to express my eternal gratitude to my family, whom this dissertation is dedicated to. This study would never have been accomplished without their help and sympathy.

TABLE OF CONTENTS

ABSTRACT	v
ÖZ	vii
ACKNOWLEDGEMENTS	x
TABLE OF CONTENTS	xi
LIST OF TABLES	xiii
LIST OF FIGURES	xv
NOMENCLATURE.....	xviii
ABBREVIATIONS	xx
CHAPTERS	
1. INTRODUCTION	1
1.1 Motivation and Scope of the Study	2
1.2 Outline of the Thesis	4
2. LITERATURE SURVEY	7
2.1 JWL Equation of State	8
2.2 Cylinder Expansion Tests	10
2.3 Measurement Techniques Used in the Tests.....	22
3. THE CYLINDER EXPANSION TEST SETUP.....	31
3.1 Design of the Test Setup in General	31
3.2 Components of the Test Setup	37
3.3 Utilization of the Setup in Cylinder Expansion Tests	45
4. THEORY	53
5.RESULT OF THE CYLINDER EXPANSION TESTS	69
5.1 Test Results and JWL Equation of State Parameters.....	69
5.2 Effects of Uncertainties on the Calculated JWL Parameters	96
6. SIMULATION OF THE CYLINDER EXPANSION TEST	105
7. CONCLUSION	123

7.1	Summary and Discussions.....	123
7.2	Suggestions for Future Work.....	126
	REFERENCES	127
APPENDICES		
A.	SAMPLE RESULTS OF CMM MEASUREMENTS	133
B.	PARAMETERS CALCULATED VIA SIMPLE FIXED POINT ITERATION TECHNIQUE.....	141
C.	PARAMETERS USED IN MODELLING OFHC COPPER AND BOOSTER	145
D.	CALCULATION OF JWL EOS PARAMETERS FOR P-1	147

LIST OF TABLES

TABLES

Table 3-1 Design Parameters for the Copper Cylinder	34
Table 3-2 Radial Positions of the Contact Pins.....	35
Table 5-1 Test Item Configurations in the Cylinder Expansion Tests.....	70
Table 5-2 Signal Times at Longitudinally Placed Optical Probes	71
Table 5-3 Velocity of Detonation Values for Explosives	76
Table 5-4 Pin Arrival Times	81
Table 5-5 Pin Data for Test-1.....	82
Table 5-6 Properties Including JWL Equation of State Parameters for P-1	85
Table 5-7 Comparison of Pressures at Selected Specific Volume Ratios for P-1 ...	86
Table 5-8 Properties Including JWL Equation of State Parameters for P-2	87
Table 5-9 Properties Including JWL Equation of State Parameters for P-3	88
Table 5-10 Properties Including JWL Equation of State Parameters for P-4	89
Table 5-11 Comparison of Pressures at Selected Specific Volume Ratios for P-3 .	92
Table 5-12 Limits of the Quantities which Affect the JWL Parameters.....	98
Table 5-13 Limits of the Parameters Resulting Lowest and Highest Pressure Values	100
Table 6-1 Cell Sizes Used in the Analyses	111
Table 6-2 Detonation Front Arrival Times for P-1 Obtained from the Analyses ..	118
Table 6-3 Test and Analysis #6 Results for Detonation Front Arrival Times	118
Table 6-4 Detonation Velocity Values for P-1 Obtained via Tests and Analysis #6	118
Table 6-5 Contact Pin Signal Times for P-1 Obtained from the Analyses	119
Table 6-6 Test and Analysis #6 Results for Contact Pin Signal Times	120
Table A-1 CMM Results for the Pin Gage Measurements	133

Table B-1 JWL Parameter Sets for P-1 Obtained via Souers' Method and Simple-Fixed Point Iteration Method	142
Table B-2 Comparison of Pressures at Selected Specific Volume Ratios for P-1 (Based on Simple Fixed-Point Iteration).....	143
Table C-1 Parameters for the Equation of State Model of OFHC Copper [10]	145
Table C-2 Parameters for the Strength Model of OFHC Copper [10].....	145
Table C-3 Parameters for the Model of Booster Material [10].....	146
Table D-1 Final Values of the Quantities in the Code for the Sample Case	155

LIST OF FIGURES

FIGURES

Figure 2-1 Detonation Wave Propagation in Hydrodynamic Theory [1]	8
Figure 2-2 Cylinder Expansion Test Setup Proposed by Lee et al. [4].....	12
Figure 2-3 Hemispherical Test Setup Proposed by Lee et al. [4]	13
Figure 2-4 Schematic of the Test Setup Used by Los Alamos National Laboratory [16]	14
Figure 2-5 Cylinder Expansion Test Setup Used by Esen et al. [5].....	17
Figure 2-6 Cylinder Expansion Test Setup Used by Elek et al. [6]	18
Figure 2-7 Test Setup Used by Goto et al. [24]	20
Figure 2-8 Streak Camera Record from the Tests Performed by Elek et al. [6]	26
Figure 2-9 Streak Camera Record from the Tests Performed by Los Alamos National Laboratory [16].....	26
Figure 2-10 Use of Pins for Measurement of Detonation Wave Propagation [33]..	28
Figure 3-1 Solid Model of the Main Test Item Assembly	33
Figure 3-2 The Cross-Section Where the Pins are Located	37
Figure 3-3 Solid Model of the Pin Holder	39
Figure 3-4 Solid Model of the Cylindrical Holder.....	40
Figure 3-5 Solid Model of the Base Plate	40
Figure 3-6 Solid Model of the Table Assembly.....	42
Figure 3-7 Solid Model of the Test Setup Assembly	43
Figure 3-8 Contact Pins and the Pin Holder.....	46
Figure 3-9 Contact Pins, Pin Holder and Base Plate.....	47
Figure 3-10 Optical Probes and Fiber Optic Cables that are used for Measuring the Detonation Velocity of the Explosive.....	48
Figure 3-11 The Test Setup Assembly.....	49
Figure 3-12 Camera Used for Visual Recording.....	50

Figure 3-13 Sample Frames from Camera Recording	51
Figure 3-14 Test Area after the Test	52
Figure 4-1 Radii at a Cross-Section of the Cylinder Casing [5]	54
Figure 4-2 Angle of Wall Deflection [6], [28].....	57
Figure 4-3 Flow Chart for the Iterative Code	68
Figure 5-1 Position vs Time Charts for the Detonation Front for P-1	72
Figure 5-2 Position vs Time Charts for the Detonation Front for P-2.....	73
Figure 5-3 Position vs Time Charts for the Detonation Front for P-3	74
Figure 5-4 Position vs Time Charts for the Detonation Front for P-4.....	75
Figure 5-5 Contact Pin Signal Record for Test-1	78
Figure 5-6 Contact Pin Signal Record for Test-3	78
Figure 5-7 Contact Pin Signal Record for Test-4	79
Figure 5-8 Contact Pin Signal Record for Test-5	79
Figure 5-9 Contact Pin Signal Record for Test-6	80
Figure 5-10 Contact Pin Signal Record for Test-7	80
Figure 5-11 Contact Pin Signal Record for Test-8	81
Figure 5-12 Radial Position of Cylinder Wall with Respect to Time for Test-1	83
Figure 5-13 Comparison of P- ν Curves for P-1 Obtained from Test Results and Literature Data	85
Figure 5-14 Comparison of P- ν Curves for P-2 Obtained from Test-3 and Test-4	90
Figure 5-15 Comparison of P- ν Curves for P-3 Obtained from Test-5 and Test-6	90
Figure 5-16 Comparison of P- ν Curves for P-4 Obtained from Test-7 and Test-8	91
Figure 5-17 Comparison of P- ν Curves among the Seven Tests	93
Figure 5-18 Comparison of P- ν Curves (for $0.8 < \nu < 1$)	93
Figure 5-19 Comparison of P- ν Curves (for $2 < \nu < 3$)	94
Figure 5-20 Comparison of P- ν Curves (for $4 < \nu < 5$)	94
Figure 5-21 Comparison of P- ν Curves (for $6 < \nu < 7$)	95
Figure 5-22 Comparison of P- ν Curves (for $9 < \nu < 10$)	95
Figure 5-23 Lower and Upper Bounds of the P- ν Curves and the $\pm 2\%$ Error Bands for P-1	101
Figure 5-24 P- ν Curves for P-1 ($0.8 < \nu < 1.0$)	101

Figure 5-25 P- v Curves for P-1 ($2.2 < v < 2.4$)	102
Figure 5-26 P- v Curves for P-1 ($6.8 < v < 7.0$)	102
Figure 5-27 P- v Curves for P-1 ($9.8 < v < 10.0$)	103
Figure 6-1 Autodyn Model of the Test Item Including P-1	107
Figure 6-2 Gauges Used for Simulating the Contact Pins	109
Figure 6-3 Boundaries where the Boundary Condition is Applied.....	110
Figure 6-4 Models with Different Cell Sizes	111
Figure 6-5 Sample Frames during the Analysis	115
Figure 6-6 Propagation of Detonation Wave and Pressure Variation in the Analysis	116
Figure 6-7 Comparison of Test Results and Analysis #6 Results for Velocity of Detonation	119
Figure 6-8 Comparison of Test Results and Analysis #6 Results for Radial Position of Cylinder Wall with Respect to Time	120
Figure B-1 P- v Curves for P-1	142

NOMENCLATURE

A	JWL equation of state parameter
B	JWL equation of state parameter
C	JWL equation of state parameter
d	distance between the tip of the contact pin and cylinder outer surface
d_i	distance between the tip of the i^{th} contact pin and cylinder outer surface
E	energy
E_c	energy of compression
$E_c(cj)$	energy of compression at the Chapman-Jouguet point
E_d	detonation energy
E_G	Gurney energy
E_o	chemical energy
E_s	specific internal energy
$E_s(cj)$	specific internal energy at the Chapman-Jouguet point
G	shear modulus
m	mass
m_{exp}	mass of the explosive
m_{case}	mass of the casing
P	pressure
P_{cj}	pressure at the Chapman-Jouguet point
R_1	JWL equation of state parameter
R_2	JWL equation of state parameter
R	initial radius
R_i	initial inner radius of the tube
R_m	initial center radius of the tube
R_o	initial outer radius of the tube

R^2	coefficient of determination
r	radius at any instant
r_i	inner radius of the tube at any instant
r_m	center radius of the tube at any instant
r_o	outer radius of the tube at any instant
Δr_m	change in the center radius of the tube at any instant
ρ	density
ρ_0	density of the unreacted explosive
t	time
t_{pin}	signal arrival time from contact pin
t_{pin_l}	signal arrival time from initial contact pin
θ	wall deflection angle
V_{exp}	volume of the explosive
V_D	detonation velocity
V_G	Gurney velocity
V_r	radial wall velocity
V_w	wall velocity
v	specific volume ratio
v_{cj}	specific volume ratio at the Chapman-Jouguet point
v_o	initial specific volume
$v(t)$	specific volume as a function of time
ω	JWL equation of state parameter
Y	yield stress

ABBREVIATIONS

ANFO	Ammonium Nitrate Fuel Oil
C-J	Chapman-Jouguet State
CMM	Coordinate Measurement Machine
EBW	Exploding Bridge-Wire
EOS	Equation of State
JWL	Jones-Wilkins-Lee
P-1	Explosive-1 (First Explosive Used in the Tests)
P-2	Explosive-2 (Second Explosive Used in the Tests)
P-3	Explosive-3 (Third Explosive Used in the Tests)
P-4	Explosive-4 (Fourth Explosive Used in the Tests)
PDV	Planar Doppler Velocimetry
TNT	Trinitrotoluene
VISAR	Velocity Interferometer for any Reflector

CHAPTER 1

INTRODUCTION

Explosives are energetic materials which release their chemical energy in a very small time interval. These materials are used both for military and commercial purposes throughout the world. Explosives are utilized in different types of munitions as well as for various civilian purposes such as mining, material cladding and even for food processing.

For determining the performance behaviour of explosives used in engineering applications, test methods, software packages or empirical formulations are used. Since empirical formulations are not very accurate and test methods are expensive and time consuming, commercial software packages such as Ansys Autodyn, LS-Dyna, etc. are occasionally preferred for modeling explosive materials and systems that contain them. For modeling an explosive in these software packages, an equation of state is required in order to define the relationship among the state parameters for the explosive. Jones-Wilkins-Lee formulation is generally used as the equation of state in most of the computer programs, since it is a simple expression and it can describe the behaviour of a variety of explosives accurately.

Formulation for JWL equation of state, which defines the relationship between pressure and specific volume ratio of gaseous products of a detonation reaction for an explosive, is presented in Equation (1.1).

$$P = A \exp -R_1 v + B \exp -R_2 v + C v^{-(\omega+1)} \quad (1.1)$$

In Equation (1.1), A , B , C , R_1 , R_2 and ω are the parameters of the JWL equation of state. These parameters are specific to each explosive composition and they have to be known in advance in order to construct the JWL equation of state for any kind of explosive.

1.1 Motivation and Scope of the Study

In order to use the JWL equation of state formulation for an explosive composition, the parameters that are used in the equation should be known. The parameters used in the equation of state are available in the literature for conventional explosives which have been used for a long time. Due to increasing and varying performance and safety requirements, however, new explosive compositions are still being synthesized in the world. These newly developed explosives, which are then used in various systems and applications, are required to be modeled in computer software packages in order to simulate the behavior of the said explosive materials. For explosive compositions with unknown equation of state parameters, these parameters are required to be determined in advance. The cylinder expansion test method is the technique used by various institutions and researchers throughout the world in order to obtain the JWL equation of state parameters of explosives.

In addition to new explosive compositions, cylinder expansion tests can also be performed in order to determine the JWL equation of state parameters of widely used explosive types and to compare the obtained data with the literature. The reason of this is that the differences in the production processes followed and variations in the chemical composition during the manufacturing of an explosive material can affect the detonation characteristics of the explosive. Therefore, for a known explosive type, the JWL equation of state parameters and other detonation characteristics of the explosive manufactured in different facilities generally deviate from the literature data. Hence, institutions and researchers sometimes prefer to determine the JWL parameters of their explosive compositions by performing

cylinder expansion tests themselves rather than using the parameters available in the literature.

Cylinder expansion tests are also used to determine several properties of explosives other than the equation of state parameters. When a cylinder expansion test is performed, the detonation velocity and Gurney velocity, which are important characteristic properties of an explosive, can also be obtained.

The main aim of this study is to design and develop a cylinder expansion test setup which can be used to determine the JWL equation of state parameters of explosives. The cylinder expansion test setup is designed with the knowledge gained from literature survey. The designed setup is employed for performing tests using four different types of explosive compositions. Two tests have been performed with each explosive material. Parameters of JWL equation of state have been obtained for these four explosive materials with the data obtained from the cylinder expansion tests. The first explosive used in the tests was TNT, which is a commonly used explosive in various applications and systems and with equation of state parameters available in the literature. The results found via the tests for TNT are compared with the data obtained from the open sources. Another explosive with known JWL equation of state parameters is also used in the tests. The other two explosive materials tested were newly synthesized explosives with no JWL data in the literature. Detonation velocity and Gurney velocity values were also determined for the explosives that are used in the tests in the scope of this study.

The test item used in the tests was also modelled in Ansys Autodyn, which is a commercial software package that is used for simulating nonlinear dynamics problems including detonation of explosives. In this software, the obtained JWL equation of state parameters were used for modelling the explosives used in cylinder expansion test items. The data obtained during the cylinder tests were also gathered from the analyses by defining gauges at sensor locations. Results obtained via the tests and the analyses were compared.

1.2 Outline of the Thesis

The chapters of this dissertation are organized as follows:

In Chapter 2, literature survey on publications discussing JWL equation of state, cylinder expansion test setups developed by various institutions throughout the world, time of arrival measurement techniques employed by different researchers and design of test setups which are used for different purposes but structurally similar to that of a cylinder expansion test are presented.

In Chapter 3, design of the test setup and its components are explained. Models of setup components and pictures taken before and after performing the test are presented. Some important steps that should be followed during the execution of the tests are also briefly discussed in this section.

In Chapter 4, the theory behind the application of the cylinder expansion test in order to obtain the JWL parameters is presented. In this chapter, the equations that are used to calculate the velocity of detonation and JWL equation of state parameters using the raw data obtained from the cylinder expansion tests are given. Moreover, the iterative method that is followed to obtain the parameters is also discussed briefly in this chapter.

In Chapter 5, JWL equation of state parameters and other explosive characteristics obtained via the tests performed in the scope of this study are presented. Pressure versus specific volume ratio curves for the explosives used in tests are provided in this section. For the explosives with equation of state parameters available in the open sources, the pressure curves obtained from the tests are compared with the pressure curves based on literature data. The upper and lower bounds of the pressure curve for explosive P-1 are also presented in this section. Discussions on the test results are also given in this chapter.

In Chapter 6, the numerical simulations performed for the models of the cylinder expansion test setup with the use of commercial software, Ansys Autodyn, are presented and the results obtained from these analyses are discussed.

In the final chapter, a general summary and the conclusion of the study are presented. Suggestions for possible future work are also given in the last chapter.

Sample CMM measurement results for the test setup components, parameters calculated using another numerical iteration method, parameters used for modelling the copper casing and the booster charges in the numerical simulations and the detailed calculation steps of the equation of state parameters for explosive P-1 are presented in the Appendices.

CHAPTER 2

LITERATURE SURVEY

As discussed in Chapter 1, the main objective of this thesis study is to design a test setup which will be used to determine the JWL equation of state parameters of explosive materials so that the parameters can be used in software packages to model the explosives. Commercial software programs are one of the most commonly used tools for modeling systems and simulating applications where explosive materials are utilized. Various general purpose commercial packages as well as several more specific computer codes are used for analyzing the performance of systems containing explosives.

When modeling high explosives in most of the commercial software packages, the hydrodynamic detonation theory is employed. In hydrodynamic detonation theory; some assumptions are made. In this theory, the detonation reaction time is assumed to be zero. Shock wave translating inside the explosive is treated as a discontinuity and named as detonation wave. Detonation velocity of the explosive is assumed to be constant during whole detonation process and the detonation product gases are assumed to be in chemical and thermodynamic equilibrium. JWL equation can be used to model the behaviour of an explosive mathematically when hydrodynamic detonation theory is employed.

The schematic representation of detonation wave propagation and regarding zones in high explosive materials in hydrodynamic theory is given by Brown [1] and shown in Figure 2-1.

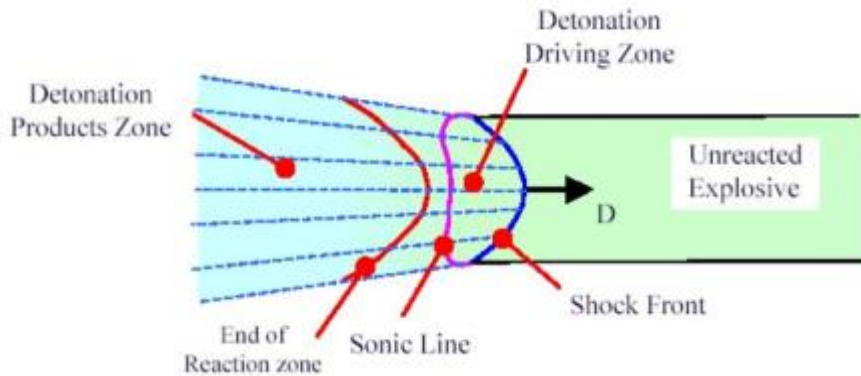


Figure 2-1 Detonation Wave Propagation in Hydrodynamic Theory [1]

2.1 JWL Equation of State

After the detonation of the explosive, reaction products occur in gas state. For predicting the behavior of explosives in the software packages in which hydrodynamic detonation theory assumptions are employed, an appropriate equation of state for the modeled explosive should be used. Generally, Jones-Wilkins-Lee (JWL) equation of state, which is a non-linear equation showing the relationship between pressure and specific volume of the gaseous detonation reaction products, is used for this purpose.

The formulation of the JWL equation of state was presented in Equation (1.1) [2], [3], [4]. In this expression, P and v are the pressure and the specific volume ratio of the gaseous detonation products, respectively. Here, the specific volume ratio, v , is the ratio of the specific volume of detonation products at an instant to the initial specific volume of these products. It has already been stated that A , B , C , R_1 , R_2 and ω are the parameters that have to be determined for any explosive composition in order to construct the equation of state for this explosive [4], [5]. Each parameter

in the equation mainly contributes to one of the stages of the expansion of the gaseous products. Parameters A and R_1 mainly contribute to modelling the behavior of the detonation products at high pressure and low expansion ratio values. Parameters B and R_2 in the equation of state define the behavior of gaseous products at the intermediate pressure zone. Parameters C and ω , on the other hand, mainly describe the pressure and specific volume relationship of the detonation products at low pressures and high expansion ratios [6].

The parameters in the JWL equation are interdependent quantities; hence, one of the parameters cannot be changed unilaterally without considering the effect of this change on the other parameters [7]. Since there are several parameters in the JWL equation of state, more than one sets of parameters, which describe the pressure and specific volume relationship of the detonation products, can be obtained for a single explosive material [6]. Therefore the JWL equation of state parameters for one type of explosive composition may differ in different sources in the literature. Hence, it is more rational to compare the behaviour described by the equation of state containing the calculated parameters, rather than the parameters themselves one by one when making a comparison between different sets for a single explosive.

Although JWL equation of state gives only an approximate representation for the pressure and specific volume relationship of an explosive composition, this formula is considered to be one of the best models describing the behaviour of explosives when compared to other mathematical models [8]. Elek et al. stated that, for modeling detonation products, JWL equation of state is more commonly used than other equation of state expressions such as Williamsburg equation of state, the polytropic expansion law, Lennard-Jones-Devonshire equation of state and Becker-Kistiakowsky-Wilson equation of state. JWL formulation is preferred over the other equation of state formulations by various authors for cases where a solid block of explosive with high velocity of detonation value is known to detonate [9], [10], [11], [12]. This equation of state is also preferred for modeling explosives in commonly used commercial software packages.

2.2 Cylinder Expansion Tests

Since new explosive materials are being synthesized, there is a necessity of determination of equation of state parameters for these new explosive compositions. Furthermore, the parameters differ for explosive compositions when they are manufactured in different facilities due to variations in the percentages of chemical components in the explosive compositions and alterations resulting from different manufacturing processes and process parameters. Moreover, the accuracy of the results obtained using the software packages has a dependency on the equation and its parameters used in modeling; therefore, more accurate parameters are always desired by scholars dealing with explosive science. Hence experimental and theoretical studies are performed in order to construct equation of state models for explosive materials.

There are various test methods which are used for determining the performance and detonation properties of explosives, such as the Truzl lead block test, ballistic mortar test, measurement of blast pressure, underwater explosion test, etc. [13], [14], [15]. Although most of these test methods can be used to determine several detonation properties of explosives and to make a comparison among the explosives in terms of performance, they cannot be directly used to determine the JWL equation of state parameters of an explosive [5], [16].

Cylinder expansion test, or the cylex test, is a test technique used for determining the performance and several detonation characteristics of explosives. During a cylinder expansion test, basically, explosive material is completely filled inside a long hollow cylindrical metallic casing. The explosive contained inside the metal casing is detonated at one end. As the detonation wave propagates and the casing expands due to the gaseous detonation products, the radial expansion of the metal is measured and recorded at a certain cross-section along the longitudinal axis of the cylinder during the test [16].

The metal tube used in a cylinder expansion test is a relatively thin walled cylinder. Generally copper is preferred as the tube material due to its high ductility, which enables the expansion of the cylinder to a large volume until its fracture after the detonation of the explosive inside the cylinder. For instance, during expansion, a copper tube radially expands twice of a steel tube before the rupture of the cylinder wall [17].

The radial expansion histogram of the cylinder is further used to calculate the Gurney velocity and the JWL equation of state parameters of the explosive used in the test. As well as the radial expansion of the tube, the detonation velocity which is along the centerline axis of the charge can also be measured while performing a cylinder expansion test. The detonation velocity of the explosive is a quantity that is required during the calculation steps of the parameters. Hence, the measured detonation velocity value, rather than a value obtained from literature or result of another test, can be used during determination of the parameters if the detonation velocity is directly measured during the test.

A significant advantage of the cylinder expansion test method is that this technique can be used to determine the pressure and expansion energy curves for explosives as functions of volume at early stages of the expansion of the detonation products, which is something that cannot be accomplished by other test methods [5].

Before the proposition of the JWL equation of state as a well-developed formulation, cylinder expansion tests had been performed in order to study the performance and metal accelerating capability of explosives. Gurney velocities had still been gathered by performing this test method. Lee et al., who constructed the formulation of JWL equation of state, proposed the cylinder expansion test method as a means for determination of the parameters used in this equation of state [4]. The cylinder expansion test has been used by various researchers to determine the JWL equation of state parameters as well as for other purposes since application of this test for this aim was suggested.

Lee et al. suggested a setup for performing cylinder expansion tests which may be used to construct the equation of state proposed by themselves. The setup proposed in their article which was published in 1960s is presented in Figure 2-2. The raw material of the cylinder was OFHC copper in this setup design. Besides the cylinder test setups, hemispherical test setups were also presented in that study (see Figure 2-3). However, the cylinder test method was preferred over the hemispherical test method and improved over the years by other researchers and scientists. Today, the cylinder expansion test setup is the preferred technique for determination of JWL equation of state parameters.

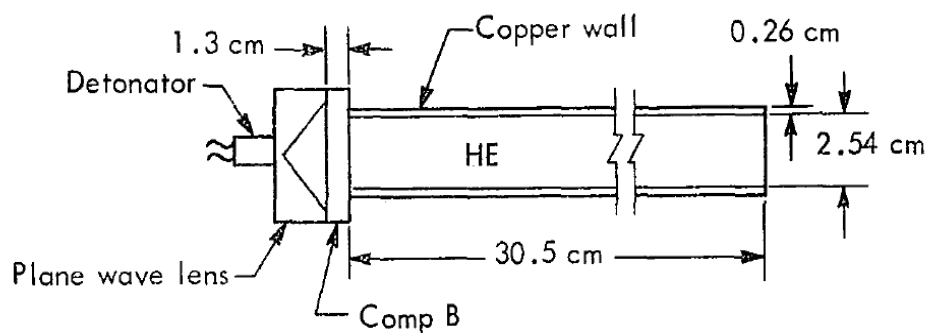


Figure 2-2 Cylinder Expansion Test Setup Proposed by Lee et al. [4]

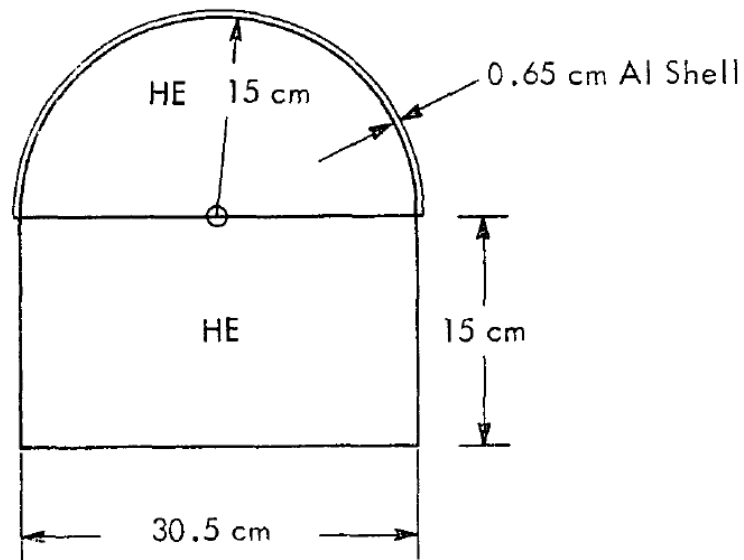


Figure 2-3 Hemispherical Test Setup Proposed by Lee et al. [4]

Los Alamos National Laboratory and Lawrence Livermore National Laboratory, two institutions of the USA, are known for pioneering the cylinder expansion tests in the world [18]. They have published several technical reports that set up the basic principles for the cylinder expansion tests that are performed by their scientists.

The schematic of the test setup used by the Los Alamos National Laboratory is demonstrated in Figure 2-4 [16]. It is stated that the cylinder expansion test is the preferred method to determine the Gurney energy and JWL equation of state parameters of an explosive composition in the report of the laboratory. The publication gives suggested tube dimensions, tolerance values and tube material for the tests that are going to be performed by the institution. Furthermore, guidelines for preparation and production of test setup components, performing the test and calculating the JWL parameters are discussed in the report. Approximately 300 mm

long oxygen free high conductivity copper tubes with 30.5 mm outer diameter and 25.4 mm inner diameter are used as the casing. For measuring the radial expansion histogram of the copper tube, a set of wired pins or a streak camera were used in most of the tests performed by this laboratory.

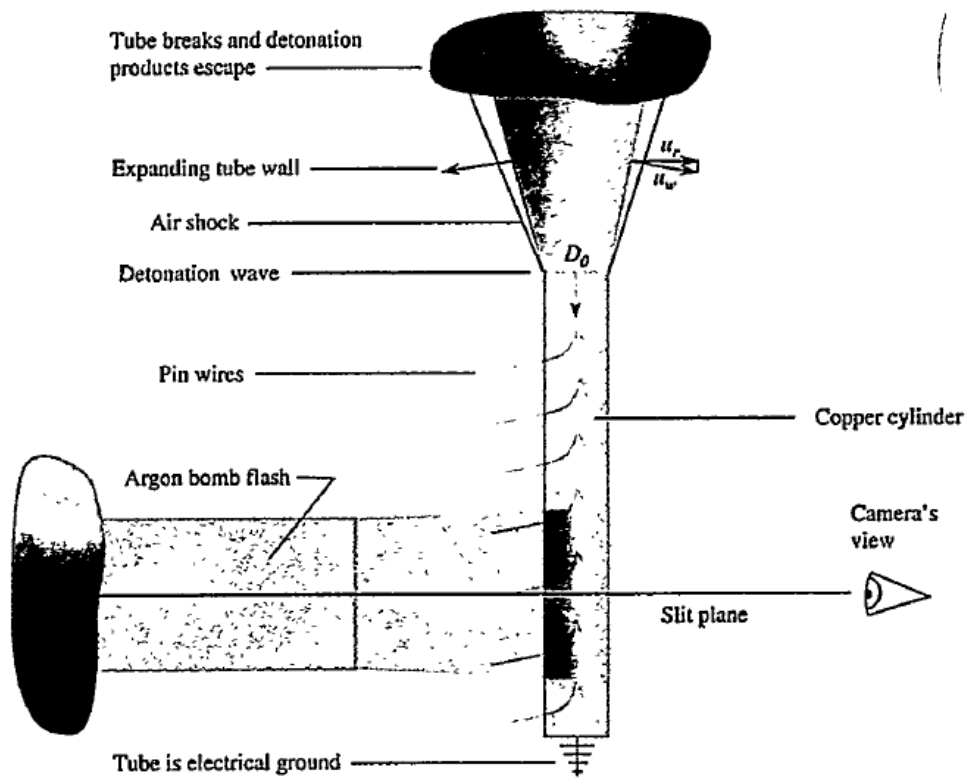


Figure 2-4 Schematic of the Test Setup Used by Los Alamos National Laboratory [16]

Esen et al. from the Swedish Blasting Research Centre (Swebrec) performed several cylinder expansion tests for different explosive compositions [5]. Their study mainly deals with commercial explosives which are used in mining and quarrying industry. The procedure followed in cylinder expansion tests is briefly stated and the results of different tests performed for several explosive compositions are presented in their study. They used OFHC copper as the tube material. The inner diameter of copper tubes used by Esen et al. varies between 40 mm and 100 mm. One of the test setups used in their studies is shown in Figure 2-5. It stated that if the wall thickness of the tube used in the test is $1/20^{\text{th}}$ of the inner diameter, which is also the diameter of the explosive charge, then the configuration is called “half-wall”; whereas the tube configuration is called “full-wall” when the wall thickness is $1/10^{\text{th}}$ of the inner diameter. Esen et al. preferred half wall tube configurations in their study; however, they stated that most of the researchers prefer the full wall configuration in their tests. 10 contact pins and a signal amplifier connected to these pins were used to gather tube expansion data. A conventional oscilloscope was used as the data acquisition device. PETN or hexotol (Composition B) boosters were used for detonating the main explosive and an EBW type detonator was utilized to initiate the explosive chain. They studied the effects of ANFO addition into emulsion type explosives and concluded that ANFO addition increases the early energy release into surroundings; however, the late energy release nearly remains same. They have also used aluminized explosives and state that the work capacity of the explosive can be improved with the addition of aluminum powder especially if the aluminum powder included in the explosive composition is fine enough. They presented pressure versus specific volume ratio curves for the explosives they tested.

Rumchick et al. [19] used cylinder expansion tests in order to determine Gurney velocity values and JWL equation of state parameters of explosive compositions. They used a standard full scale setup and a scaled-down setup with smaller dimensions in their tests. The diameter of the tube used in the full scale setup was 25.4 mm, whereas the tube with the scaled-down dimensions had a diameter of

12.7 mm. Oxygen free high conductivity copper was the raw material for the cylindrical casing. Streak camera records were employed to determine the expansion histogram of tube.

Hodgson and Handley [20] performed cylinder expansion tests in order to determine the JWL equation of state parameters for an explosive material designated as EDC35. The inner diameter of the cylinder was 25.4 mm and the radial expansion of the wall was measured up to 20 mm from the initial position of the wall surface. Both a streak camera and a set of ionization probes were used for radial expansion histogram in their study. For determining the JWL equation of state parameters using the data obtained from the cylinder expansion tests, they followed an iterative method. In this iterative method, the equation parameters are changed with each step till the simulations they make with their in-house developed code matches with the results of the experiment. In their paper, it is stated that changing the parameters manually to calibrate the equation of state is also possible and a commonly followed method.



Figure 2-5 Cylinder Expansion Test Setup Used by Esen et al. [5]

Elek et al. used cylinder expansion test results in order to obtain the JWL equation of state parameters for five different explosive compositions [6]. Several assumptions, which are inherent to a cylinder expansion test and the hydrodynamic detonation theory, were made. The tube wall was assumed to be incompressible; reflections of shock wave inside the cylinder were neglected; the detonation wave was assumed to be planar and at steady state; explosive material was assumed to transform to detonation products instantaneously when the detonation wave arrives and the gaseous detonation products were assumed to be inviscid. For determination of JWL equation of state parameters using the test results, they followed an

analytical approach in which the parameters are calculated iteratively. Similar to the method suggested by Souers [21], Elek et al. changed the parameters until the difference between the values of the detonation parameters of the explosive calculated via analytical expressions and from the test results become small enough. It is stated that a computer program was established for the iterative calculations. The schematic of the cylinder expansion test setup used by Elek et al. is provided in Figure 2-6. In this figure which describes the test setup, L is the length of the explosive charge; c is the distance from the explosive surface to the cross-section where the radial expansion of the tube is recorded; whereas r_{10} and r_{20} are the inner and outer radii of the cylinder. Copper was the raw material the cylindrical tube was manufactured from. A streak camera was utilized for recording the radial expansion of the cylinder wall.

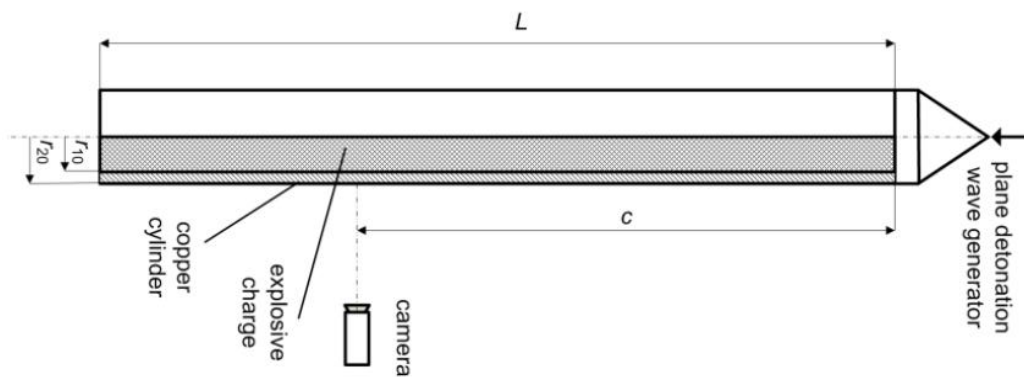


Figure 2-6 Cylinder Expansion Test Setup Used by Elek et al. [6]

Renick et al. [22] performed a series of laboratory experiments, field tests and theoretical studies to characterize the ATX-27 explosive composition. During their study, cylinder expansion tests were employed in order to determine the detonation velocity and JWL equation of state parameters of the explosive.

Gold et al. [23] used the JWL equation of state for modeling the explosives in their study of natural fragmentation of explosive filled metal cases. They studied the non-fractured phase of the natural fragmentation, which is a similar phenomenon to the expansion of a copper tube during a cylinder expansion test. They used equation of state parameters which had already been calibrated via cylinder expansion tests. It is stated that the predictions for the velocities of the expanding case at the non-fractured phase are reasonably accurate due to the fact that the parameters of the equation of state had been calibrated by cylinder expansion tests.

Goto et al. [24] studied the fracture and natural fragmentation of steel and copper hollow cylinders filled with explosive. Although cylinder expansion tests have not been performed in order to calculate the JWL equation of state parameters of explosives in this publication, the test setup used in order to examine the fracture behavior of metal cases was similar to that of a cylinder expansion test setup. The test setup is presented in Figure 2-7.

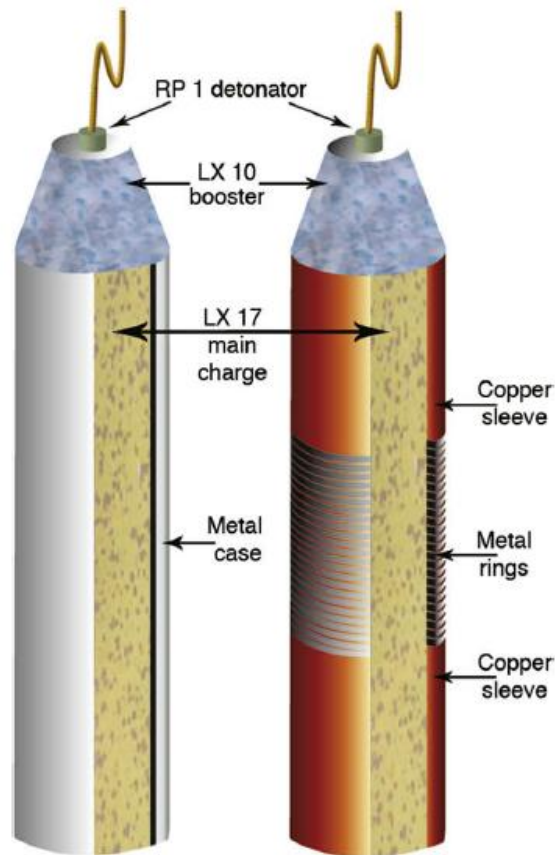


Figure 2-7 Test Setup Used by Goto et al. [24]

There are several important issues to be considered when designing the cylinder expansion test setup. In a cylinder expansion test, different values have been used as the internal diameter of the metal tube, i.e. the diameter of the explosive charge. In the cylinder expansion test setups presented in the literature, inner diameter values ranging between 20 mm and 100 mm are employed for the cylinder. It is suggested to select the inner diameter of the tube at least 25 mm in order that the detonation of the explosive approximates the behavior encountered at the theoretically infinite diameter [4], [8]. Moreover, the explosive diameter should be larger than the critical diameter of the explosive. The critical diameter for an explosive is the minimum

diameter value required to obtain a developed detonation in the explosive charge. Another important issue which must be considered is that the length to diameter ratio of the tube should be large enough to obtain plane wave detonation at the cross-section where the pins are located [5], [6]. When performing a test for determining the velocity of detonation of an explosive, it is suggested that the length to diameter ratio of the test item should not be lower than 8. This is necessary for obtaining a steady state detonation velocity and a detonation front with constant curvature [17]. Therefore these criteria should be considered during the design of the cylinder expansion test item.

For determination of JWL equation of state parameters using the data obtained from the cylinder expansion tests, a numerical iteration method has to be employed. Various iteration methods for solving sets of nonlinear equations have been developed and information is available on these techniques in the literature [25], [26]. Open domain numerical methods such as Newton's method, secant method, Muller's method and fixed-point iteration method or closed domain numerical methods such as bisection method or regula falsi method can be employed for solving nonlinear equations iteratively. Open domain methods do not search for the root in a bracketed region, unlike the closed domain methods. Therefore open domain methods may diverge. However, these methods find the roots faster and there is no need for bracketing an interval where the root certainly exists. In this thesis study a computer code was utilized for performing the iterations and an open domain iteration method, which is specifically used for data reduction from cylinder expansion tests and was proposed by Souers [21], was used in the code. For obtaining the radial position of the cylinder wall as a function of time using the contact pin signal time values, non-linear least squares regression is employed for curve fitting.

2.3 Measurement Techniques Used in the Tests

Since measurement of detonation velocity and radial expansion histogram are necessary in a cylinder expansion test, the papers discussing measurement techniques and apparatus used for this purpose are also examined in the scope of this study.

During a classical cylinder expansion test, detonation velocity of the explosive used in test item is also measured. It should be noted that the detonation velocity of an explosive increases with increasing charge diameter. The detonation velocity measured during the cylinder test is a value for the charge diameter selected. However, when the diameter of the charge is larger than 25 mm, for most of the explosives, the velocity of detonation approaches to the theoretical value which is the velocity of detonation of a charge with infinite diameter. Therefore, the measured detonation velocity of a charge with a diameter of more than 25 mm and contained inside a metal casing is representative for the explosive. The obtained value can also be compared to the data in the literature, if available. Furthermore, the detonation velocity measured during a cylinder expansion test is applicable to use in the calculation steps of the JWL equation of state parameters.

There are several methods for measurement of the velocity of detonation. The method is generally selected considering the available equipment and capabilities, since it is stated that any method does not have a prominent advantage over another one [17]. Most commonly used measurement methods for detonation velocity are named the electrical method, the optical method and the optical probe method. In the electrical method, the closing or opening of an electric circuit due to the pressure induced by the detonation generates the signal. By this way, the arrival of detonation front at a desired location can be measured. In optical method, a streak camera is used to record the position of the detonation front during the detonation of the test explosive. This is achieved by observing the expansion of the casing which is used as the housing for the explosive. In the optical probe method, probes

sensitive to light are employed for generating signal and the probes are generally connected to data acquisition equipment via fiber-optic cables.

For measurement of the detonation velocity, authors and researchers have generally used one the three methods discussed or a variation of one of them. Bocksteiner et al. measured the detonation velocity of both confined and unconfined explosives [27]. Although the optical method employing a streak camera is available in their institution, the researchers used the electrical method in their study and they employed a number of ionization probes to measure the detonation velocity of PBXW-115 explosive composition. For confined explosives, they used two different types of metal tubes with inner diameters of 22 mm and 50 mm and wall thicknesses of 3 mm and 5 mm. The length to diameter ratio of the tubes was approximately 5. Various types of pressed booster pellets were utilized in the detonation chain design of their setup. Other than the three methods that are mainly preferred, there are some other techniques for measurement of detonation velocity. Reader can refer to Suceska's publication for more detailed discussions on these methods [28].

When performing a cylinder expansion test, the most important issue is to measure the radial expansion of the cylinder wall accurately. There are various methods for observing the radial expansion of the cylinder wall during the test. Electronic pin probes or contact pins, flash x-ray techniques, shadowgraph, various velocity interferometer techniques, streak camera and high frame rate camera can be given as examples of instruments and methods that can be used for measuring and recording the radial expansion of the cylinder wall.

Flash x-ray radiography is one of the methods that can be used for recording dynamics events occurring with high speed. This method can be used for measuring the dynamic behaviour of materials in ballistic events as well as for measuring other high speed phenomena. Flash x-ray is used to obtain visual data of processes which occur within a few microseconds employing devices which produce intense

radiographic rays. However, it is difficult to protect the necessary equipment near an explosion and it is not logical to replace such expensive equipment in every test. Furthermore, the data obtained using flash x-ray radiography can be obscured due to factors such as dust and luminous effects [29], [30]. Therefore the flash x-ray radiography is not commonly preferred by the scholars as a recording technique for cylinder expansion tests.

The shadowgraph technique is another optical method that can be followed for observing high speed events. In this technique, the object that is to be observed is illuminated by a light source and the shadow of the observed items is recorded by suitable equipment. This method is generally used to observe the non-homogeneities in a fluid flow. The shadowgraph technique is mainly employed for observing the shock waves rather than the acceleration of metal casings in events including detonation of an explosive material [31].

Velocity interferometers are optical velocity measurement systems. They are used to obtain images with a high rate. VISAR (Velocity Interferometer for any Reflector) is an optical velocity interferometer method for obtaining images during a dynamic event occurring within a small time interval. The line-VISAR, which is an improved version of the classical VISAR technique, is a promising method for measuring the velocities with respect to time or position; however, it is a recently developed method and has not been used extensively for research purposes [32]. PDV (Planar Doppler Velocimetry) is also an optical method for determination of instantaneous velocities of moving particles or solid material. The PDV method is based on the Doppler effect in light waves for determining the three dimensional velocity vectors for moving objects. This is also a relatively new technique for velocity measurement [33]. Fabry Perot interferometer is another velocity interferometer design for obtaining the velocities of solids in motion. VISAR, PDV and Fabry Perot interferometer are not generally preferred in cylinder expansion tests when compared to other measurement techniques.

One of the instruments that is commonly used in order to determine the expansion histogram of the cylinder tube is the streak camera. A streak camera, or a smear camera, is an instrument which records the changes of light reaching at the camera with a very high rate. In a cylinder expansion test, the streak camera can be used both for determining the velocity of detonation of the explosive and the arrival times of the hollow tube at several radial positions at a cross-section [17]. Although, if protected well during tests, a streak camera can be used in many tests without need of replacement, the significantly high cost of a high precision streak camera is a hindrance. Moreover, in order to obtain clear images from a streak camera, an external source of light such as an exploding wire, a flash bulb or an argon bomb is generally utilized. Use of such a light source during each test adds more complication to the test setup and this is another factor which increases the recurring cost of the tests. Sample frames from the streak camera records taken during cylinder expansion tests and presented in publications are given in Figure 2-8 and Figure 2-9 [6], [16]. High speed camera or high frame rate camera is another visual recording apparatus that is proposed for recording the radial expansion of the cylinder. However, the streak camera is a better instrument than a standard high speed camera for recording fast events. Therefore, if a camera is used for obtaining the radial expansion histogram during a cylinder expansion test, streak cameras are preferred rather than classical high frame rate cameras.

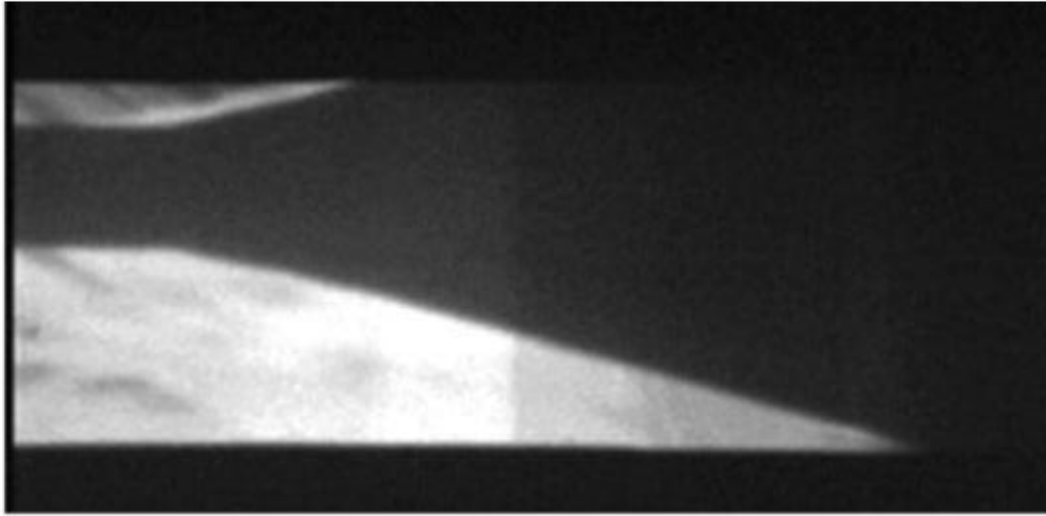


Figure 2-8 Streak Camera Record from the Tests Performed by Elek et al. [6]

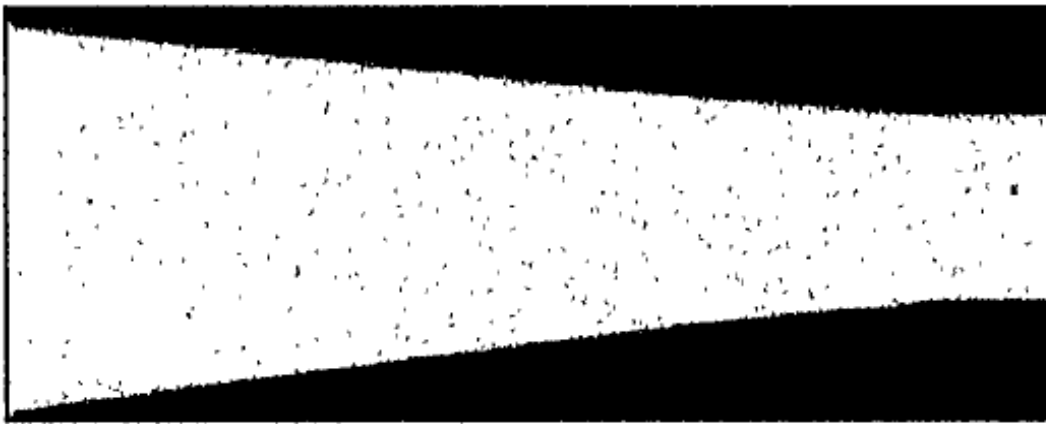


Figure 2-9 Streak Camera Record from the Tests Performed by Los Alamos National Laboratory [16]

Use of contact pins is another commonly employed method that can be used for measurement of the radial expansion of the cylinder wall in a cylinder expansion test. Contact pins are used for measurement purposes by various scientists and institutions as position transducers or time of arrival detectors [34]. They produce electrical signal when impacted by a fast moving object or when subjected to a shock front at their sensory end. Ionization pins, shorting pins and piezoelectric pins are the commonly used types of contact pins. Piezoelectric pins are not needed to be exposed to an excitation to generate signal, whereas ionization pins and shorting pins require an external excitation source. Esen et al. [5] used off-the-shelf ionization contact pins in their cylinder expansion test setup. The contact pins were used efficiently in this setup and the measurements obtained using these pins were accurate enough for the study.

The Lawrence Radiation Laboratory used to prefer streak camera for recording the wall velocity and pin probe method for determining the detonation velocity of the explosive in the past. Today, the Lawrence Livermore National Laboratory (previously the Lawrence Radiation Laboratory) employs both streak cameras and contact pins for recording the radial expansion histogram of the cylinder wall. Atomic Weapons Research Establishment of the United Kingdom prefers to use both electronic pin probes and streak cameras to record the wall expansion, and pin probes to measure the detonation velocity during cylinder expansion tests [17], [35].

Contact pins are also used in other types of experimental setups for measurement purposes. Forbes et al. [36] used piezoelectric type of contact pins for measurement of wave propagation resulting from the reaction due to thermal cook-off of a cylindrically confined high explosive. The setup used by Forbes et al. is shown in Figure 2-10. Chen et al. measured the arrival times of micro-jetting particles resulting from explosively shock-melted lead employing lithium neonate piezoelectric contact pins as well as high speed photography [37]. Jackson et al. [38] studied detonation of ammonium-nitrate-fuel-oil (ANFO) which is confined inside aluminum tubes with an inner diameter of 76 mm. The configuration of the

test setup is similar to that of a cylinder expansion test setup. They measured the detonation velocity, shape of the detonation front and response of the aluminum casing to the detonation. They utilized crystal pins for measuring the wave profile.

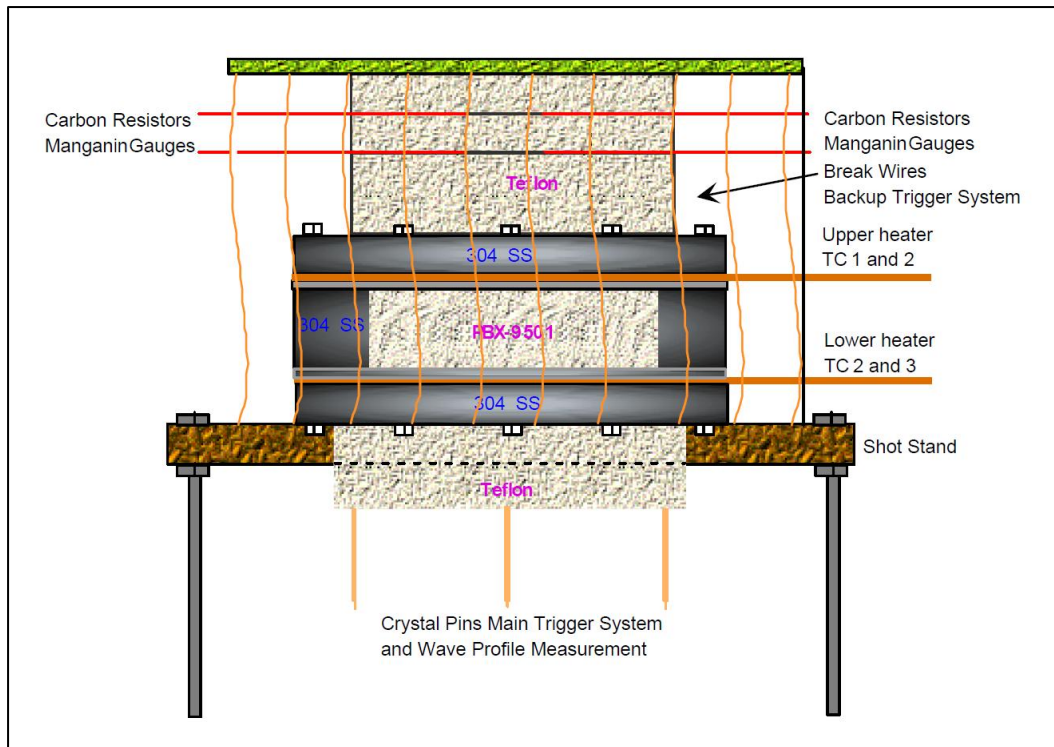


Figure 2-10 Use of Pins for Measurement of Detonation Wave Propagation [33]

Shock initiation and critical diameter of liquid isopropyl nitrate were studied by Zhang and Murray [39]. In this study, times of arrival of detonation front at certain locations inside the liquid explosive are measured utilizing piezoelectric pins and velocity of detonation of the explosive is calculated using the measured arrival times. Piezoelectric pins and photoelectric probes were used in order to measure the time of arrival values of detonation wave while investigating the detonation

properties of gaseous mixtures inside closed chambers [40], [41]. Pits et al. [42] used ionization pins for measuring the arrival times of shock waves resulting from combustion of hydrogen gas inside a closed residential garage. Similar ionization and piezoelectric pins are also used as measurement sensors or triggers for data acquisition systems in other experimental studies [43], [44].

Among the various apparatus that are used for recording the wall expansion histogram, the streak camera and the contact pins are the most commonly used ones for recording the radial expansion of the casing in a cylinder test. Conolly compares different recording methods and states that ionization contact pins and optical fiber probes are preferable over other instruments including the streak camera. The main reason for selecting the contact pins is that the initial and recurring costs of metrology techniques which utilize contact pins are lower than other expansion data recording methods [45]. Another advantage of the contact pin method is that, this method provides more accurate expansion data than the streak camera record for the early stages of the cylinder wall expansion [17]. Furthermore image processing has to be employed for the records obtained from visual recording techniques such as velocity interferometers, streak cameras, high speed cameras or flash x-ray radiography. On the other hand, when contact pins and a digital data acquisition system are used for gathering the expansion data, there is no need for post-processing of images after the test. Due to these advantages, contact pins were used for measurement of the radial position of the cylinder wall as a function of time in the tests performed in the scope of this dissertation.

CHAPTER 3

THE CYLINDER EXPANSION TEST SETUP

3.1 Design of the Test Setup in General

A cylinder expansion test setup was designed and developed in the scope of this study following the guidelines and suggestions given in the publications which have been presented in the literature. The setup consists of the main test item, the components which are used for positioning the test item and measurement apparatus, the off-the-shelf components used for signal amplification and data acquisition, and other auxiliary parts and components.

The solid model of the main test item assembly, which consists of the hollow copper cylinder filled with main explosive and the ignition chain, is presented in Figure 3-1. The main explosive is the composition for which the JWL equation of state parameters are to be obtained. During the test, the main explosive is detonated from one side. At the side where the explosive is detonated, an ignition chain is utilized. The ignition chain consists of two booster pellets and an EBW type detonator. A booster pellet is an explosive charge which has smaller size and higher sensitivity than the main explosive in a system, munition or test item that contains explosive materials. Boosters are utilized prior to the main explosive in ignition chains and are employed for initiating detonation in the main explosive charges. In this setup, the booster charges and a detonator handling part are assembled to the main explosive using an appropriate adhesive material. One of the booster charges is larger than the other one. The larger booster is mounted on the explosive and then the smaller booster pellet is mounted over the large booster. Finally the detonator handling part, which has the same diameter as the small booster pellet, is pasted

over the small booster part. It is important to use an appropriate adhesive material for fixing the booster pellets and the detonator handling part. In this design, an adhesive material which was compatible with the main explosive materials and the booster pellets was used for mounting purposes.

Diameters of the booster pellets used in the ignition chain are 35 mm and 25 mm; whereas the lengths for these boosters are 60 mm and 10 mm for the big and small pellets respectively. Use of two booster pellets with increasing masses and diameters assists obtaining a planar detonation front rather than a detonation front with curvature when the detonation front fully develops inside the cylinder. Use of a single booster with a complex geometry like a conic one in order to achieve a planar detonation front and therefore production of a pressing tool for such a complex geometry were avoided by using two booster pellets. Simulations were performed using a commercial hydrocode both before and after the cylex tests. In the analyses performed before the tests, the geometry of the detonation front that is going to be encountered when the setup with the selected booster charges is used in a test was able to be studied. In the hydrocode analyses, the test item was modeled and the test was simulated in its entirety. Results of these hydrocode simulations have shown that the designed detonation chain is sufficient for a planar detonation wave. The booster pellets used in the tests were manufactured by pressing explosive with ex-proof pressing machines. Pressing moulds were employed for the manufacturing of the pellets. Various explosives can be used as the booster material. In this design, PBXN-5, which is a pressable polymer bonded explosive, is selected as the raw explosive material for both booster pellets.

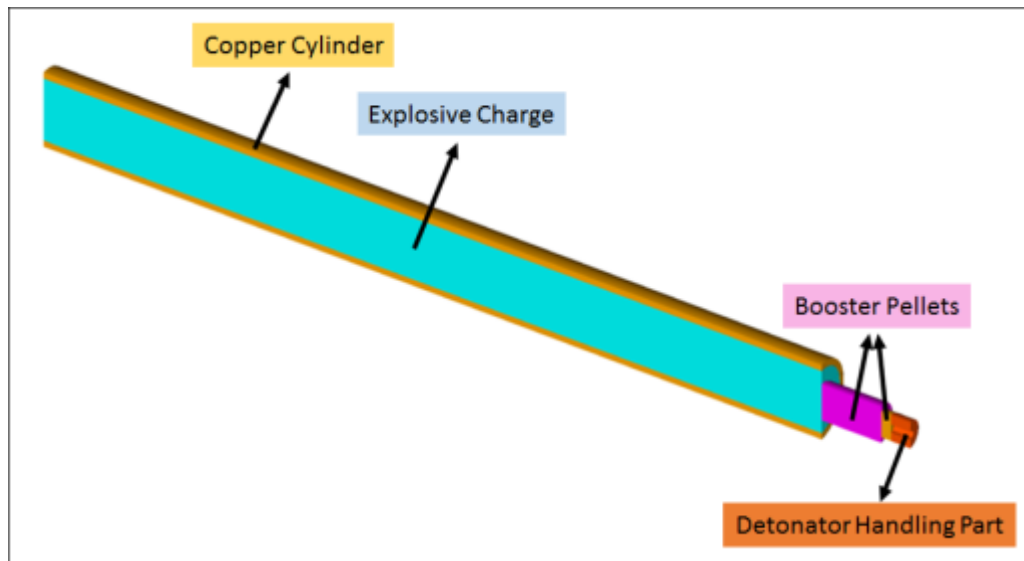


Figure 3-1 Solid Model of the Main Test Item Assembly

The hollow cylinder is filled with explosive by casting process. The amount of explosive in a single test item is approximately 3.6 kg; however the exact explosive mass in every test item depends on the type of the explosive composition and its bulk density used in that test item. During the cylinder expansion test, the wall of the cylindrical casing expands radially during the propagation of the detonation wave inside the explosive after the explosive is detonated. The cylinder was produced of OFHC copper. OFHC copper is a highly pure material with a copper percent of at least 99.95%. During the design of the copper casing, the inner and outer diameters of the casing were selected as 60 mm and 72 mm respectively. Therefore the wall thickness of the casing in the test item is 6 mm. Since the wall thickness is one tenth of the inner diameter of the tube, the tube configuration is full-wall, rather than half-wall. The length of the copper cylinder is selected as 800 mm. The length to inner diameter ratio for the main explosive charge is approximately 13. This ratio is large enough for achieving steady state detonation inside the cylinder. The important design parameters for the copper case geometry are summarized in Table 3-1. The dimensions are given with their tolerances.

Table 3-1 Design Parameters for the Copper Cylinder

Parameter	Value	Tolerances (mm)
Inner Diameter	60 mm	+0.0; -0.1
Outer Diameter	72 mm	+0.0; -0.1
Wall Thickness	6 mm	-
Length	800 mm	+0.0; -0.2
Material	OFHC Copper	-

As explained before, two quantities are measured during the cylinder expansion test, namely the detonation velocity of the explosive and the radial expansion of the cylinder wall at a single cross-section. The measured data are later processed to obtain the JWL equation of state parameters.

Detonation velocity of the explosive is the velocity of the detonation front in the direction of longitudinal cylinder axis. In this design, four optical probes connected to fiber-optic cables are used for measurement of the detonation velocity. In order to place these probes later inside the explosive, four equally spaced holes are drilled along the cylinder before the explosive is casted inside the cylinder. Moreover, four dummy metallic pins are placed inside these holes during explosive casting such that the tips of each pin reach to the axis of the cylinder. By this way, clear spaces are shaped within the explosive and these spaces are used afterwards for inserting the optical probes inside the explosive before the test. The distance between each consecutive hole pair and therefore each probe is 100 mm. The diameter of each hole is 3 mm, which is an enough clearance for the probes that are to be inserted in.

During the tests, signals are gathered from each optical probe. The time of signal for each probe indicates the time of arrival of detonation wave at the location of that probe. Since the position and time of arrival of the detonation front are known for

these four points, an average velocity of detonation is calculated for each test item after the tests.

The other quantity which is necessary to measure during the test is the radial position function of the cylinder wall with respect to time during its expansion. In this design, ten contact pins are employed for measurement of wall expansion. The pins are located at a single cross-section along the cylinder axis. The cross-section where the pins are located is at a distance of 590 mm from the end where the explosive is detonated. The ratio of this distance to the diameter of the main explosive charge is approximately 10, which is a suitable value for achieving a steady state detonation wave before the detonation front arrives at the cross-section where the radial expansion histogram of the cylinder wall is recorded. The pin axes are orthogonal to the copper cylinder surface and the tip of each pin is pointed to the outer surface of the cylinder. The radial position of each pin measured from the cylinder outer surface, i.e. the distance between each pin tip and the surface of the cylinder, is different. The radial positions of the contact pins are presented in Table 3-2. Design and manufacturing tolerances for the dimensions are also given in the table.

Table 3-2 Radial Positions of the Contact Pins

Pin No.	Dimension	Radial Position (d) (mm)	Tolerances (mm)
1	d ₁	0.10	+0.05; -0.00
2	d ₂	8.10	+0.05; -0.05
3	d ₃	16.10	+0.05; -0.05
4	d ₄	24.10	+0.05; -0.05
5	d ₅	32.10	+0.05; -0.05
6	d ₆	40.10	+0.05; -0.05
7	d ₇	48.10	+0.05; -0.05
8	d ₈	56.10	+0.05; -0.05
9	d ₉	64.10	+0.05; -0.05
10	d ₁₀	72.10	+0.05; -0.05

The pin distances equally increase for each consecutive pin. During the expansion of the cylinder wall, the outer surface of the cylinder gets in contact with the pins one after another and signals are gathered from each pin consecutively. Time of each signal indicates that the cylinder surface reaches the pin location at that instant. By this way, the radial position of the cylinder wall is obtained as a function of time. For gathering the signals, a signal amplifier and a data acquisition system are employed. The difference between the radial positions of each consecutive pin pair is 8 mm. The position of the last pin from the cylinder outer surface is 72.10 mm. The cross-section where the contact pins are located is shown in Figure 3-2. Distances between pin tips and the outer surface of the copper cylinder, d_i , are illustrated on the figure. The radius of the copper cylinder at this position during expansion is 108.10 mm, since the initial outer radius is 36 mm. Therefore the radial expansion of the cylinder wall is measured till the point where the cylinder radially expands approximately up to a radius three times of its original outer radius. Use of 10 contact pins and measuring the radial expansion up to a radius ratio of 3 enables gathering data over a wide range with adequate resolution. An advantage of using this many contact pins is that in case that signal cannot be gathered from some of the pins, the remaining measurements will be sufficient for obtaining an accurate radial expansion histogram of the cylinder wall during its expansion.

Performing radiographic inspections on the test items before the tests was considered during this study due to the fact that discrepancies in the explosive such as cracks, bubbles, foreign substances affect the performance of the explosive and the detonation front. However, the x-ray equipment that was available during the course of the study was not powerful enough to penetrate 12 mm thick copper casing used in the test item, which has a density value higher than many other metals; therefore, distinguishable visual radiographic films could not be obtained.

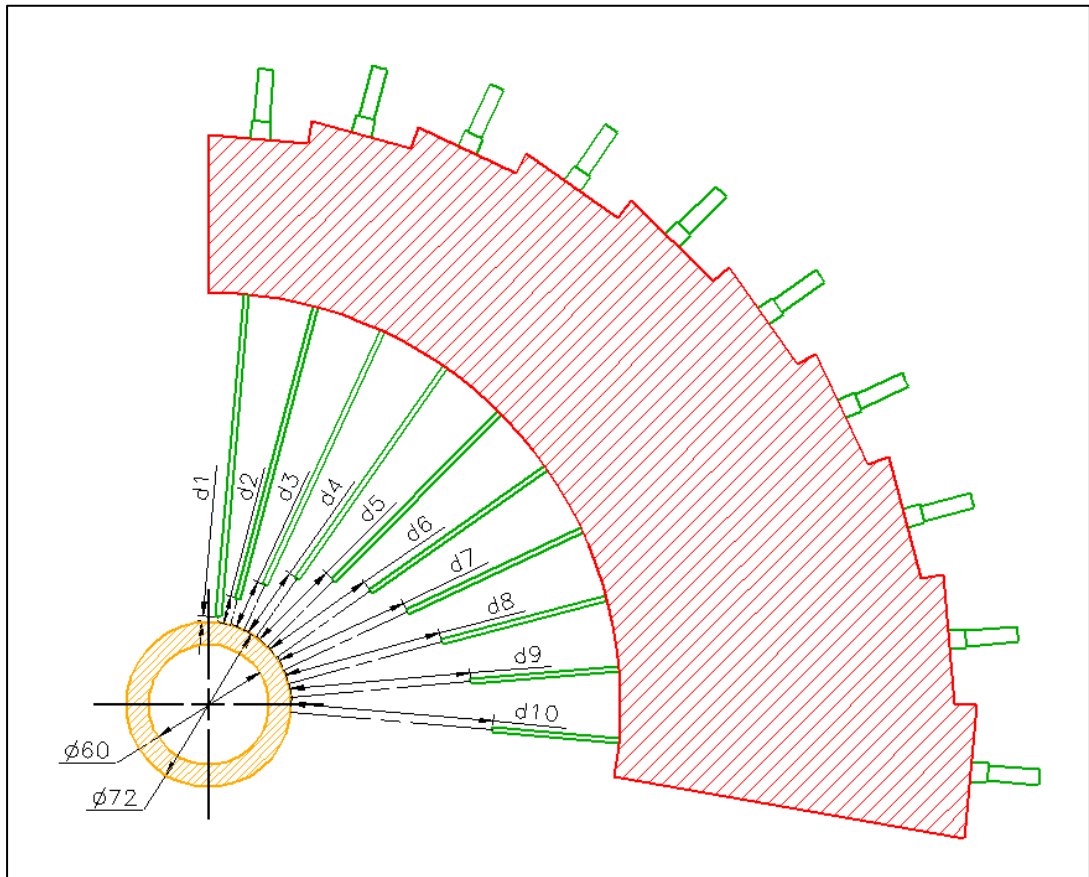


Figure 3-2 The Cross-Section Where the Pins are Located

3.2 Components of the Test Setup

In the test setup, there are auxiliary parts for positioning and handling the main test item assembly and measurement apparatus. These sub-components are the pin holder, the cylindrical holder, the base plate and the wooden table assembly. These parts are described in the following paragraphs. The solid models of the components are presented as cut from half for better comprehensibility.

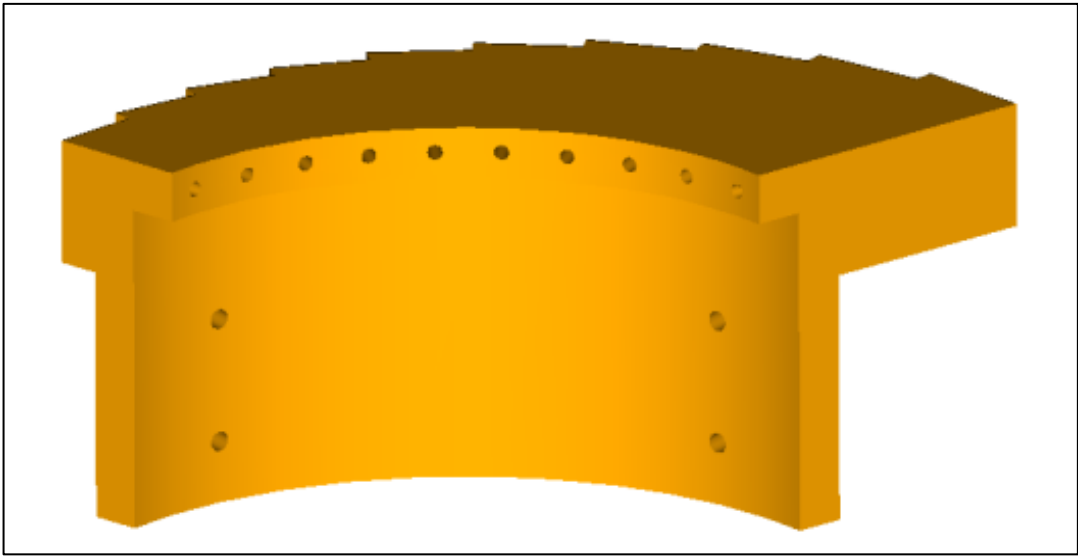
The pin holder is the component on which the ionization contact pins are screwed. The views of the 3-D model of the pin holder are given in Figure 3-3. There are

10 threaded holes on the pin holder for positioning the contact pins. The pin holder is designed as a stepped part with varying diameters at different sections where each pin is positioned. Since the distance between the cylinder surface and different pins is not constant, such a pin holder part is designed. Several metals including steel and aluminum alloy and several polymer materials were considered as the raw material candidates for this part during design. Aluminum alloy was selected as the raw material, since its density is lower than that of steel, which results in a considerably lighter part. Using a relatively light part is important since a heavy pin holder could topple down when mounted on other components. Any polymer material was not employed due to the fact that there is a strict tolerance requirement for the dimensions of the pin holder and strict tolerances can be achieved more easily if a metallic material is used. The pin holders used in the tests were produced by machining.

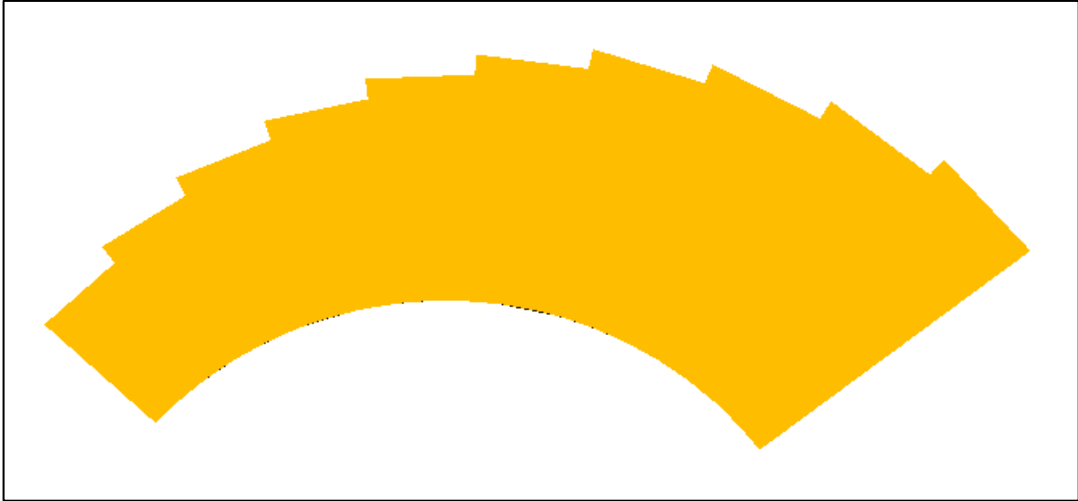
The pin holder is screwed to a part called the cylindrical holder in the test setup. Although the pin holder is required to be a light part for avoiding toppling, this part should be a relatively heavy one because mounting the pin holder on it moves the center of gravity of the assembly to one side. Therefore the cylindrical holder was manufactured from steel. The pin holder is mounted on the cylindrical holder using four bolts. The view of the solid model prepared for the cylindrical holder is presented in Figure 3-4.

The main test item which is the explosive filled copper cylinder should be placed inside the cylindrical holder before the test. The copper cylinder should be concentric with the cylindrical holder, since the pin holder is mounted on the holder. For achieving the concentricity, a thin steel part, called the base plate, is used as a template for placing the explosive filled copper tube. The model of this base plate is given in Figure 3-5. The inner diameter of the base plate was the same as the outer diameter of the copper cylinder; whereas the outer diameter of the base plate and the inner diameter of the cylindrical holder was the same at their nominal values. Dimensions for the inner and outer diameters of the base plate with their

tolerances are 72 (+0.3 ; +0.1) mm and 300 (-0.5 ; -0.7) mm, respectively. The tolerances of the inner and outer diameters of the base plate is important for tight positing of the copper cylinder.



(a)



(b)

Figure 3-3 Solid Model of the Pin Holder
(a) General View (b) View from Top

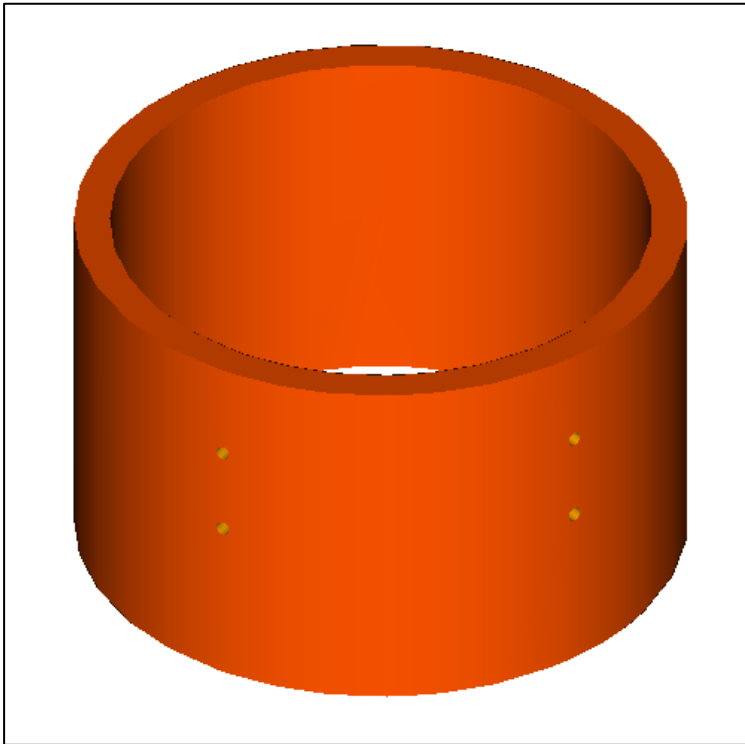


Figure 3-4 Solid Model of the Cylindrical Holder

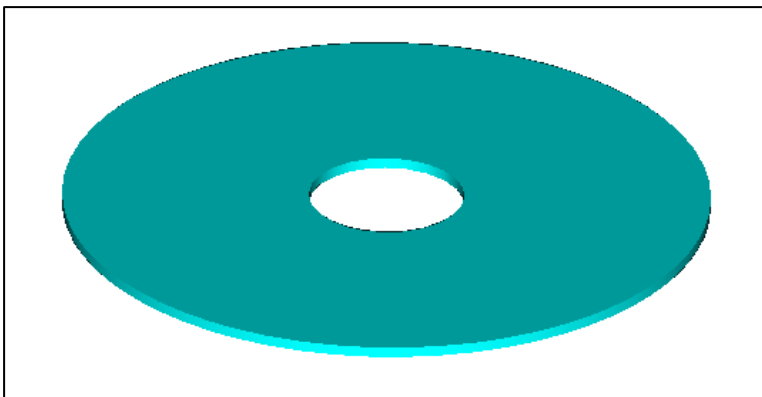


Figure 3-5 Solid Model of the Base Plate

The distances between the tip of each contact pin and the outer surface of the cylinder wall are different, as stated before. Each pin should be positioned accurately and strict tolerance values must be employed for pin positions in order to obtain precise values for the radial velocity of the cylinder wall during expansion. Therefore a stepped part with varying diameters was used as a gauge for placing the pins at accurate positions before conducting the tests. This stepped part is designed such that the differences between the outer diameter of each step and the inner diameter of the part are equal to the values of radial pin locations measured from the cylinder wall outer surface. The thickness of each step on the part has a total tolerance value of 0.1 mm. The gauge is placed over the surface of the cylinder during adjusting the positions of the contact pins. Each contact pin is then screwed to the pin holder such that its tip will be in contact with the gauge after positioning. Since the gauge is used for positioning each pin during every test, it should be a relatively light part for easy handling. The stepped gauge was manufactured from aluminum alloy.

The components that have been described up to now are placed to their positions on a wooden table assembly before the test. The model of the table assembly is presented in Figure 3-6. The explosive filled cylinder is placed vertically on the table assembly before the tests such that its center axis will be orthogonal to the horizontal ground surface. There exists a hole at the top side of this table for supporting the explosive filled copper cylinder. The diameter of this hole is equal to the outer diameter of the copper cylinder. Standard materials such as timber nails and timber glue are used for mounting the sub-components of the wooden table to each other.

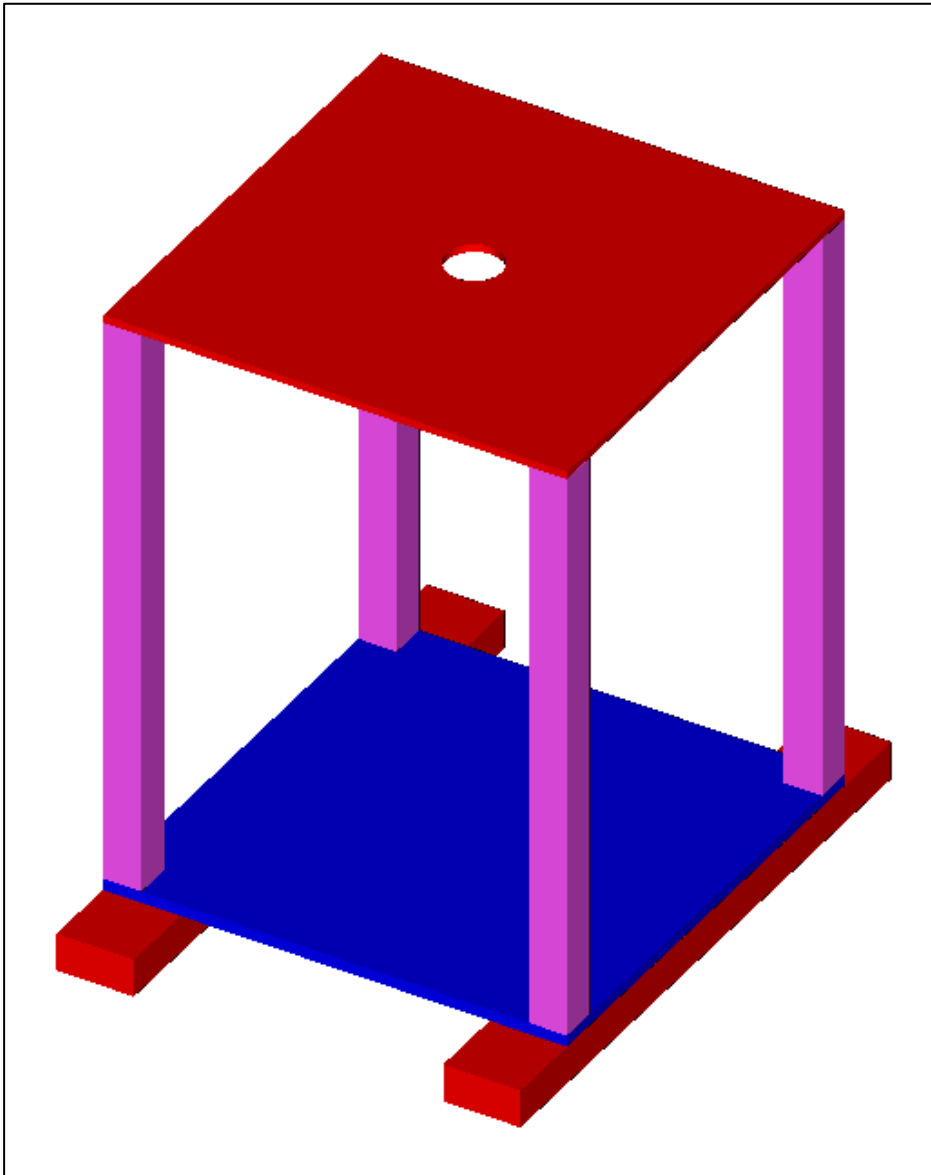


Figure 3-6 Solid Model of the Table Assembly

The final assembly of the test setup is constructed on the test area before performing the tests. The model of the final setup assembly with the components in this assembly is shown in Figure 3-7.

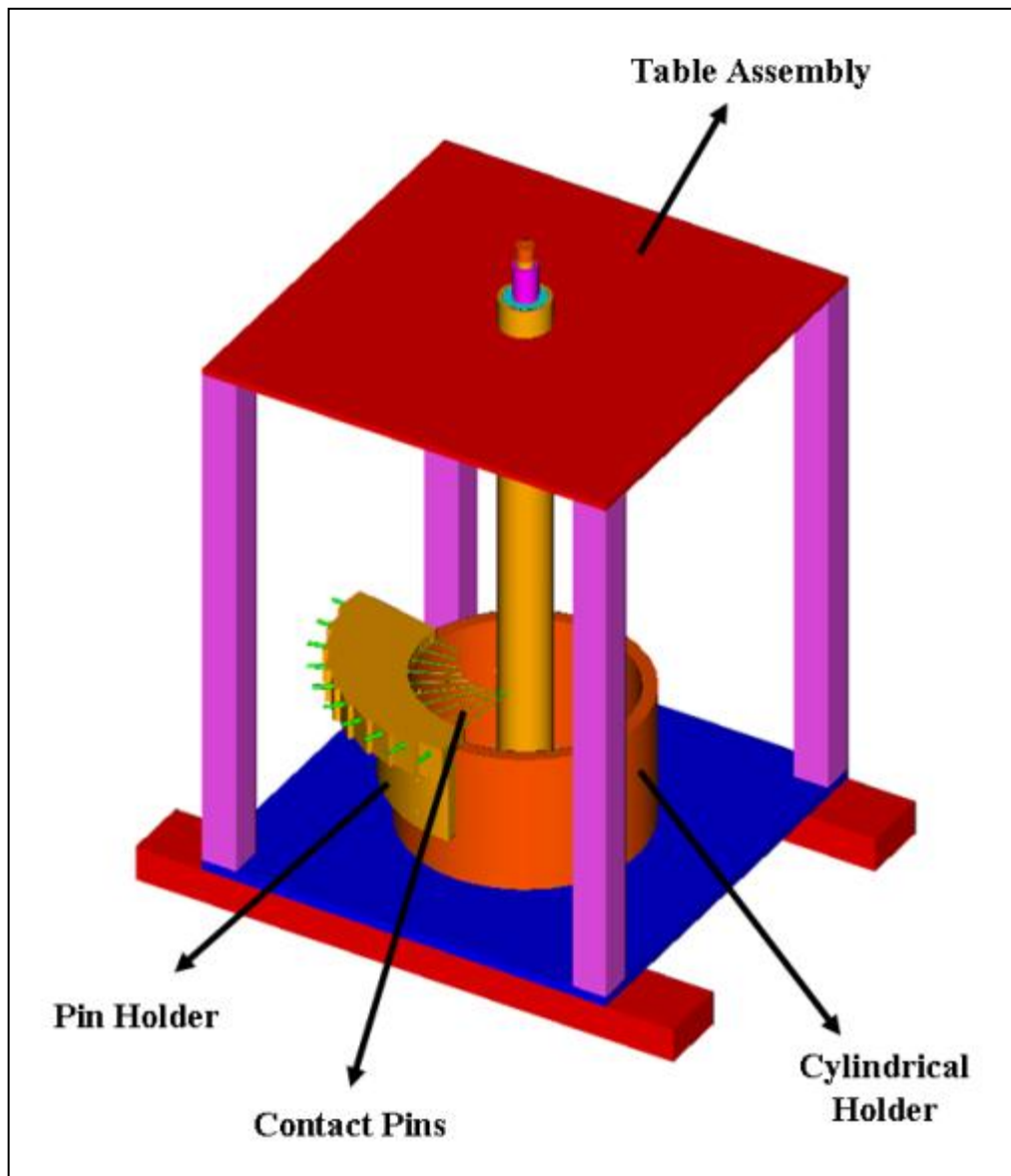


Figure 3-7 Solid Model of the Test Setup Assembly

The tolerances for the important dimensions of the test setup components were presented previously within the text. Geometric dimensioning and tolerancing were also utilized for the setup components when necessary. The dimensions with their tolerances have been controlled by conventional quality control tools whenever

possible. For more complex parts like the stepped cylinder, conventional methods for metrology were not appropriate. For such components, a CMM was utilized to check whether the critical dimensions were within the design tolerances. Sample results of these CMM measurements are provided in Appendix A.

In several systems containing explosives, some chemicals or polymeric materials are used as an interface material or component between the metallic casing and the explosive material. These liner materials may be employed for several purposes such as providing insulation between the metal and explosive, protecting and conserving the explosive against hazardous environmental effects and preventing undesired interactions between the casing and the explosive. Moreover, strength of the bonding or adhesion between the explosive and the metal may be wanted to be enhanced or reduced according to the design considerations and requirements of the said system. Adhesion of the main explosive charge to the metallic casing components may be desired locally or as a whole, or it might be desired to be prevented at all in different systems. The decision for this is made according to the specific requirements of the systems. In several systems, for instance, it is not desired to have any adhesion between explosive and the casing due to the difference between the coefficient of thermal expansion between the explosive and the metallic casing, which may lead to cracking inside the explosive when the assembly is subjected to excessively high or low temperature. For several other systems like artillery or mortar munitions, on the other hand, the designer may prefer some adhesion between the explosive and the casing at least locally due to high acceleration values the system will be exposed to during flight. The lower and higher limits for the temperature range or the magnitudes of the acceleration that the component will be subjected to are imposed by the requirements of the weapon system. However, such insulating liners and adhesive enhancing or preventing materials are generally used in munitions that are used in mortar, rocket and missile systems. Since long term shelf time is required and environmental requirements for such systems are defined due to general system needs. The environmental requirements are imposed to such systems according to life cycle conditions of the

system as a whole. However, the test items used in the cylinder expansion tests are not stored for a long time before the tests and therefore there is no long term shelf life requirement. Furthermore there is no imposed environmental condition requirement such as temperature range, transportational or operational vibration on the test item since it is not used in a weapon system. Therefore any liner material has not been designed to employ between the explosive and the casing in the test item. The adhesion issues for the explosive has not been considered during design either, since this is not critical for test items which do not undergo a long term life cycle. Similarly, no insensitive munitions mitigation techniques were followed in the design of the explosive filled copper cylinder, because it is a test item rather than a component used in a weapon system.

3.3 Utilization of the Setup in Cylinder Expansion Tests

The designed setup has been utilized in the cylinder expansion tests which have been performed in the scope of this dissertation. The tests were performed in the energetic material test area of Mechanical and Chemical Industry Corporation of Turkey. Tests were performed using four different types of explosives, which are named as P-1, P-2, P-3 and P-4 in the context of this dissertation. The explosive composition designated as P-1 is actually TNT, which is commonly used explosive material and properties of this explosive are known well. Since detonation properties and JWL equation of state parameters for TNT are available in the open sources, comparison of the test results with the literature data was possible for this explosive. The energetic manufacturing processes followed for production of the test items such as explosive casting, booster pressing and booster assembling were performed in Roketsan facilities. Technical drawings have been prepared for mechanical components of the setup and they were produced in accordance with these technical drawings. Quality control measurements and activities were performed for both the metallic and the energetic components as discussed before.

The test setup was assembled in the test area with the previously manufactured components. Initially, the contact pins which are used to record the cylinder wall expansion are screwed to the pin holder which is further mounted on the cylindrical holder (Figure 3-8). Then the pin holder is placed on the wooden table. The base plate which is used as a template for positioning the main test item is placed inside the cylindrical holder (Figure 3-9). The main test item, which comprises of the explosive filled copper cylinder and the ignition chain elements, is placed to its position on the table. The base plate placed inside the cylindrical holder and the supporting hole at the top of the wooden table enable the positioning of the main test item correctly. After the cylinder is placed to its position on the table assembly, the positions of the pins are fine tuned with the help of the stepped gauge.



Figure 3-8 Contact Pins and the Pin Holder



Figure 3-9 Contact Pins, Pin Holder and Base Plate

The pins are connected to a signal amplifier via flexible coaxial cables and BNC type cable connectors. The signal amplifier is further connected to a digital data acquisition system. The flexible cables used for connecting the contact pins and the signal amplifier was long enough to place the signal amplifier and the data acquisition system at a distant position protected from the effects of the explosion.

Four optical probes that are connected to the fiber optic cables are mounted to the holes which were opened beforehand on the copper cylinder (Figure 3-10). The optical probes are fixed on their positions on the main test item with the help of adhesive bands. The fiber-optic cables are connected to a device that stores the signal times in its memory. The signal times obtained from these probes are then used to calculate the velocity of detonation of the explosive.

During several stages of the construction of the test setup, the horizontal planarity of the test setup was checked using a digital protractor and a spirit level.

The photograph of the final setup assembly is presented in Figure 3-11. After the construction of the setup is completed, the signal amplifier, the digital data acquisition system and the video camera are started and the test is performed. During the test all the personnel leave the test area and stay inside a protective bunker. The ignition of the EBW detonator is triggered inside the bunker utilizing an igniter unit that provides the electric current necessary for activating the detonator.



Figure 3-10 Optical Probes and Fiber Optic Cables that are used for Measuring the Detonation Velocity of the Explosive



Figure 3-11 The Test Setup Assembly

During one of the tests, visual data was obtained utilizing high speed camera. The recording speed of this high frame rate camera during the test was 15000 frames per second. The camera records were for recording the tests rather than data gathering purposes. Therewithal, the camera records were obscure due to detonation of explosive and the visual images was not appropriate for post-processing calculations. Instead of the high frame rate camera, a standard hand camera was employed in some of the other tests for video recording. The camera was covered

with a portative metal bunker during the tests for protection against blast and fragmentation effects caused by the test item (Figure 3-12). Different frames of the camera recording obtained with the high frame rate camera are presented in Figure 3-13 as samples.



Figure 3-12 Camera Used for Visual Recording



Figure 3-13 Sample Frames from Camera Recording

The test setup is completely destroyed in each test and the surrounding area is affected by the explosion. The photograph of the test area after the test is completed is shown in Figure 3-14. After the test, the data gathered during the test is recorded for further data processing calculations.



Figure 3-14 Test Area after the Test

CHAPTER 4

THEORY

Several detonation properties, namely the detonation velocity, Gurney velocity and JWL equation of state parameters of an explosive, can be obtained performing the cylinder expansion test.

As discussed before, the time of arrival values of the detonation wave at distinct points along the tube axis and the radial expansion histogram of the tube at a certain cross-section are measured during a cylinder expansion test. Using the arrival times along the tube, the velocity of detonation of the explosive used in the test is calculated. The arrival times are measured at several points, the distances among which are known. Therefore, using the distance between these points and the time of arrival values, an average detonation velocity for the explosive used in the test is obtained.

In order to obtain the Gurney velocity and the JWL equation of state parameters of the explosive, the radial position of the tube wall as a function of time should be known [5], [21]. Arrival times measured during the test are for the outer surface of the casing. These arrival times, initially, are used for obtaining the radial position and radial velocity of the tube after the detonation occurs and during the detonation products expand. For a relatively thin-walled cylinder, the radial expansion histogram belonging to the outer surface could be used in the rest of the calculations; in order to obtain more accurate results, however, it is proposed to use the time of arrival values for the center circle or the mid-wall of the tube [5], [6]. The radial position values for the outer surface of the tube can be converted to the

radial position values for the center circle of the tube. For this purpose, the radii of the center circle at the pin locations should be calculated.

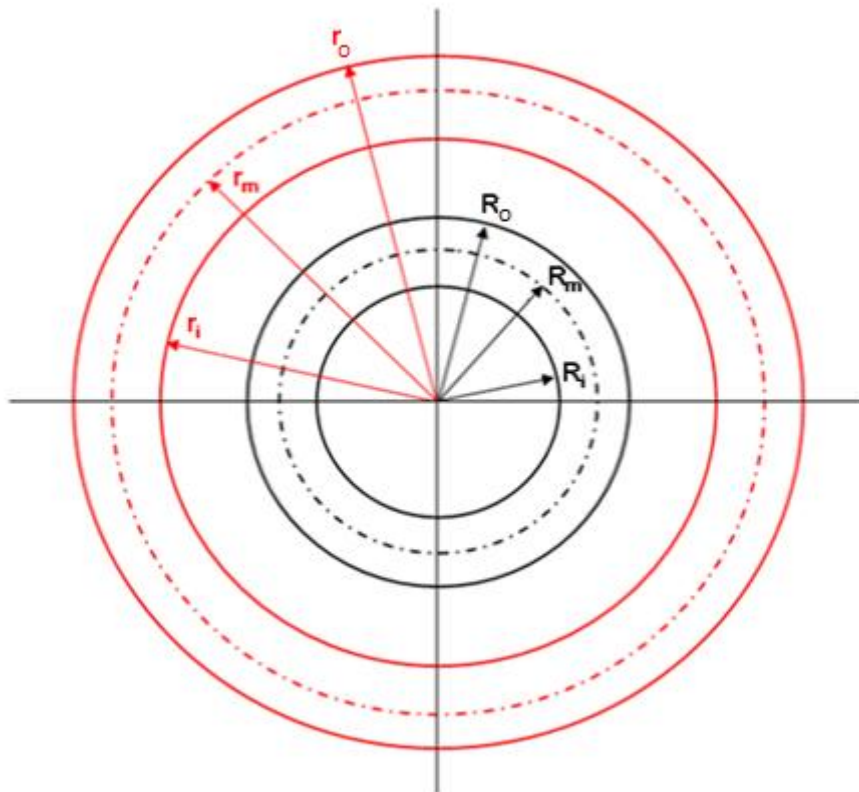


Figure 4-1 Radii at a Cross-Section of the Cylinder Casing [5]

The schematic showing a cross-section of a hollow cylinder is given in Figure 4-1. In Figure 4-1, R_i , R_o and R_m are the radii of the inner, outer and mean circles at the initial position; whereas r_i , r_o , and r_m are the radii of the inner, outer and mean circles at any time and position during the expansion of the hollow tube. In the case

of a cylinder expansion test, R_i and R_o are the inner and outer radii of the tube and hence they are known constants. When the outer casing reaches at the tip of any of the pins during expansion, the instantaneous outer radius of the casing, r_o , is the radial position, d_i , for that pin. In order to obtain the expansion histogram of the center circle, values of r_m at pin locations should be determined. As the center circle is defined as the circle which divides the cross-section to two regions having equal areas, Equation (4.1) can be written. Further, if the cross-sectional surface area is assumed to be constant during expansion, Equation (4.2) can be constructed. Then, Equation (4.3) is obtained combining Equation (4.1) and Equation (4.2)

$$\pi r_o^2 - r_m^2 = \pi r_m^2 - r_i^2 = \frac{1}{2} \pi r_o^2 - r_i^2 \quad (4.1)$$

$$\pi r_o^2 - r_i^2 = \pi R_o^2 - R_i^2 \quad (4.2)$$

$$r_o^2 - r_m^2 = \frac{1}{2} R_o^2 - R_i^2 \quad (4.3)$$

From Equation (4.3), Equation (4.4) can be written for r_m .

$$r_m = \sqrt{r_o^2 + \frac{R_i^2 - R_o^2}{2}} \quad (4.4)$$

Similarly, Equation (4.5) can be obtained for R_m .

$$R_m = \sqrt{\frac{R_i^2 + R_o^2}{2}} \quad (4.5)$$

The difference between the instantaneous radius and the initial radius values is the change in the center radius for any instant during expansion of tube. Using Equation

(4.4) and Equation (4.5), the change in the center radius during expansion in terms of known parameters can be written as:

$$\Delta r_m = r_m - R_m = \sqrt{r_o^2 + \frac{R_i^2 - R_o^2}{2}} - \frac{R_i^2 + R_o^2}{2} \quad (4.6.a)$$

Similarly, Equation (4.6.b) can also be written for Δr_m . In Equation (4.6.b), r_i is used as a parameter instead of r_o .

$$\Delta r_m = r_m - R_m = \sqrt{r_i^2 + \frac{R_o^2 - R_i^2}{2}} - \frac{R_i^2 + R_o^2}{2} \quad (4.6.b)$$

Using Equation (4.6.a), the radial position of the center circle of the tube cross-section for any radial position of the tube outer surface can be calculated. This expression can be employed in order to obtain the center circle radius for the instants when the outer surface of tube contacts with the pins. The number of radial position and arrival time values for the center circle will be equal to the number of contact pins used in the test. After these values are obtained, the radial position of the tube can be written as a continuous function of time employing curve fitting. Several forms for the radial position function are proposed in the literature. The form of the function $r(t)$ used in this study is [5];

$$\Delta r_m = a \left(t - \frac{1}{b} \right) \left(1 - e^{-bt} \right) \quad (4.7)$$

The form of the expression relating Δr_m and t is given as Equation (4.7) since it is known that this form of the equation fits the data accurately and its derivative with respect to time, which is the expression for radial velocity of the tube wall, can be obtained with ease. In this dissertation, parameters a and b used in Equation (4.7) were obtained with least squares regression since distinct values of Δr_m at different t

values are obtained from the cylinder expansion test. By taking the derivative of Equation (4.7) with respect to time, the radial expansion velocity of the tube can also be obtained as a function of time. The radial velocity, V_r can be expressed as:

$$V_r = \frac{d\Delta r_m}{dt} = a (1 - e^{-bt}) \quad (4.8)$$

Although, the tube wall velocity has a radial component after the detonation, the wall expands along an axis which is at an angle to the tube surface normal. This angle between the tube normal and expansion velocity vector of the tube wall is called the wall deflection angle or the cylinder inclination angle [5], [18], [28]. The expansion path of a single point on the cylinder wall and the wall deflection angle, θ , are illustrated in Figure 4-2 [6].

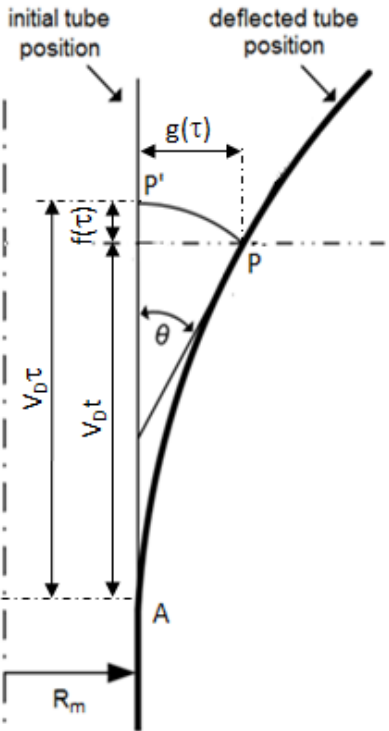


Figure 4-2 Angle of Wall Deflection [6], [28]

In Figure 4-2, the path of a point P on the cylinder wall during expansion is shown. The original location of this point before expansion is P'. A contact pin placed at point P records the time of arrival as t. During this time, the detonation front translates a distance of V_D times t [28]. Actually, the point P already starts to expand before being in contact with the pin. Therefore, the actual time of particle motion is τ , which has a larger value than t. The distance between point P' and the location of detonation front when the point P is contacted with the pin is $V_D \cdot \tau$.

If the coordinates of point P' with respect to P are defined as g and f, which are functions of τ , these parameters can be written as in Equation (4.9) and Equation (4.10).

$$g \tau = r_m t - R_m \quad (4.9)$$

$$f \tau = V_D \tau - V_D t = V_D (\tau - t) \quad (4.10)$$

Then for the wall deflection angle, θ , Equation (4.11) can be written. With manipulating and simplifying this equation, Equation (4.14) can be obtained for θ . The results obtained from the tests performed in the scope of this study have shown that the wall deflection angle, θ , is around 10° during tube expansion.

$$\tan \theta = \frac{dg \tau}{d(V_D t)} = \frac{d(r_m t - R_m)}{d(V_D t)} \quad (4.11)$$

$$\tan \theta = \frac{1}{V_D} \cdot \frac{d(r_m t)}{dt} \quad (4.12)$$

$$\tan \theta = \frac{V_r}{V_D} \quad (4.13)$$

$$\theta = \tan^{-1} \frac{V_r}{V_D} \quad (4.14)$$

As discussed before, the resultant velocity, or the true velocity, of the tube wall, V_w , has both axial and radial components. Equation (4.15) can be written for the true wall velocity [28].

$$V_w = \sqrt{\left(\frac{dg}{d\tau}\right)^2 + \left(\frac{df}{d\tau}\right)^2} \quad (4.15)$$

Equation (4.15) can be manipulated as explained below and finally Equation (4.28) can be obtained for V_w , where θ is given by Equation (4.14).

$$V_w = \sqrt{\left(\frac{dg}{dt}\right)^2 + \left(\frac{df}{dt}\right)^2} \quad (4.15)$$

$$\frac{dg}{d\tau} = \frac{d(r_m t - R_m)}{dt} \cdot \frac{dt}{d\tau} \quad (4.16)$$

$$\frac{df}{d\tau} = \frac{d(V_D(\tau - t))}{d\tau} \quad (4.17)$$

$$\frac{d\tau}{dt} = \sqrt{1 + \frac{1}{V_D^2} \left(\frac{dr_m t}{dt}\right)^2} \quad (4.18)$$

$$\frac{d\tau}{dt} = \frac{1}{\cos \theta} = \sec \theta \quad (4.19)$$

$$\frac{dt}{d\tau} = \cos \theta \quad (4.20)$$

$$\frac{dg \tau}{d\tau} = V_r \cdot \cos \theta \quad (4.21)$$

$$\frac{df \tau}{d\tau} = V_D \cdot \frac{d \tau - t}{d\tau} = V_D \cdot (1 - \cos \theta) \quad (4.22)$$

$$V_w = \sqrt{V_r \cdot \cos \theta^2 + V_D \cdot (1 - \cos \theta)^2} \quad (4.23)$$

$$V_w = \sqrt{V_D \cdot \tan \theta^2 \cdot \cos^2 \theta + V_D^2 \cdot (1 - \cos \theta)^2} \quad (4.24)$$

$$V_w = \sqrt{V_D^2 \cdot \sin^2 \theta + V_D^2 \cdot (1 - 2 \cos \theta + \cos^2 \theta)} \quad (4.25)$$

$$V_w = \sqrt{V_D^2 \cdot (2 - 2 \cos \theta)} \quad (4.26)$$

$$V_w = 4 V_D^2 \cdot \frac{1 - \cos \theta}{2} \quad (4.27)$$

$$V_w = 2 \cdot V_D \cdot \sin \frac{\theta}{2} \quad (4.28)$$

Gurney velocity and Gurney energy are two terms related with explosives named after Ronald Wilfred Gurney. In 1940s, using conservation of energy and conservation of momentum principles, R. W. Gurney suggested that, for a metal casing filled with explosive, the energy transfer from explosive to the casing after detonation of explosive is related to the metal mass to explosive mass ratio [46]. Gurney energy is a representative value for the work done by the explosive for

accelerating metal casings. Expressions relating Gurney energy, the velocity of metal wall after detonation of explosive and metal mass to explosive mass ratio based on Gurney's methodology for explosive filled casings have long been used by various researchers and authors [13], [47], [48], [49], [50]. Although Gurney velocity or Gurney constant, V_G , is considered to be equivalent of true wall velocity, V_w , by some researches [5]; in most of the sources available in the literature the Gurney velocity is defined as a property of the explosive different than the true wall velocity. The expression for the Gurney velocity is given in Equation (4.29) [35]:

$$V_G = \sqrt{2E_G} \quad (4.29)$$

Gurney energy, E_G , for a cylindrical tube filled with explosive can be calculated using the tube wall velocity at the later stages of expansion, V_w , mass of the explosive charge, C , and mass of the metal, M , in the test item. Equation (4.30) gives the Gurney energy of an explosive composition, which is filled inside a metal casing, per unit mass of explosive.

$$E_G = \frac{V_w^2}{2} \cdot \frac{M}{C} + \frac{1}{2} \quad (4.30)$$

Gurney energy is actually an intensive property for an explosive composition. However, different Gurney energy values can be calculated for different phases of the wall expansion using the wall velocity values at different points during expansion of the metal tube in Equation (4.30). Using Equations (4.7), (4.28), (4.14) and (4.30), Gurney energy of the explosive can be calculated using different wall velocities at different times during expansion of the tubes. Using the Gurney energy and the density of the explosive, one can also obtain the Gurney energy per unit volume.

The method for determining the JWL equation of state parameters of an explosive using was explained by Souers [21]. The method suggested by Souers employs an open iteration method for calculation of the parameters. This methodology is used in this study and it is explained in the following paragraphs.

As stated when describing Equation (1.1), the JWL equation of state represents the relationship between the pressure and specific volume of detonation products during the reaction and expansion of the metal casing takes place. The Chapman-Jouguet point is the condition where the velocity of the shock front reaches the detonation velocity of the explosive and the detonation is considered to reach a state of equilibrium. In the hydrodynamic theory of detonation, Equation (4.31) can be written for the pressure at the Chapman-Jouguet point [51].

$$P_{cj} = \rho_o \cdot V_D^2 \cdot 1 - v_{cj} \quad (4.31)$$

At the Chapman-Jouguet point the specific internal energy, E_s , is assumed to be the sum of the chemical energy, E_o , and the energy of compression, E_c . Therefore, Equation (4.32) can be further written for this point.

$$E_s(cj) = E_o + E_c(cj) \quad (4.32)$$

The energy of compression is the work done by compression of the gaseous products and this can be written in terms of pressure and the specific volume ratio. At the Chapman-Jouguet point;

$$E_c(cj) = \frac{1}{2} \cdot P_{cj} \cdot 1 - v_{cj} \quad (4.33)$$

By combining Equation (4.32) and Equation (4.33), the specific internal energy at the Chapman-Jouguet point can be written in terms of pressure and specific volume ratio.

$$E_S(cj) = E_o + \frac{1}{2} \cdot P_{cj} \cdot 1 - v_{cj} \quad (4.34)$$

The JWL equation of state was stated in Equation (1.1). The integral of Equation (1.1) with respect to v gives the specific internal energy, E_s , of the explosive in terms of the JWL equation of state parameters.

$$E_S = \frac{A}{R_1} \exp(-R_1 v) + \frac{B}{R_2} \exp(-R_2 v) + \frac{C}{\omega v \omega} \quad (4.35)$$

After combining the Equations (1.1) and (4.35) by eliminating parameter C , Equation (4.36) can be obtained for the pressure.

$$P = A \left[1 - \frac{\omega}{R_1 v} \right] \exp(-R_1 v) + B \left[1 - \frac{\omega}{R_2 v} \right] \exp(-R_2 v) + \frac{\omega E_S}{v} \quad (4.36)$$

It should be noted that Equation (4.36) is another form of the JWL equation of state that gives the relationship between P , v and E_s .

By combining Equations (4.32), (4.33) and (4.35), the expression for the pressure at the Chapman-Jouguet point can be written as Equation (4.37). Solving for P_{cj} in Equation (4.37), one can obtain Equation (4.38).

$$P_{cj} = A \left[1 - \frac{\omega}{R_1 v_{cj}} \right] \exp(-R_1 v_{cj}) + B \left[1 - \frac{\omega}{R_2 v_{cj}} \right] \exp(-R_2 v_{cj}) + \frac{\omega}{v_{cj}} \left[E_o + \frac{1}{2} P_{cj} (1 - v_{cj}) \right] \quad (4.37)$$

$$P_{cj} = \frac{A \left(1 - \frac{\omega}{R_1 v_{cj}}\right) \exp(-R_1 v_{cj}) + B \left(1 - \frac{\omega}{R_2 v_{cj}}\right) \exp(-R_2 v_{cj}) + \frac{\omega E_o}{v_{cj}}}{1 - \frac{\omega(1-v_{cj})}{2v_{cj}}} \quad (4.38)$$

Equations (4.31) and (4.38) are two expressions for the Chapman-Jouguet pressure for the explosive. Equation (4.31) includes the term V_D detonation velocity, and Equation (4.38) includes the term E_o , chemical energy of the explosive. These quantities can also be stated in terms of JWL equation of state parameters.

In order to express the detonation velocity in terms of the equation of state parameters; the derivate of both Equation (1.1) and Equation (4.31) can be taken with respect to v , giving Equation (4.39) and Equation (4.40), respectively. Then the resultant equations are combined. Finally Equation (4.41), an expression for detonation velocity in terms of JWL equation of state parameters and the specific volume ratio, is obtained.

$$\frac{dP}{dv} = -A R_1 \exp(-R_1 v) - B R_2 \exp(-R_2 v) - \frac{C(w+1)}{v^{(w+2)}} \quad (4.39)$$

$$\frac{dP_{cj}}{dv} = -\rho_o V_D^2 \quad (4.40)$$

$$V_D = \frac{1}{\rho_o} \frac{A R_1 \exp(-R_1 v) + B R_2 \exp(-R_2 v) + \frac{C(w+1)}{v^{(w+2)}}}{1} \quad (4.41)$$

The internal energy inside the explosive is totally transferred to the detonation products when the detonation products theoretically expand to an infinite volume [21]. Therefore the detonation energy in other words the energy of compression is equal to the chemical energy at infinity; whereas the specific internal energy of the explosive diminishes at infinity. During the expansion process of the detonation products, however, the detonation energy can be written as:

$$E_d(v) = E_O - E_S(v) \quad (4.42)$$

Combination of Equation (4.35) and Equation (4.42) gives Equation (4.43), which is the expression for chemical energy, E_d , in terms of the detonation energy and the equation of state parameters.

$$E_O = E_d(v) - \frac{A}{R_1} \exp(-R_1 v) + \frac{B}{R_2} \exp(-R_2 v) + \frac{C}{\omega v^\omega} \quad (4.43)$$

Since the energy of detonation, E_d , is mainly used for metal accelerating during a cylinder expansion test, the calculated Gurney energy values can be equated to the energy of detonation, E_d , for those points [18]. Therefore, the values of $E_d(v)$ can be calculated using Equation (4.30) and results of the cylinder expansion test for different values of specific volume ratios, v . It should be noted that for a cylinder assumed to be expanding in two dimensions, the ratio of the specific volume of gaseous products at an instant, $v(t)$, to the initial specific volume, v_0 , is equal to the square of the ratio of the radius of the cylindrical tube at that instant, r_i , to the initial radius of the tube, R_i . Since values of R_i and v_0 are known values and value of r_i at any instant can be determined using the results of the cylinder expansion test, values of v can further be calculated for any point of interest and be used in the equations.

$$v = \frac{v(t)}{v_0} = \frac{r(t)}{R_i}^2 \quad (4.44)$$

Using Equations (4.31), (4.38), (4.41) and (4.43), one can compute the equation of state parameters iteratively. For this purpose, initial guesses have to be made for the equation of state parameters. During the iterations, the difference between the P_{cj} values calculated via Equations (4.31) and (4.38), as well as the difference between V_D values calculated from Equation (4.41) and directly measured during the cylinder expansion test are tried to be minimized.

Before performing the iterations which will give the JWL equation of state parameters, initial guesses have to be made for these parameters. In order that the results converge, initial guesses for the parameters should be in the proximity of the true values of the parameters. For this purpose, the initial guesses for the parameters are taken close to known JWL parameters which are used for different explosives and available in the literature. During the iterations, parameters R_1 and R_2 are not changed. As discussed before, JWL equation of state parameters are interdependent quantities; therefore computing only A , B , C , and ω during the calculations give a set of parameters that can describe the P - v relationship of the gaseous detonation products [7], [21].

For performing the iterations that are necessary to obtain the equation of state parameters, a simple computer program has been developed for this study. At the beginning of the calculations, initial guesses are made for the JWL equation of state parameters of A , B and ω as well as the unknown value of the specific volume at the Chapman-Jouguet point, v_{cj} . Before starting the iteration loop, values of energy of detonation, E_d , are calculated for different values of v using Equations (4.7), (4.28), (4.14) and (4.30). After that, explosive chemical energy, E_o , is calculated using the initial guesses, one of the E_d values found before, the corresponding value of v and Equation (4.43).

Then, the calculations that will be performed in each iteration block begin. The pressure at Chapman-Jouguet point, P_{cj} and the new value of parameter C are calculated using Equation (4.38) and Equation (1.1), respectively. E_d values for different values of v are recalculated using new values and Equation (4.43). After that V_D is calculated using Equation (4.41). Then for comparison, value of P_{cj} is obtained using both Equation (1.1) and Equation (4.31). At the end of the calculations, the relative errors are calculated for P_{cj} and V_D . The relative error for P_{cj} is calculated using the values obtained via Equation (1.1) and Equation (4.31). The relative error for V_D is calculated by comparing the value of V_D directly

obtained from the cylinder expansion test data and the one obtained using Equation (4.31). Then the values of A, B, C and v_{cj} are changed if the calculated errors for P_{cj} and V_D are not below the previously determined tolerance value. Differences between new and old values of E_d are used while determining the new value of v_{cj} , which will be used in the next iteration. Whereas the differences between the P_{cj} and V_D values are used for obtaining the new values of A and B, respectively. Then the next step in the iterative calculations is started by recalculating the values of P_{cj} and parameter C.

In this study, the iterations have been performed until the relative errors for both the pressure at the Chapman-Jouguet point, P_{cj} , and the detonation velocity, V_D , of the explosive gets below a predetermined tolerance value. After the iterations are terminated, the value of parameter ω is recalculated employing Equation (4.45) presented by Souers [21].

$$0.7\omega = \frac{E_o - E_d(v = 10)}{E_o - E_d(v = 7)} \quad (4.45)$$

The comparison of the results with the literature values and has shown that obtained parameters are accurate enough and hence the limit value taken for the relative error is an appropriate one. Furthermore, the comparison between the tests results and analysis results were in close proximity. The flow chart for the code used for the iterative calculations is given in Figure 4-3.

The calculation steps of the JWL equation of state parameters for P-1 (TNT) using the data obtained from Test-1 is presented in more detail as a sample case in Appendix D.

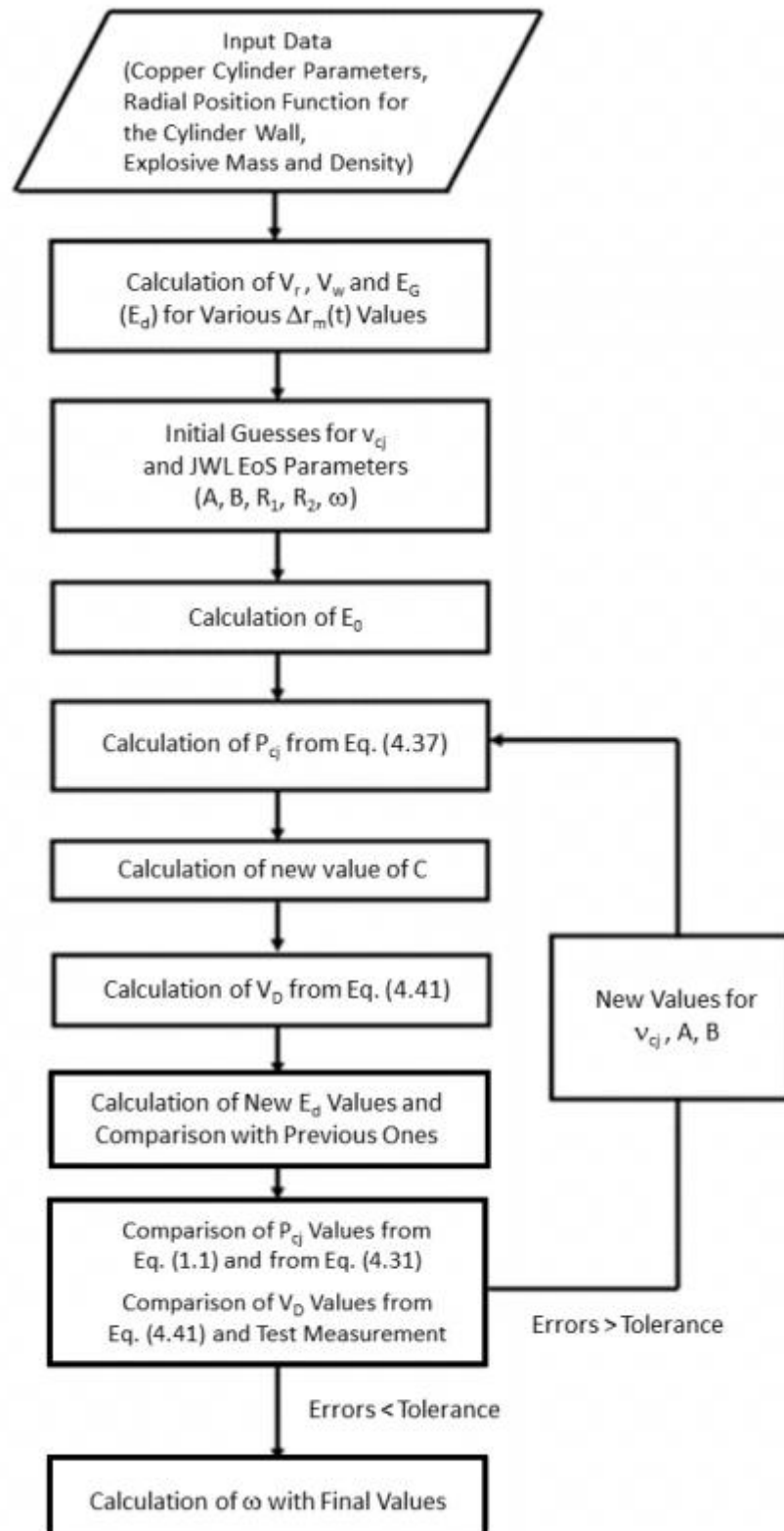


Figure 4-3 Flow Chart for the Iterative Code

CHAPTER 5

RESULT OF THE CYLINDER EXPANSION TESTS

5.1 Test Results and JWL Equation of State Parameters

In the scope of this study, cylinder expansion tests were performed for four types of explosive compositions which are designated as P-1, P-2, P-3, and P-4. The explosive designated as P-1 is TNT, which is a composition commonly used throughout the world and the JWL equation of state parameters for this composition are available in the literature. P-3 is another explosive with parameters available in the literature. One of the aims of the tests performed with P-1 and P-3 is to make a comparison with the data available in the literature and to verify that the parameters obtained using the designed setup describe the pressure - specific volume relationship of the tested explosive accurately. However, the values available in the literature may not give accurate results for P-1 and P-3 when used in analysis software due to differences in manufacturing processes and variations of the raw material components in the chemical composition. Therefore another aim of using these two explosives in the tests is to obtain the JWL equation of state parameters from the tests and use the test results instead of literature data when performing analyses in simulation software. The explosive designated as P-2 and P-4, on the other hand, are new type of compositions designed and synthesized by Roketsan. Therefore, JWL equation of state parameters of explosive P-2 and P-4 cannot be found by literature survey and hence performing cylinder expansion tests for this composition was a must. Two tests have been performed for each of the explosive materials.

Type of the explosive used in each test item configuration in the cylinder expansion tests and the corresponding explosive and copper cylinder mass values are presented in Table 5-1.

Table 5-1 Test Item Configurations in the Cylinder Expansion Tests

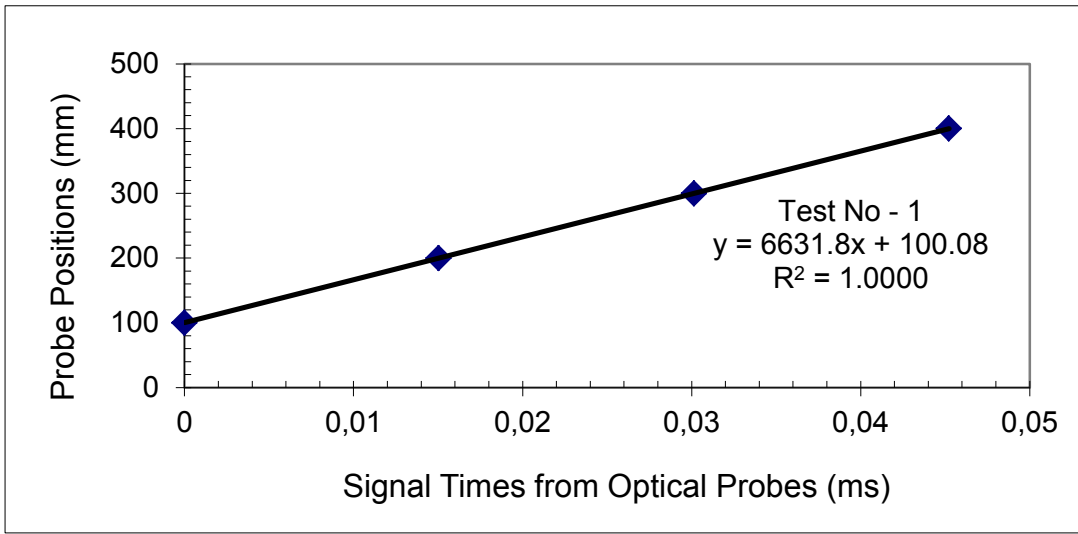
Test No.	Explosive Type	Explosive Mass (kg)	Copper Cylinder Mass (kg)
1	P-1 (TNT)	3.473	8.856
2	P-1 (TNT)	3.497	8.874
3	P-2	3.709	8.902
4	P-2	3.711	8.881
5	P-3	3.617	8.865
6	P-3	3.610	8.860
7	P-4	3.804	8.913
8	P-4	3.798	8.907

In Test-2, which was performed with P-1, the radial expansion histogram of the cylinder wall was measured with the contact pins successfully; however, the data gathered could not be recorded after the test due to a power loss in the data acquisition system. Therefore, only the velocity of detonation measurement record is available for this test. Velocity of detonation and radial wall expansion were measured and recorded successfully in the other seven tests. Another data acquisition error that was encountered during the tests was that signal could not be gathered from the tenth contact pin in Test-1; however the remaining recordings were adequate for determining the radial position function of the cylinder wall as a function of time and calculating the JWL equation of state parameters. Signal could be gathered from all contact pins in the other tests.

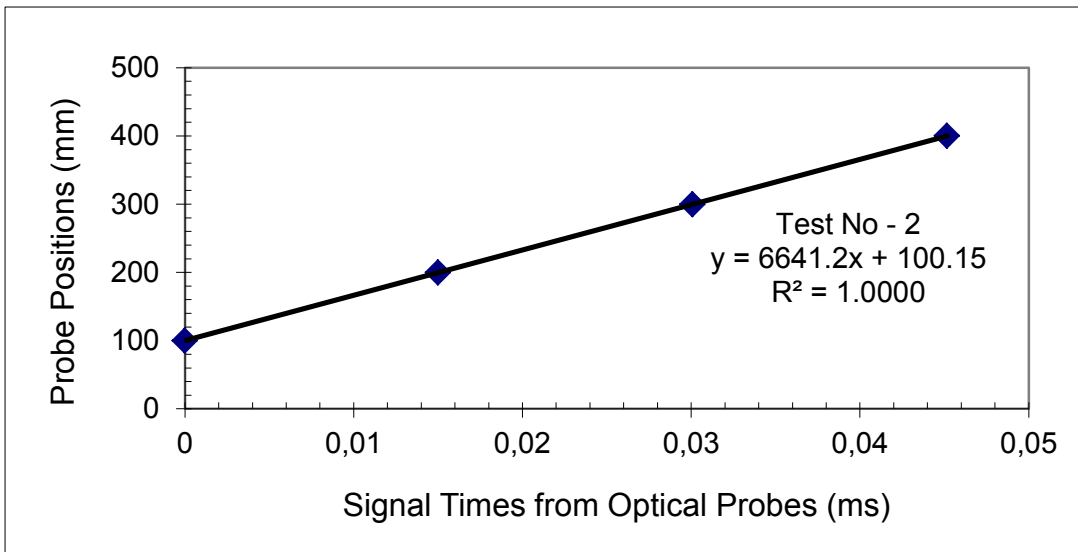
The velocity of detonation was calculated using the data gathered from the four optical probes placed along the longitudinal axis of the test item during each test. The arrival times of the detonation wave at the probe locations are presented in Table 5-2. Since data acquisition system connected to the optical probes is triggered when the first signal arrives, the arrival time of the detonation front to the first pin in each test is zero. The distance between the explosive surface where the detonation is initiated and the first optical probe location, as well as the distance between each consecutive probe is 100 mm. With the distances between pins and the signal arrival times, position curves for the detonation front with respect to time are obtained for each test employing linear curve fitting. The detonation front position versus time charts obtained for the explosive compositions P-1, P-2, P-3 and P-4 are presented in Figure 5-1, Figure 5-2, Figure 5-3 and Figure 5-4, respectively. The slopes of these curves are the detonation velocity values for the explosives obtained from the corresponding test. Detonation velocity values calculated using the data gathered from the tests are given in Table 5-3.

Table 5-2 Signal Times at Longitudinally Placed Optical Probes

Test No.	Explosive Type	Detonation Front Arrival Time (μ s)			
		First Probe	Second Probe	Third Probe	Fourth Probe
1	P-1 (TNT)	0	15.05	30.15	45.24
2	P-1 (TNT)	0	15.01	30.08	45.14
3	P-2	0	14.30	28.43	42.51
4	P-2	0	14.04	28.38	42.46
5	P-3	0	13.50	27.50	41.39
6	P-3	0	13.20	27.10	40.80
7	P-4	0	13.70	27.70	41.20
8	P-4	0	13.70	27.40	41.31

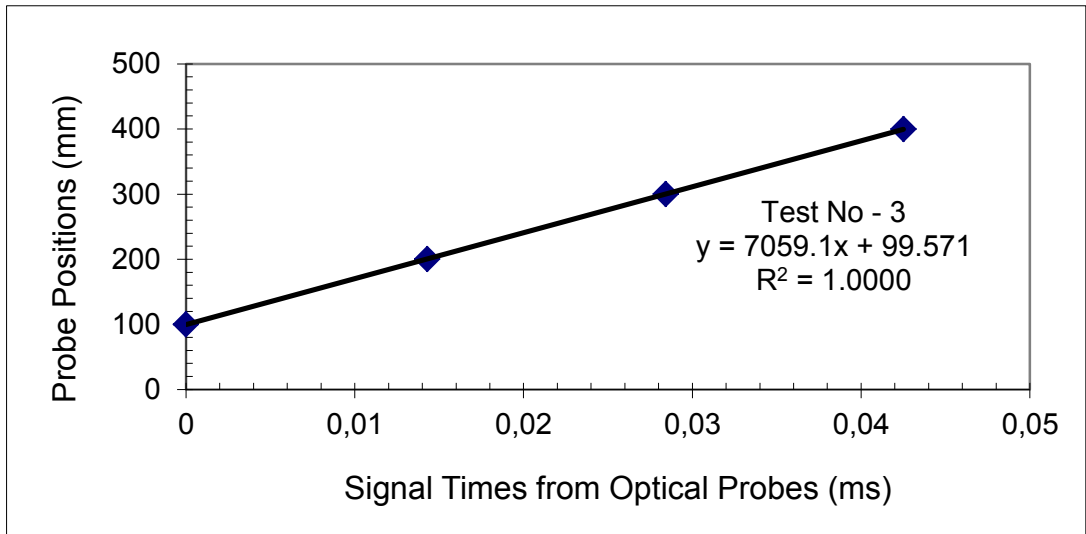


(a)

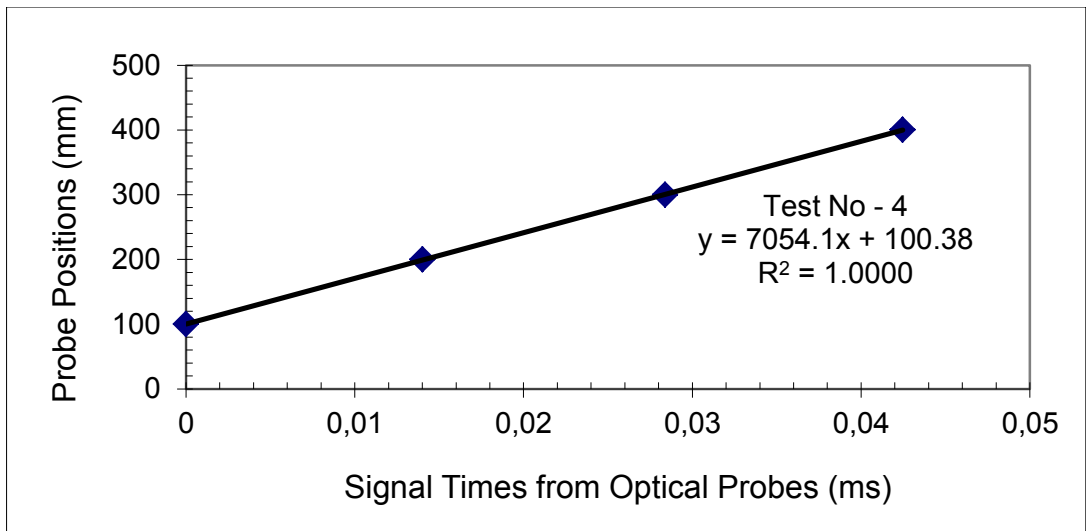


(b)

Figure 5-1 Position vs Time Charts for the Detonation Front for P-1
 (a) Results of Test-1 (b) Results of Test-2

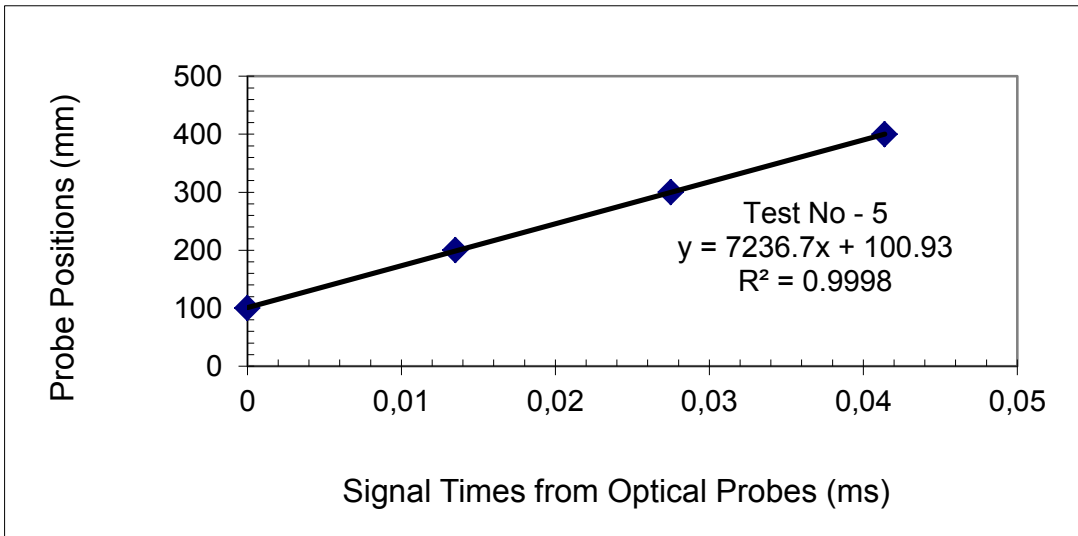


(a)

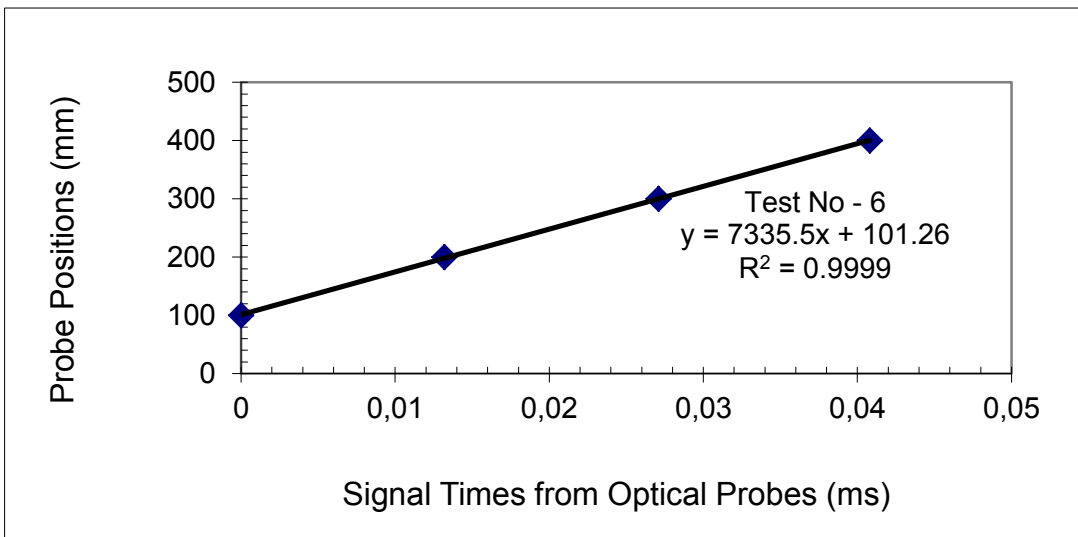


(b)

Figure 5-2 Position vs Time Charts for the Detonation Front for P-2
 (a) Results of Test-3 (b) Results of Test-4

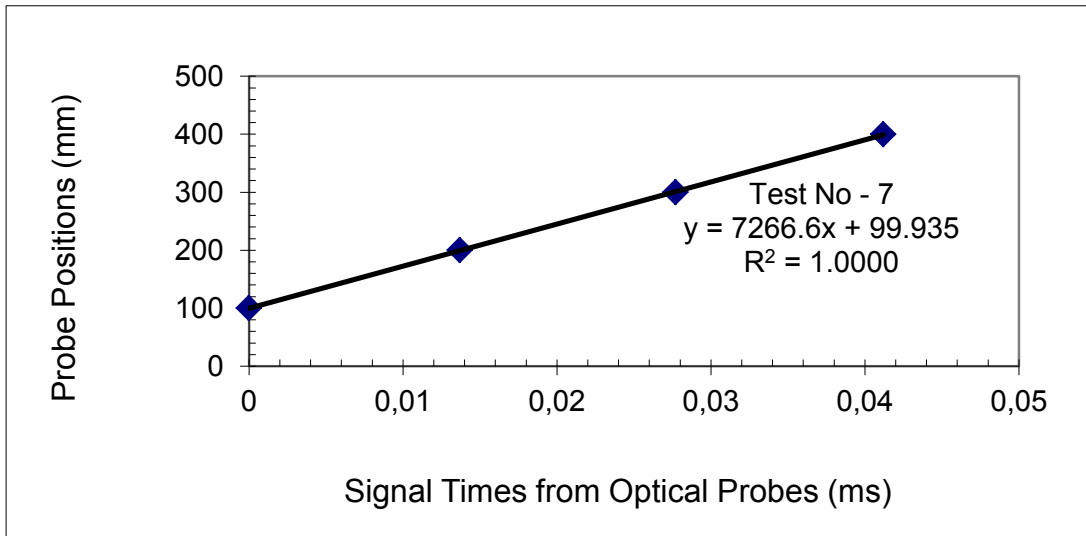


(a)

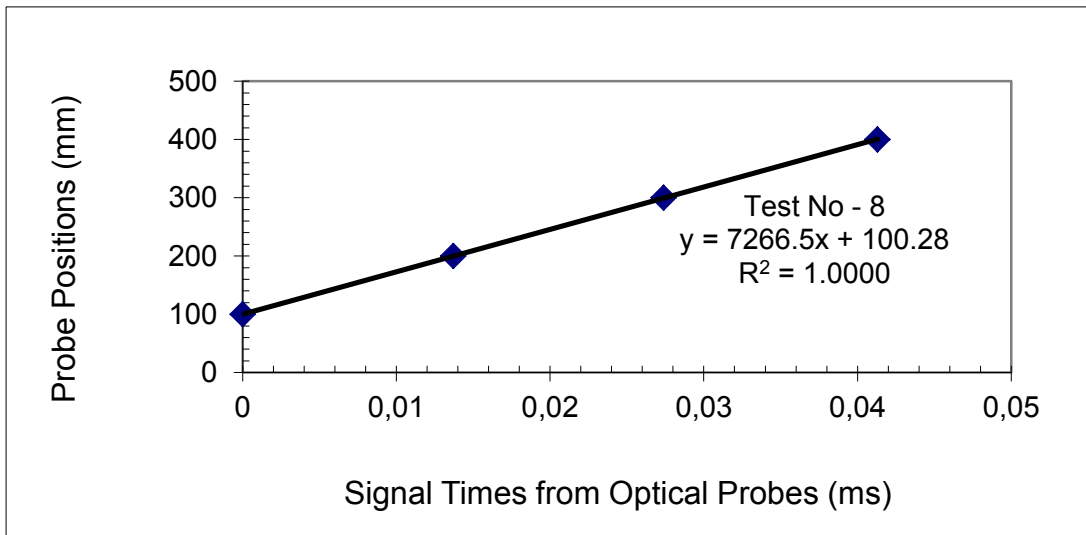


(b)

Figure 5-3 Position vs Time Charts for the Detonation Front for P-3
 (a) Results of Test-5 (b) Results of Test-6



(a)



(b)

Figure 5-4 Position vs Time Charts for the Detonation Front for P-4
 (a) Results of Test-7 (b) Results of Test-8

Table 5-3 Velocity of Detonation Values for Explosives

Test No.	Explosive	Velocity of Detonation (V_D) (m/s)
1	P-1 (TNT)	6632
2	P-1 (TNT)	6641
3	P-2	7059
4	P-2	7054
5	P-3	7237
6	P-3	7335
7	P-4	7273
8	P-4	7268

Since explosive property data is available for P-1 in several publications, the velocity of detonation obtained from the test can be compared with literature data. The average value of the velocity of detonation of explosive composition P-1 obtained from Test-1 and Test-2 is 6636 m/s. The velocity of detonation for P-1 is given to be about 6900 - 6950 m/s [10], [13], [32], [52], [53]. The velocity of detonation value obtained from the test is approximately 4% lower than the values provided in the literature. However, the velocity of detonation is greatly dependent on the density of the explosive block and the density of the composition used in the test was 2.5% lower than the explosive density values in the literature. Moreover, detonation velocity may vary according to various factors such as proportions of the components in the chemical composition of the explosive within the tolerances, manufacturing process of explosive and filling methodology of explosive into the casing. Therefore a difference of 4% is an acceptable error for the velocity of detonation. When the detonation velocity values obtained for P-3 via the tests are compared with the values available in the open sources, it was seen that a relative

error very similar to that in the case of P-1 is present between the test results and literature data.

The JWL equation of state parameters for the explosive compositions are calculated as discussed in Chapter 4. Cylinder wall expansion data gathered during the tests utilizing the contact pins are used for this purpose. The signals obtained via the contact pins are recorded in the data acquisition system during the tests. The screen captures of the recordings taken by the data acquisition system for Test-1 and Tests-3 to 8 are shown in Figure 5-5 to Figure 5-11. Since contact pin data could be gathered but not be saved after Test-2, the recording for this test could not be presented nor used for calculations of equation of state parameters. Each peak in the recordings indicates the signal time for a different pin. The software of the data acquisition system enables to track values from any data point on the curve. Therefore the contact times of the cylinder wall with each contact pin could be obtained from the signal recording curves. The radial positions of the contact pin tips and the arrival times for each test are presented in Table 5-4. The presented arrival times are normalized such that the arrival time for the first pin is equated to zero.

As discussed before, data could not be gathered from the tenth contact pin in Test-1; however, the rest of the pins produced signals and the data gathered from these pins was sufficient for obtaining the radial position and velocity functions for the cylinder wall.

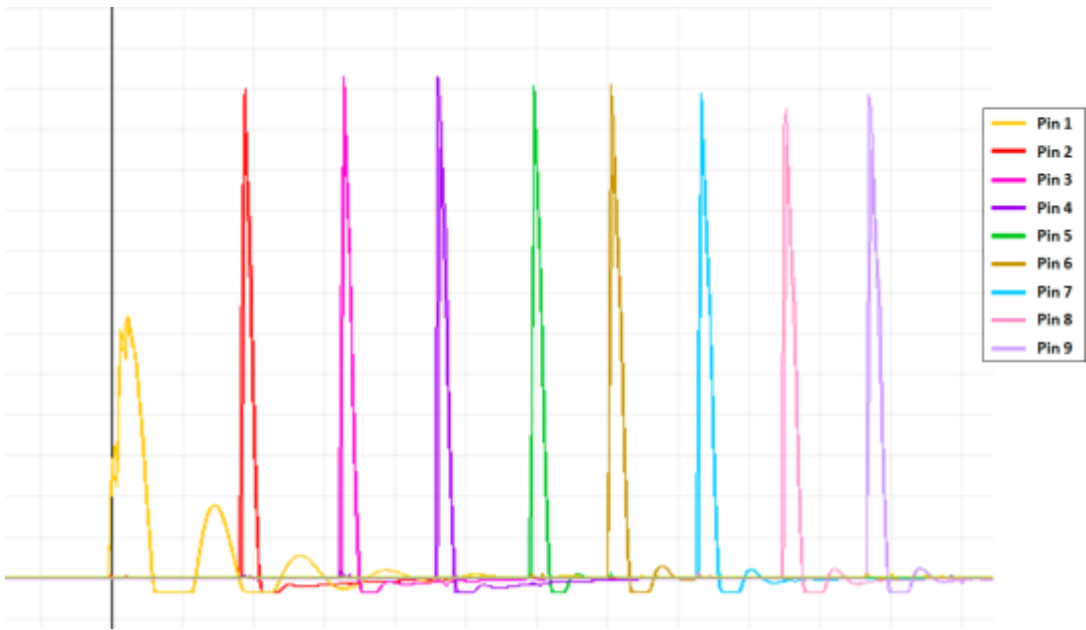


Figure 5-5 Contact Pin Signal Record for Test-1

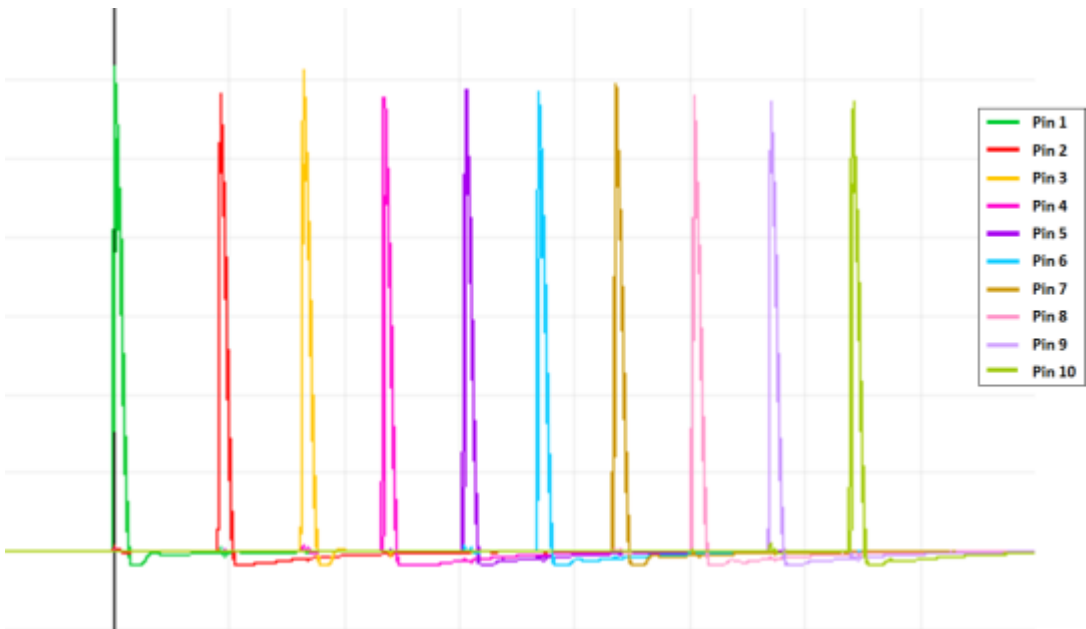


Figure 5-6 Contact Pin Signal Record for Test-3

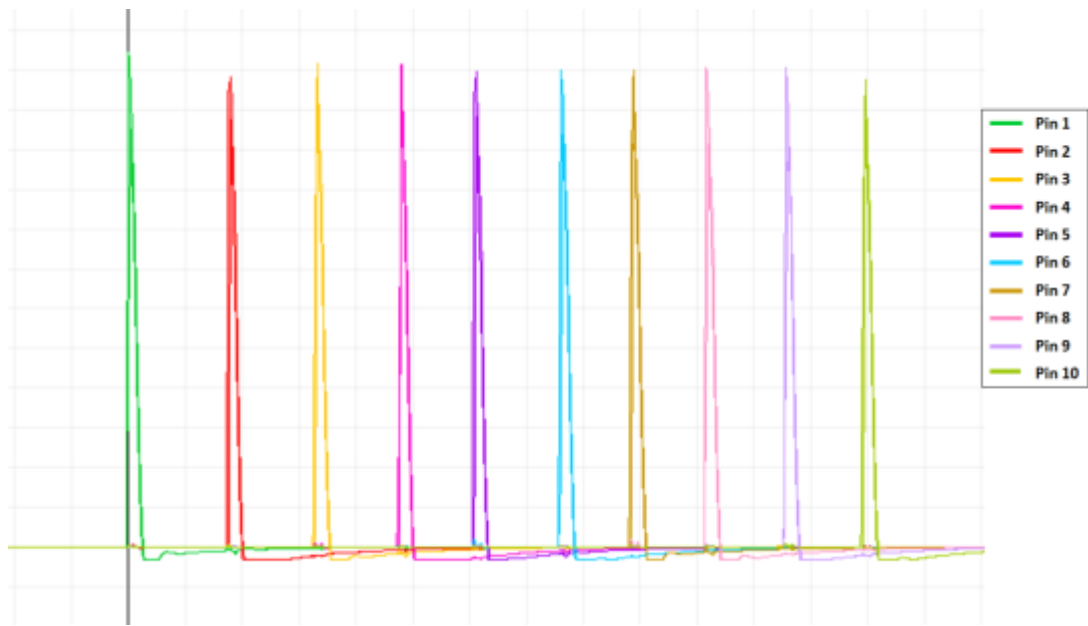


Figure 5-7 Contact Pin Signal Record for Test-4

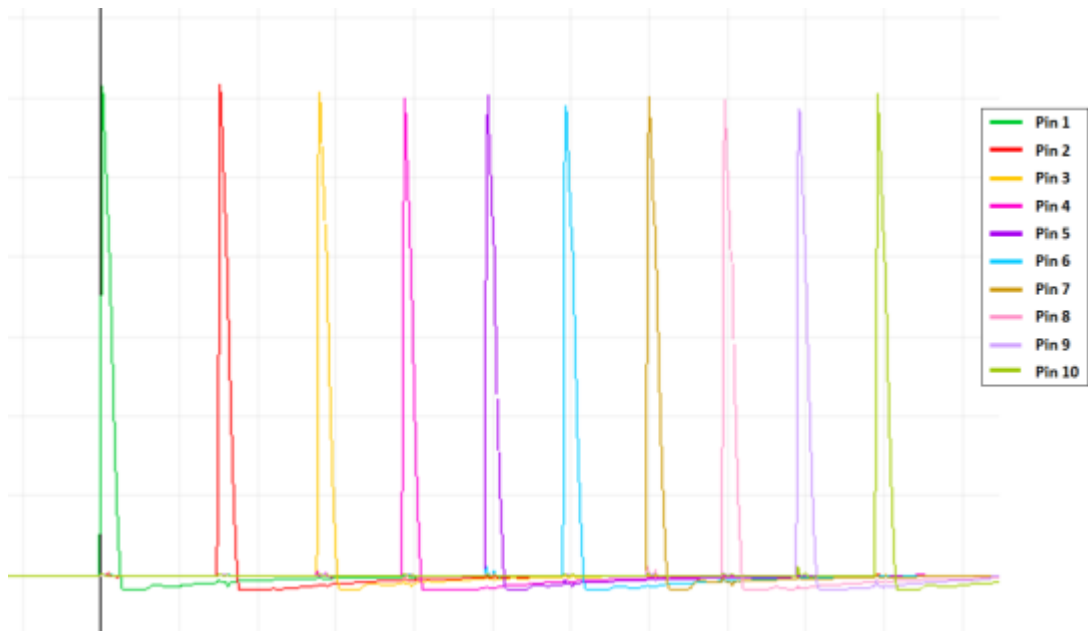


Figure 5-8 Contact Pin Signal Record for Test-5

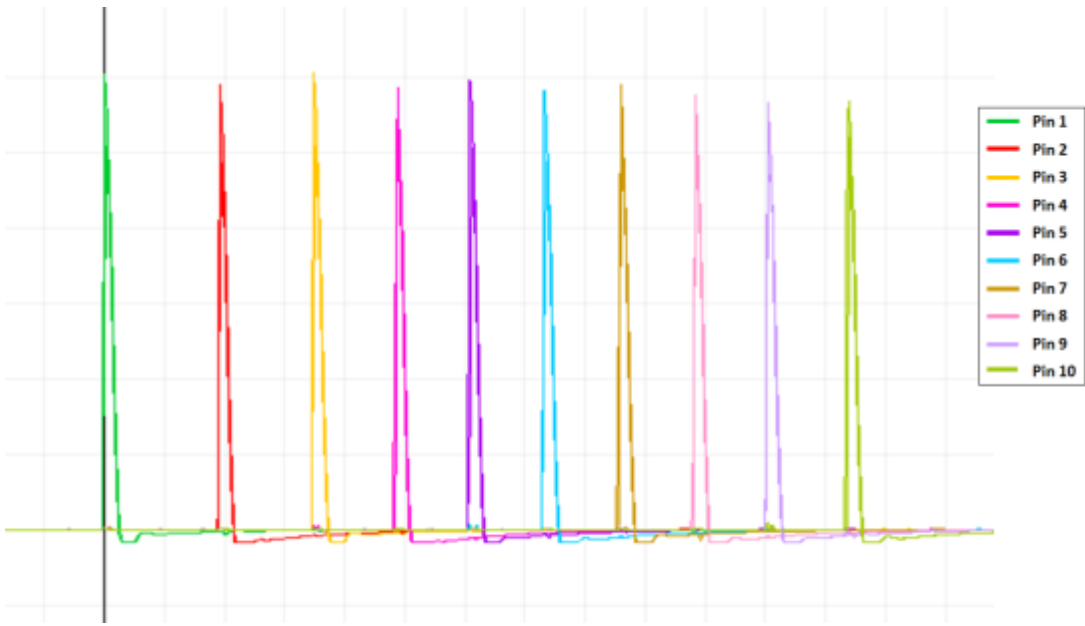


Figure 5-9 Contact Pin Signal Record for Test-6

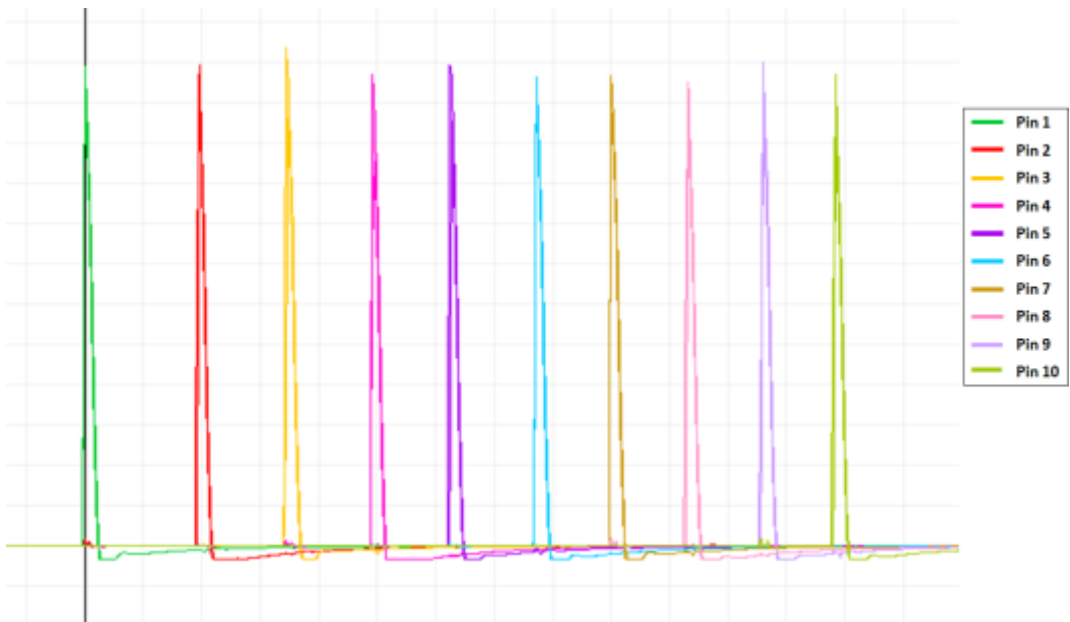


Figure 5-10 Contact Pin Signal Record for Test-7

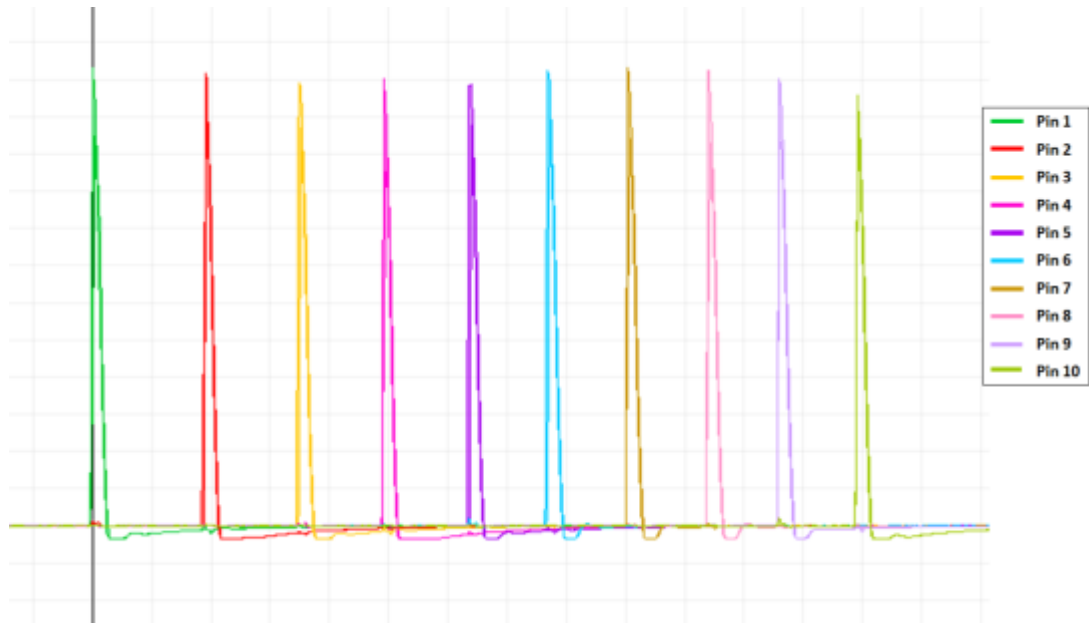


Figure 5-11 Contact Pin Signal Record for Test-8

Table 5-4 Pin Arrival Times

Pin No	Radial Position of the Pin Tip (d) (mm)	$t_{pin} - t_{pin_1}$ (μs)						
		Test-1	Test-3	Test-4	Test-5	Test-6	Test-7	Test-8
1	0.10	0.0	0.0	0.0	0.0	0.0	0.0	0.0
2	8.10	9.3	9.2	8.9	9.5	9.6	9.7	9.5
3	16.10	16.3	16.4	16.5	17.3	17.4	17.2	17.4
4	24.10	23.1	23.4	23.9	24.2	24.3	24.6	24.6
5	32.10	29.7	30.5	30.5	30.4	30.4	31.2	31.9
6	40.10	35.2	36.8	38.0	36.8	36.6	38.5	38.4
7	48.10	41.5	43.5	44.3	42.7	42.9	45.0	45.2
8	56.10	47.5	50.3	50.8	49.1	49.1	51.5	52.0
9	64.10	53.4	57.0	57.8	55.0	55.2	57.9	58.0
10	72.10	-	64.1	64.7	61.6	61.9	64.1	64.5

Δr_m values for the pin locations are calculated as explained in Chapter 4. Then the radial position function of the cylinder wall is obtained as a function of time using Δr_m values and times of arrival. Contact pin data and the curve of the radial position function of cylinder wall for Test-1 are presented in Table 5-5 and Figure 5-12, respectively. The expression for radial position function of cylinder wall presented in Figure 5-12 is in the form of Equation (4.7). The values of constants a and b with their units are 1271.697 mm/ms and 212.684 ms⁻¹, respectively. These constants were obtained using least squares regression. The coefficient of determination, R^2 , which indicates how well the obtained regression curve represents the data, is calculated to be 0.9994 for Test-1 as seen in the curve presented in Figure 5-12. The coefficient of determination for this curve was calculated with a polynomial regression assumption, although the regression curve is a nonlinear one. After obtaining the radial wall position as a function of time, the Gurney velocity and JWL equation of state parameters for explosive composition P-1 were calculated as explained in Chapter 4.

Table 5-5 Pin Data for Test-1

Pin No.	Time of Arrival (ms)	$t_{pin} - t_{pin_1}$ (ms)	d (mm)	d-d₁ (mm)	r_y (mm)	Δr_m (mm)
1	241914.9363	0.0000	0.10	0.00	36.10	0.0932
2	241914.9456	0.0093	8.10	8.00	44.10	7.6382
3	241914.9526	0.0163	16.10	16.00	52.10	15.3145
4	241914.9594	0.0231	24.10	24.00	60.10	23.0730
5	241914.9660	0.0297	32.10	32.00	68.10	30.8863
6	241914.9715	0.0352	40.10	40.00	76.10	38.7377
7	241914.9778	0.0415	48.10	48.00	84.10	46.6167
8	241914.9838	0.0475	56.10	56.00	92.10	54.5164
9	241914.9897	0.0534	64.10	64.00	100.10	62.4319

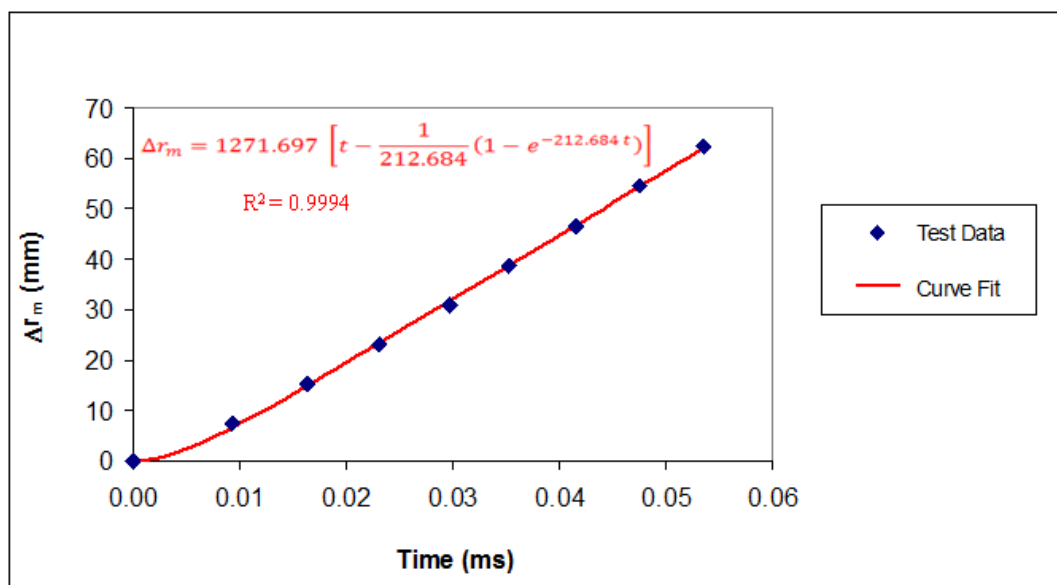


Figure 5-12 Radial Position of Cylinder Wall with Respect to Time for Test-1

The JWL equations of state parameters for explosive composition P-1 obtained via the cylinder expansion tests and the literature data for this explosive are presented in Table 5-6. As well as the results obtained from the cylinder expansion tests, the value of the density of the explosive, which is calculated before the tests, is also given in this table since the density of the explosive is usually presented as a part of this set in various literature sources. Since the JWL equation of state can be used to obtain pressure versus specific volume ratio of explosives, P-v curves could be generated using both the test results and the literature data. It is more appropriate to compare the P-v curves obtained using the JWL equation of state parameters rather than the parameters themselves due to the fact that more than one set can be obtained in order to describe the behaviour of a single explosive material. Comparison of the curves based on the tests and the literature data is provided in Figure 5-13.

Pressure values for selected values of specific volume ratio read from the two curves are presented in Table 5-7. Relative differences between the results based on test data and the values based on the literature values are also given in this table. The curve based on the cylinder expansion test results is in good agreement with the curves obtained using the literature data for specific volume ratio values lower than 1 and higher than 3. There are deviations in pressure values based on the test results and based on literature data for specific volume ratios around 2. The main reason of this difference is the effect of parameter B, which is the main parameter that defines the behaviour for moderate specific volume ratio values. Since parameter B obtained from the test results is relatively higher than the values in the literature, pressure values obtained for moderate specific volume ratios are also higher.

Such differences between the values are acceptable since the JWL parameters and properties for an explosive is dependent on many factors including the raw explosive material manufacturing processes, casting process of the explosive into the casing, the bulk density of the casted explosive, etc. At several points, the relative difference between the pressure values obtained based on two different literature data sets also reach approximately 55%. Actually, the presence of these differences is one of the reasons for performing cylinder expansion tests for explosive compositions with JWL data available in the literature. Therefore it can be concluded that such a difference between the P-v curves is acceptable and the designed setup is a reliable one for obtaining the JWL equation of state parameters of explosives.

Table 5-6 Properties Including JWL Equation of State Parameters for P-1

Parameter/ Property	Unit	Test-1	Literature Value [52]	Literature Value [53]
V_D	m/s	6632	6900	6930
V_G	m/s	2348	-	2440
ρ	g/cm^3	1.59	1.63	1.63
E_o	kJ/m^3	5.675×10^6	6.000×10^6	7.000×10^6
P_{cj}	kPa	2.033×10^7	2.100×10^7	2.100×10^7
A	kPa	4.531×10^8	3.738×10^8	3.712×10^8
B	kPa	1.560×10^7	3.747×10^6	3.231×10^6
C	kPa	5.765×10^5	7.340×10^5	1.045×10^6
R_1	-	5.15	4.15	4.15
R_2	-	1.00	0.90	0.95
ω	-	0.344	0.350	0.300

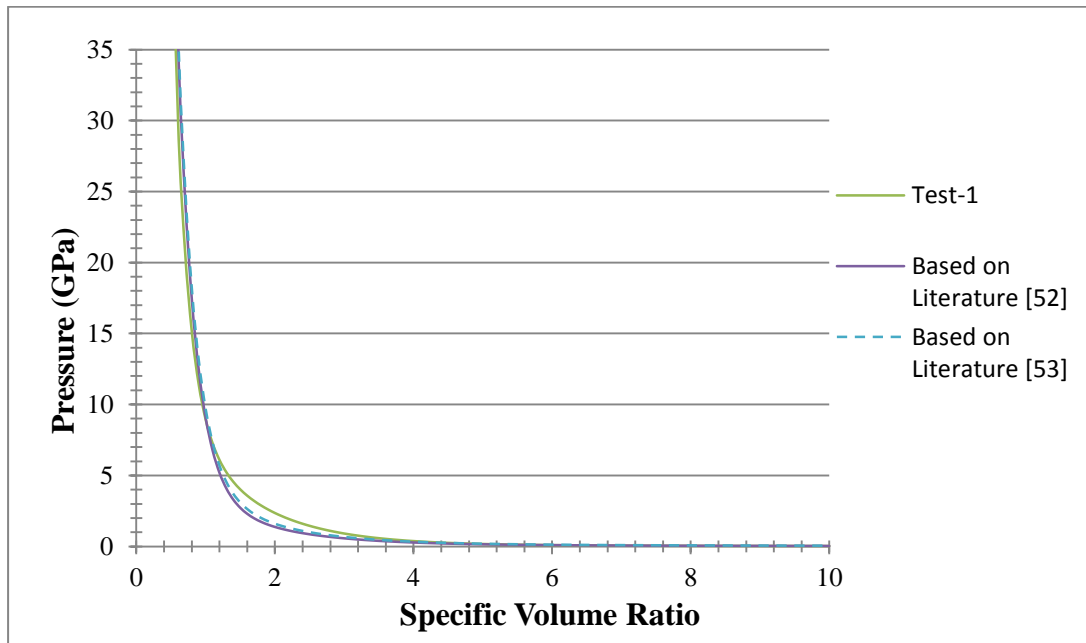


Figure 5-13 Comparison of P-v Curves for P-1 Obtained from Test Results and Literature Data

Table 5-7 Comparison of Pressures at Selected Specific Volume Ratios for P-1

v	P (GPa) (based on Test-1)	P (GPa) (based on Ref. [52])	Relative Difference (Test-1 and Ref. [52])	P (GPa) (based on Ref. [53])	Relative Difference (Test-1 and Ref. [53])	Relative Difference (Ref. [52] and Ref. [53])
0.2	179.481	174.453	3%	176.309	2%	1%
0.4	70.168	77.789	11%	78.965	11%	2%
0.8	15.146	17.426	15%	18.198	18%	4%
1.2	6.088	5.181	15%	5.689	7%	10%
1.6	3.577	2.299	36%	2.634	36%	15%
2.0	2.355	1.373	42%	1.598	47%	16 %
2.4	1.596	0.935	41%	1.092	46%	17%
3.2	0.758	0.490	35%	0.577	31%	18%
4.0	0.376	0.277	26%	0.334	13%	22%
6.0	0.091	0.092	1%	0.126	27%	36%
8.0	0.041	0.049	18%	0.074	44%	51%
10.0	0.027	0.034	22%	0.053	48%	58%

Two tests were performed for each of the remaining three explosives, which are P-2, P-3 and P-4. In a similar approach to the one followed for explosive P-1, the properties and JWL equation of state parameters for these explosive compositions were also determined using the raw data obtained from the cylinder expansion tests. Since data could be gathered from the two tests were performed employing P-2, P-3 and P-4, two sets of parameters could be obtained for these explosive compositions. The time of arrival values measured by contact pins for the tests were given in Table 5-4. The properties and equation of state parameters for P-2, P-3 and P-4 are presented in Table 5-8, Table 5-9 and Table 5-10, respectively. The relative differences between the results of two tests performed for each explosive are also shown on these tables. The P-v curves for P-2, P-3 and P-4 generated using the data

gathered from the corresponding tests are presented in Figure 5-14, Figure 5-15 and Figure 5-16, respectively. The parameters obtained using the data of both tests for each explosive are relatively close. The P-v curves based on two different tests for each explosive material are also very close to each other. Hence the repeatability of the tests with the design setup could be ensured.

Table 5-8 Properties Including JWL Equation of State Parameters for P-2

Parameter / Property	Unit	Test-3	Test-4	Relative Difference Between Two Test Results
a	mm/ms	1157.291	1140.117	1%
b	1/ms	305.386	307.952	1%
V _D	m/s	7059	7054	0.1%
V _G	m/s	2032	1995	2%
ρ	g/cm ³	1.66	1.66	0.0%
E _o	kJ/m ³	4.892 x 10 ⁶	4.771 x 10 ⁶	2 %
P _{cj}	kPa	1.892 x 10 ⁷	1.856 x 10 ⁷	2%
A	kPa	1.813 x 10 ⁸	1.883 x 10 ⁸	4%
B	kPa	2.217 x 10 ⁷	2.098 x 10 ⁷	5%
C	kPa	6.247 x 10 ⁵	5.830 x 10 ⁵	7%
R ₁	-	6.623	6.623	0.0%
R ₂	-	1.367	1.367	0.0%
ω	-	0.137	0.136	1%

Table 5-9 Properties Including JWL Equation of State Parameters for P-3

Parameter / Property	Unit	Test-5	Test-6	Relative Difference Between Two Test Results
a	mm/ms	1148.241	1244.117	8%
b	1/ms	184.980	187.604	1%
V _D	m/s	7273	7335	1%
V _G	m/s	2175	2183	0.4%
ρ	g/cm ³	1.62	1.62	0.0%
E _o	kJ/m ³	5.431 x 10 ⁶	5.453 x 10 ⁶	0.4%
P _{cj}	kPa	2.009 x 10 ⁷	2.104 x 10 ⁷	5%
A	kPa	1.362 x 10 ⁹	1.376 x 10 ⁹	1%
B	kPa	2.384 x 10 ⁷	2.391 x 10 ⁷	0.3%
C	kPa	8.464 x 10 ⁵	8.476 x 10 ⁵	0.1%
R ₁	-	6.250	6.261	0.2%
R ₂	-	1.350	1.344	0.4%
ω	-	0.170	0.170	0.0%

Table 5-10 Properties Including JWL Equation of State Parameters for P-4

Parameter / Property	Unit	Test-7	Test-8	Relative Difference Between Two Test Results
a	mm/ms	1167.926	1162.189	0.5%
b	1/ms	217.089	214.586	1%
V _D	m/s	7273	7268	0.1%
V _G	m/s	2050	2070	1%
ρ	g/cm ³	1.70	1.70	0.0%
E _o	kJ/m ³	4.977 x 10 ⁶	4.910 x 10 ⁶	1%
P _{cj}	kPa	1.967 x 10 ⁷	1.938 x 10 ⁷	1%
A	kPa	2.143 x 10 ⁹	2.064 x 10 ⁹	4%
B	kPa	2.152 x 10 ⁷	2.138 x 10 ⁷	1%
C	kPa	1.213 x 10 ⁶	1.238 x 10 ⁶	2%
R ₁	-	6.64	6.64	0.0%
R ₂	-	1.37	1.37	0.0%
ω	-	0.134	0.134	0.0%

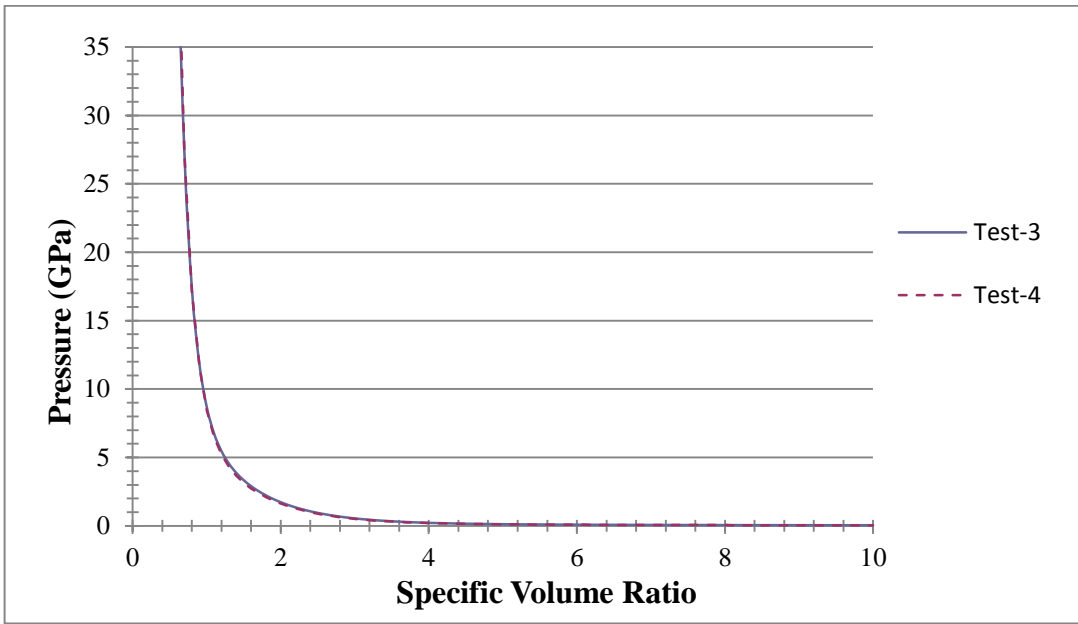


Figure 5-14 Comparison of P-v Curves for P-2 Obtained from Test-3 and Test-4

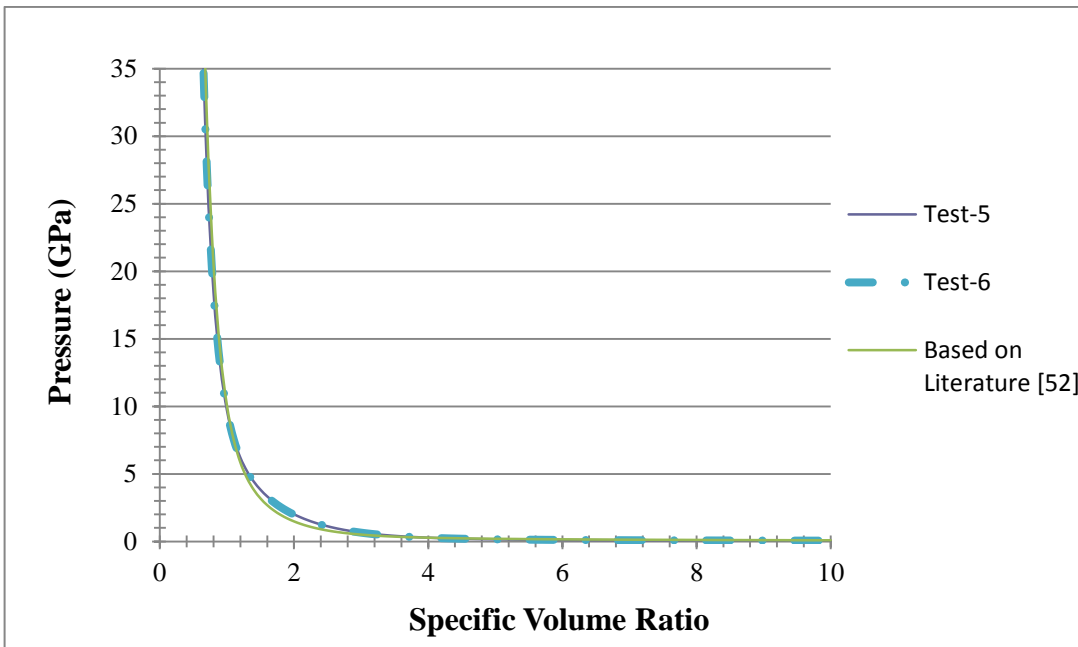


Figure 5-15 Comparison of P-v Curves for P-3 Obtained from Test-5 and Test-6

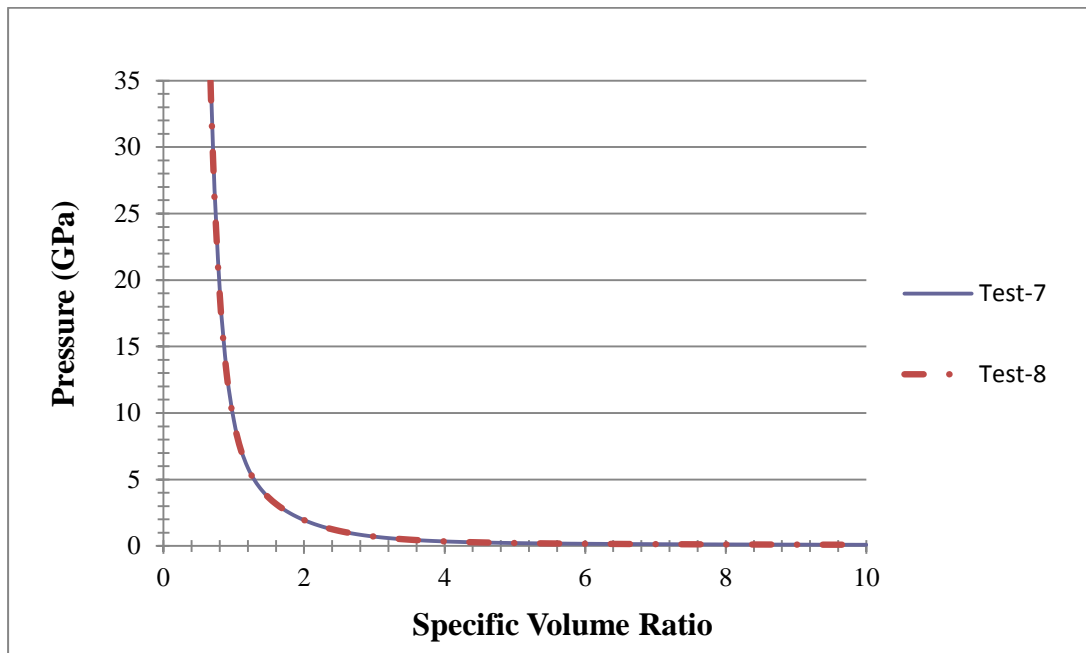


Figure 5-16 Comparison of P-v Curves for P-4 Obtained from Test-7 and Test-8

Since the explosive P-3 is a material with available parameters in the literature, like P-1, the P-v curve based on the literature data could also be obtained for this explosive and it is presented for comparison in Figure 5-15. As presented for P-1 before, pressure values for several values for specific volume ratio are tabulated and given in Table 5-11. It can be seen that, the relative differences for pressure values based on test results and literature data set for P-3 are smaller while v is around 2 when compared to the relative differences calculated for P-1. The relative difference between the values gets larger for higher values of v . However, the absolute difference between the values are not too high since the pressure drops at higher values of specific volume ratio. As discussed before, the relative differences are within an acceptable margin.

Table 5-11 Comparison of Pressures at Selected Specific Volume Ratios for P-3

v	P (GPa) (based on Ref. [52])	P (GPa) (based on Test-5)	relative difference (Test-5 and Ref [52])	P (GPa) (based on Test-6)	relative difference (Test-5 and Ref [53])
0.2	436.009.	417.210	5%	413.982	5%
0.4	141.603	128.896	10%	128.165	10%
0.8	20.530	18.449	11%	18.372	12%
1.2	5.844	6.202	6%	6.155	5%
1.6	2.685	3.334	19%	3.300	19%
2.0	1.482	2.008	26%	1.983	25%
2.4	0.902	1.255	28%	1.238	27%
3.2	0.433	0.542	20%	0.534	19%
4.0	0.277	0.278	0%	0.275	1%
6.0	0.156	0.112	28%	0.111	29%
8.0	0.110	0.074	32%	0.075	32%
10.0	0.084	0.057	32%	0.057	32%

The pressure versus specific volume ratio curves obtained from the seven tests are presented in a single graph in Figure 5-17. Several sections of this graph are presented for smaller specific volume ratio intervals in Figures 5-18 to 5-22 for distinguishing different curves more clearly. One can compare the pressure values for different stages of the expansion of the detonation products by examining these figures.

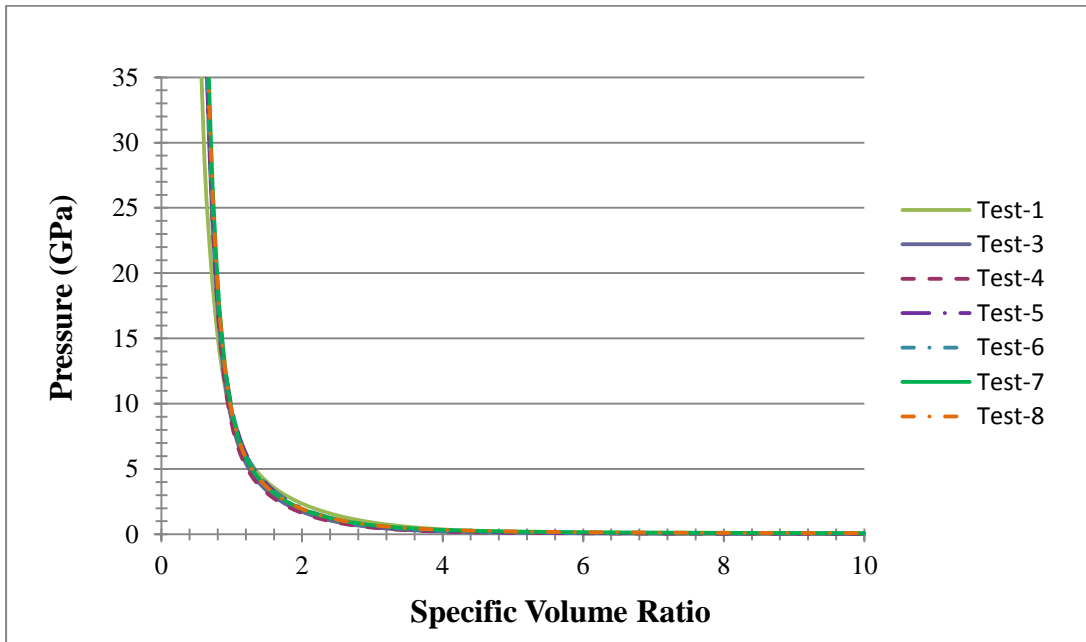


Figure 5-17 Comparison of P-v Curves among the Seven Tests

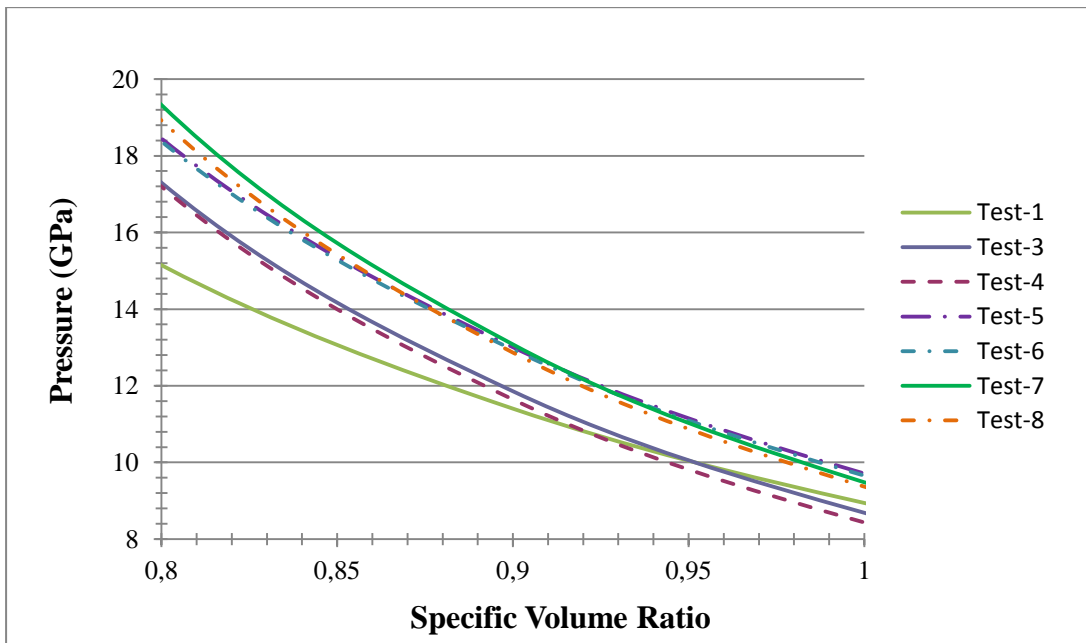


Figure 5-18 Comparison of P-v Curves (for $0.8 < v < 1$)

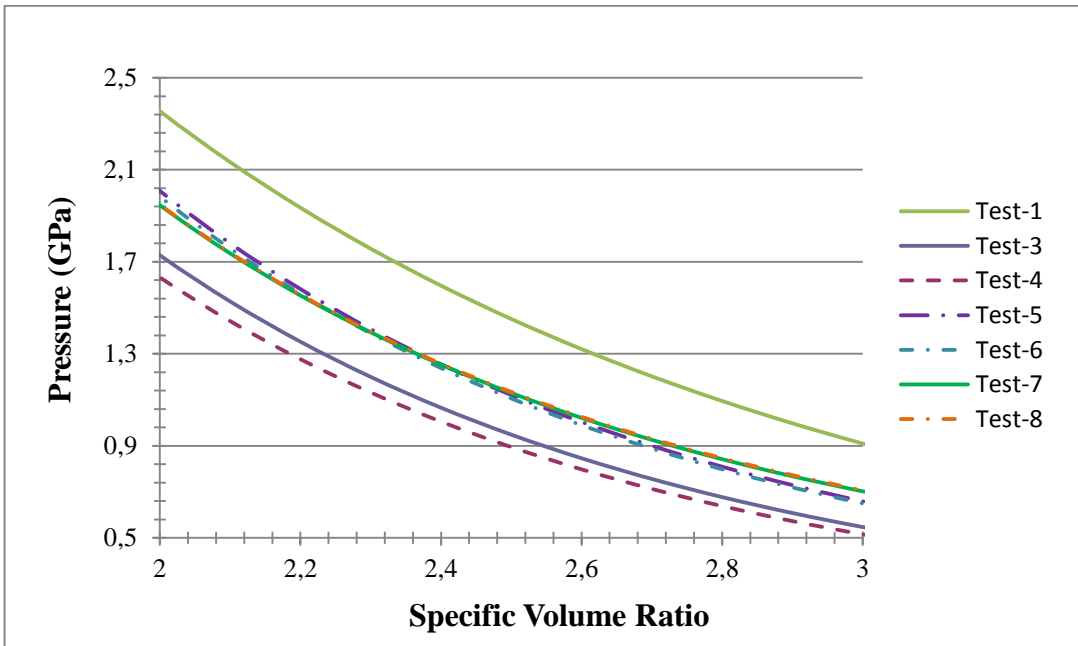


Figure 5-19 Comparison of P-v Curves (for $2 < v < 3$)

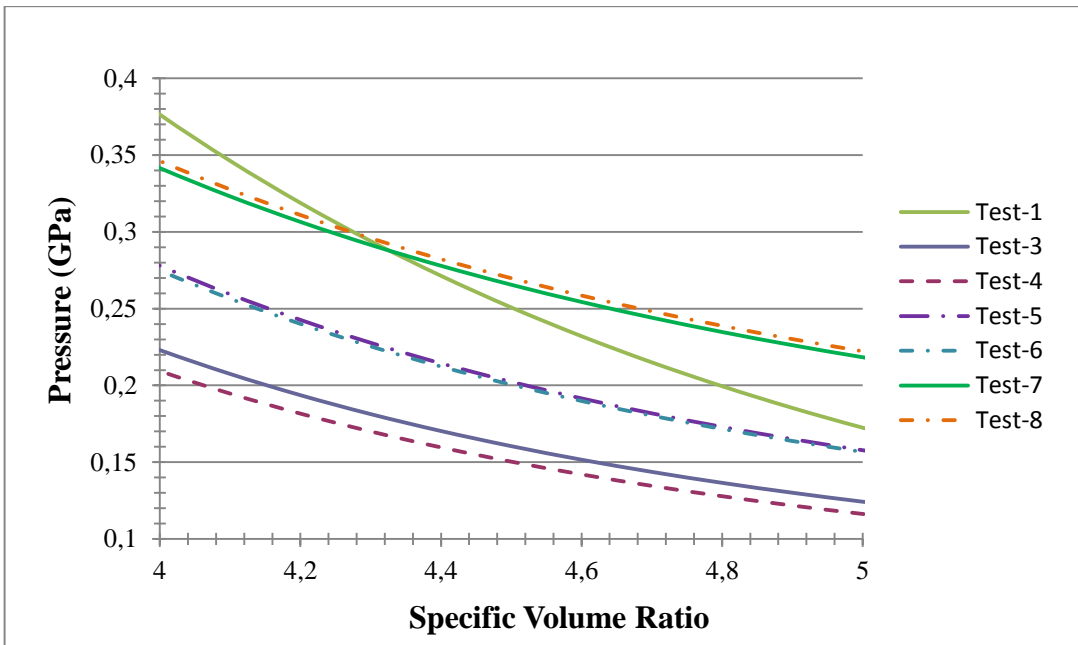


Figure 5-20 Comparison of P-v Curves (for $4 < v < 5$)

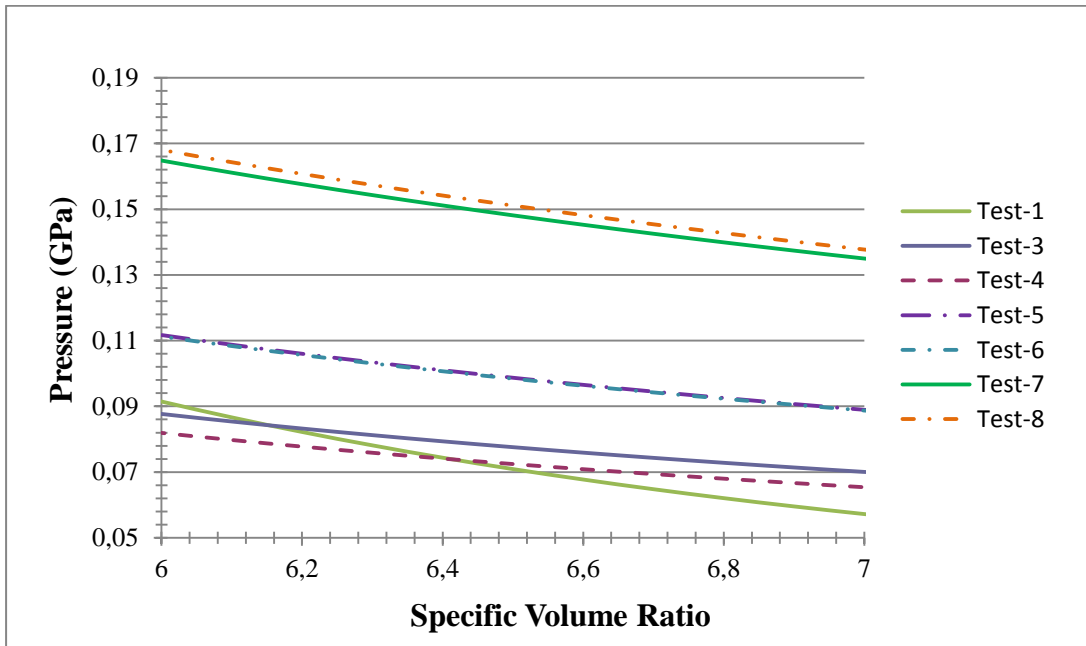


Figure 5-21 Comparison of P-v Curves (for $6 < v < 7$)

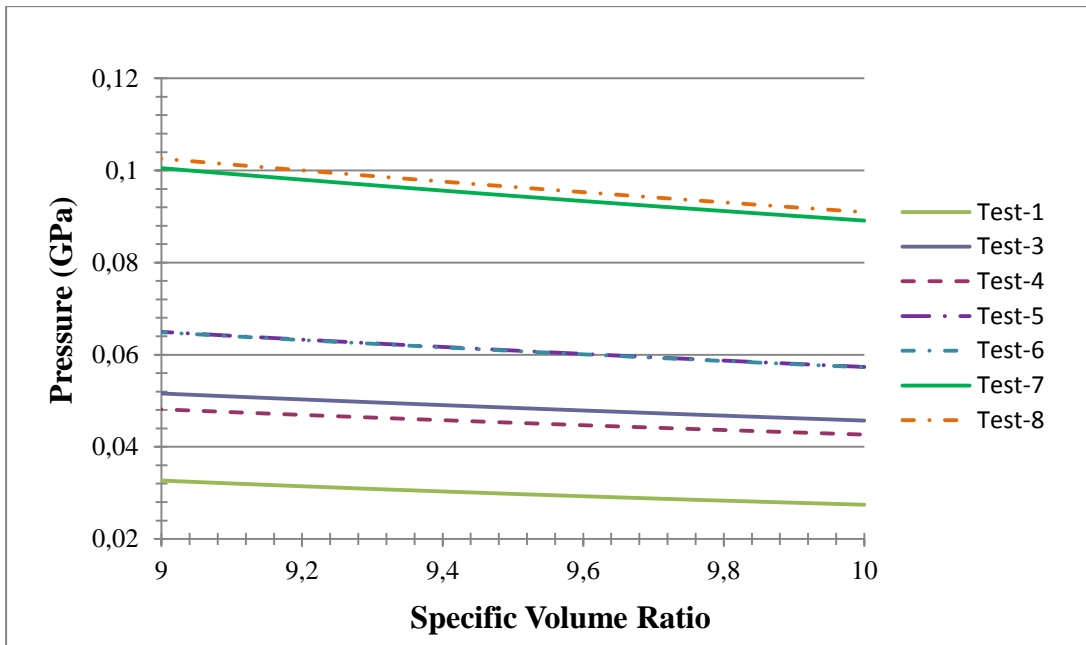


Figure 5-22 Comparison of P-v Curves (for $9 < v < 10$)

In addition to the iterative method suggested by Souers, which is specifically used for obtaining the JWL equation of state parameters from cylinder expansion tests, fixed-point iteration method for a set of nonlinear equations was also used for determining the JWL parameters from the raw experimental data for explosive P-1 only. Fixed-point iteration is an open method used for solving either a single nonlinear equation or a set of nonlinear equations [25], [54]. When this method is used for solving a nonlinear system, each variable is left alone at one side of an equation and stated in terms of all the variables. A single initial value is guessed for each variable. The next value of each variable is calculated via the equation written for that variable. The set of equations and the corresponding P-v curve obtained via the fixed-point iteration technique is given in Appendix B. It was seen that the results obtained using this technique do not represent the behaviour of the explosive as accurate as the results based on Souers' method.

5.2 Effects of Uncertainties on the Calculated JWL Parameters

Correct positioning of the optical probes and the contact pins is critical in order to gather accurate measurements in the cylinder expansion tests. As discussed before, strict tolerance values have been selected during design of the cylinder expansion test setup components when necessary, especially for the positions of the measurements sensors. However, there is a limit for narrowing down the manufacturing tolerances due to restrictions resulting from production processes. Employing too strict tolerances may cause complications and difficulties in production of the part or may increase the cost of production to extreme values. Therefore, there are deviations from the nominal design dimensions and parameters for the parts produced. Additionally, although quality control measurements were performed for the components of the setup after they had been manufactured, there are uncertainties resulting from the nature of the metrology techniques in controls. Therefore there are uncertainties in the quantities in any engineering application.

In order to analyze the effects of the uncertainties in a cylinder test on the JWL equation of state parameters, the JWL parameters were calculated using the tolerance limits of quantities that affect the calculation of the JWL parameters. For remaining on the safe side and obtaining a larger margin for the resulting errors, limits of the tolerances were used when available rather than the value measured during quality controls. The analysis for the test performed with P-1 is presented in this study.

The tolerance limits for the parameters used in the calculations of the JWL equation of state parameters of P-1 are presented in Table 5-12. The sets for limits for the parameters are grouped such that the limits that result in the lowest pressure are given in one column; whereas limits that lead to the highest pressure values are given in the other column. For instance, the lower limit for explosive mass and the higher limit of the wall thickness result in low values of pressures and they are given in the same column in Table 5-12.

For the uncertainty of measurements for mass values, the tolerance limit of the calibrated mass measurement scale was used. For the uncertainty values of the dimensional quantities, design tolerances were used for the lower and higher limits of the values rather than the values measured during quality controls in order to remain on the safe side and obtain conservative bounds for the probable lower and higher bounds for the pressure values.

Table 5-12 Limits of the Quantities which Affect the JWL Parameters

Quantity	Unit	Nominal Value	Value Resulting in Lowest Values of Pressures	Value Resulting in Highest Values of Pressures
m_{exp}	kg	3.4730	3.4725	3.4735
m_{case}	kg	8.8560	8.8565	8.8555
R_i	mm	30	30	29.5
R_o	mm	36	36	35.5
d_1	mm	0.10	0.15	0.10
d_2	mm	8.10	8.15	8.05
d_3	mm	16.10	16.15	16.05
d_4	mm	24.10	24.15	24.05
d_5	mm	32.10	32.15	32.05
d_6	mm	40.10	40.15	40.05
d_7	mm	48.10	48.15	48.05
d_8	mm	56.10	56.15	56.05
d_9	mm	64.10	64.15	64.05
d_{10}	mm	72.10	72.15	72.05
ρ	g/cm^3	1.59	1.57	1.60

Using the quantity sets that will result in lowest and highest pressure values, the JWL equation of state parameter sets were recalculated. These parameter sets are given in Table 5-13. The corresponding lower and upper bound pressure versus specific volume ratio curves as well as the curve showing the nominal values and the $\pm 2\%$ pressure curves drawn based on the nominal values are given in Figure 5-23. However since all the curves are very close to each other, several smaller intervals of the specific volume ratio values the corresponding pressures are presented graphically in Figure 5-24 to Figure 5-27. The differences between the curves can be identified in these figures. As the charts are examined, it is seen that the nominal values for pressure and corresponding upper and lower bounds are within the $\pm 2\%$ interval curves. Therefore it can be concluded that the pressure values obtained using the parameters calculated based on the cylinder expansion tests are within $\pm 2\%$ error. The unpredictable test errors are not included in this analysis.

Table 5-13 Limits of the Parameters Resulting Lowest and Highest Pressure Values

Parameter/ Property	Unit	Nominal	Value Resulting Lowest Values of Pressures	Value Resulting Highest Values of Pressures
a	mm/ms	1271.697	1271.195	1272.206
b	1/ms	212.684	215.139	210.276
V _D	m/s	6632	6629	6656
ρ	g/cm ³	1.59	1.57	1.60
E _o	kJ/m ³	5.675 x 10 ⁶	5.672 x 10 ⁶	5.678 x 10 ⁶
P _{cj}	kPa	2.033 x 10 ⁷	2.031 x 10 ⁷	2.038 x 10 ⁷
A	kPa	4.531 x 10 ⁸	4.372 x 10 ⁸	4.607 x 10 ⁸
B	kPa	1.560 x 10 ⁷	1.591 x 10 ⁷	1.540 x 10 ⁷
C	kPa	5.765 x 10 ⁵	5.692 x 10 ⁵	5.833 x 10 ⁵
R ₁	-	5.15	5.15	5.15
R ₂	-	1.00	1.00	1.00
ω	-	0.334	0.336	0.334

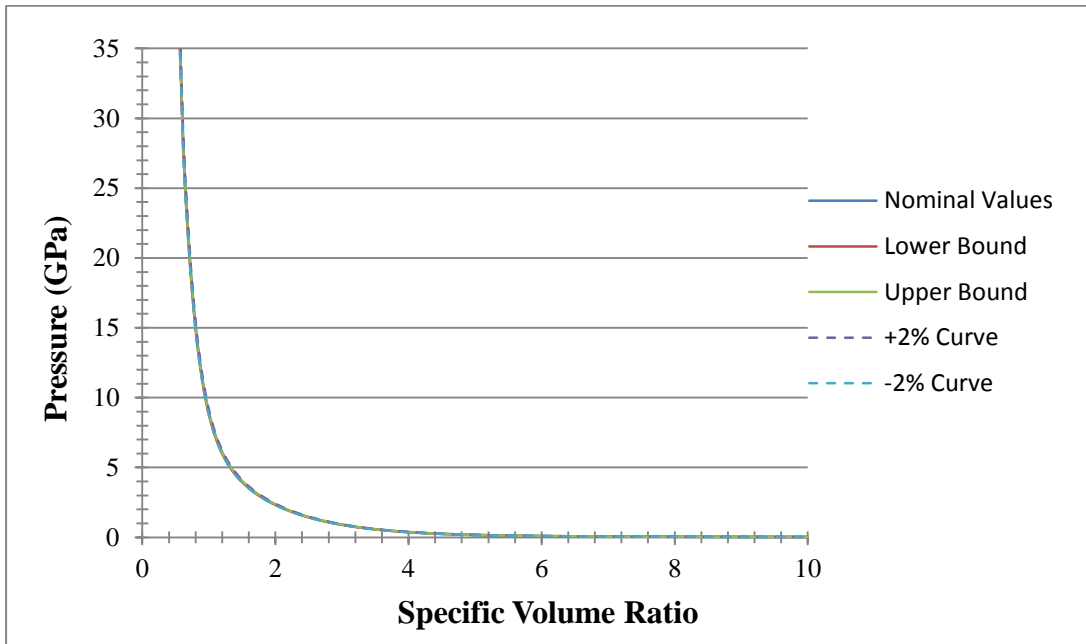


Figure 5-23 Lower and Upper Bounds of the P-v Curves and the $\pm 2\%$ Error Bands for P-1

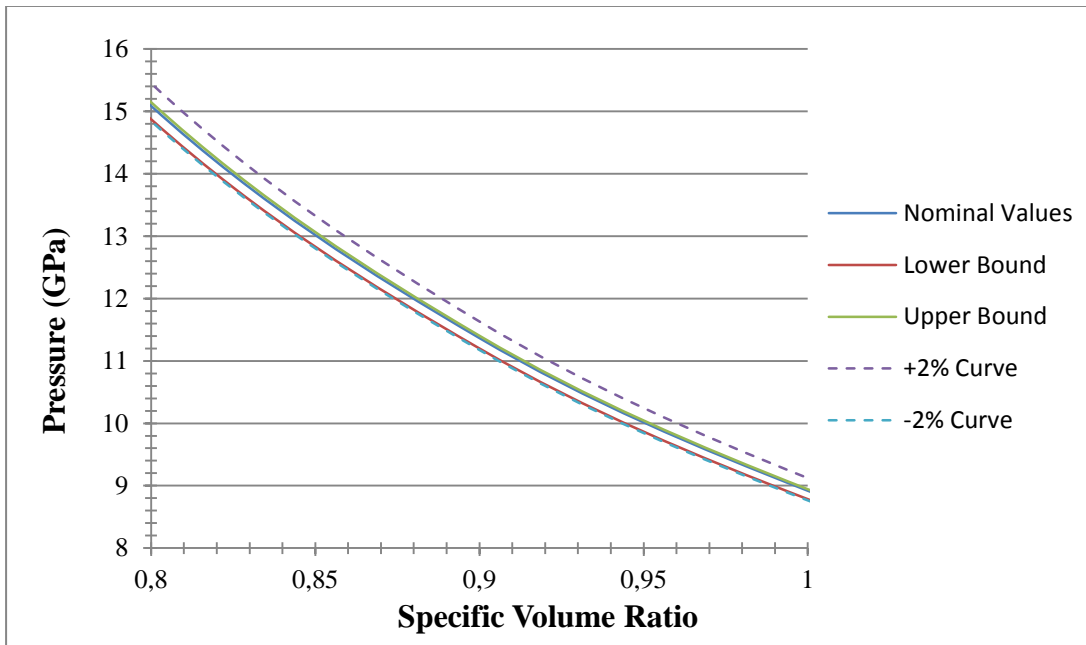


Figure 5-24 P-v Curves for P-1 ($0.8 < v < 1.0$)

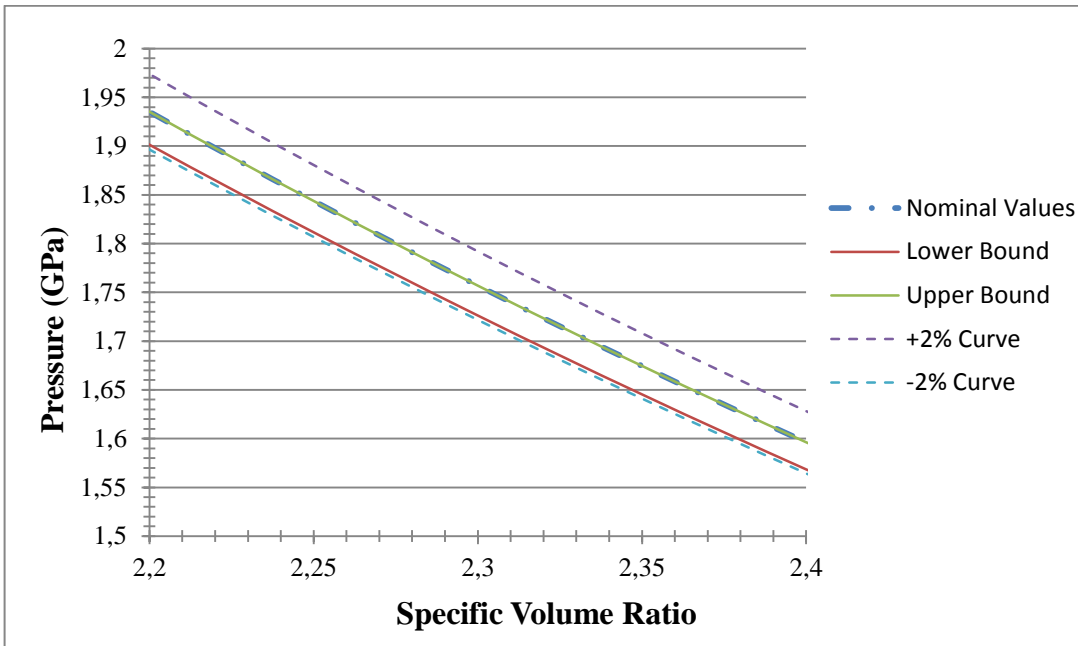


Figure 5-25 P- v Curves for P-1 ($2.2 < v < 2.4$)

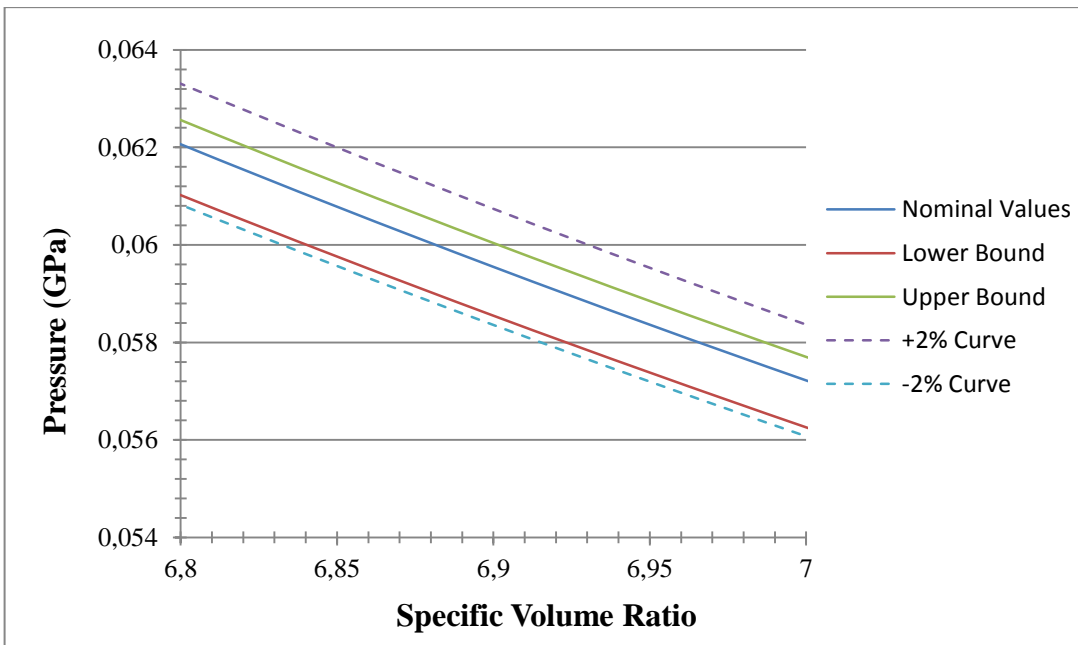


Figure 5-26 P- v Curves for P-1 ($6.8 < v < 7.0$)

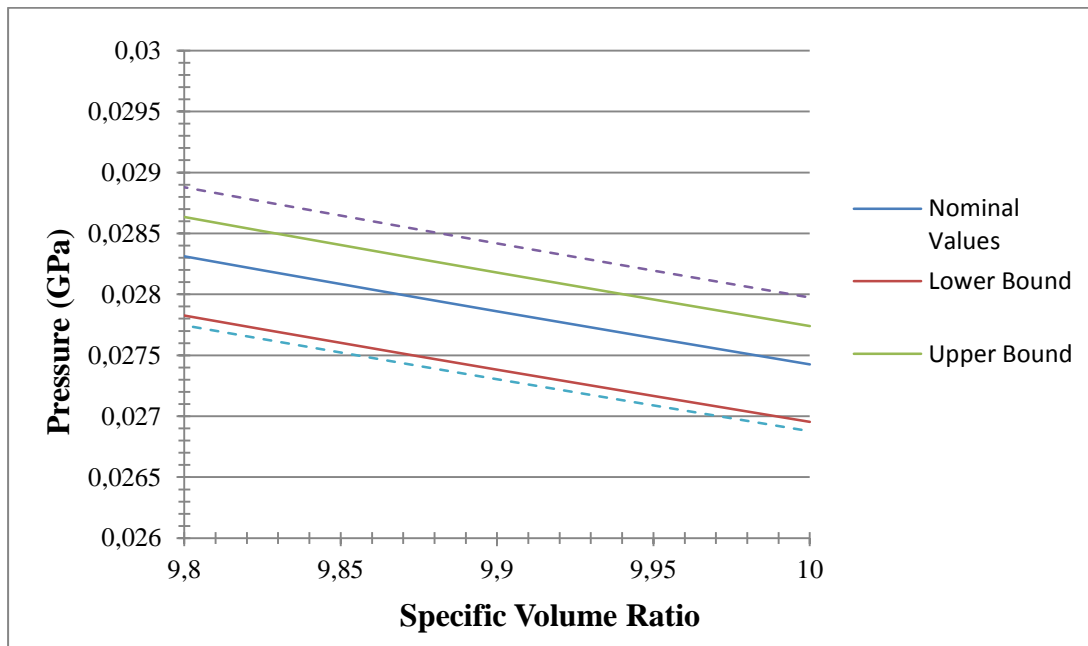


Figure 5-27 P- ν Curves for P-1 ($9.8 < \nu < 10.0$)

CHAPTER 6

SIMULATION OF THE CYLINDER EXPANSION TEST

The cylinder expansion test is modeled and simulated using Ansys Autodyn, which is a commercial tool employing hydrocode. Autodyn is explicit finite element analysis software which is used for modeling and simulating nonlinear and time-dependent dynamics of materials and their interactions [10]. The software includes finite element solvers for structural dynamics, finite volume solvers for computational fluid dynamics, mesh free solvers for smoothed particle hydrodynamics and multi-solver couplings. Autodyn can be used for modeling problems which involve interactions of multiple systems of structures, fluids and gases. Therefore this software can be used for performing analyses for systems including detonation of explosive materials and interaction between the detonation products and the structural elements modeled.

The test item used in the tests is modeled in the numerical simulations performed. Autodyn has a Euler solver that incorporates a control volume method for solving conservation of mass, momentum and energy equations. This solver is generally preferred for situations that involve large deformations and fluid flow. As well as a Euler solver, the software includes a Lagrange solver which is usually employed when a faster simulation time is desired and when there is no excessive material transform and deformations. However; the software employs several methods to extend the application of the Lagrange solver to events including high distortion. Moreover, since the software uses Euler-Lagrange coupling technique, both Euler and Lagrange cells can be employed in a single simulation. In this technique, Euler cells define a stress profile for the Lagrange parts at the interaction zone of coupling; whereas the Lagrange interface defines a geometric constraint for material

flow in the Euler grid [10]. Therefore the Euler-Lagrange coupling feature can be used for modelling systems with fluid-structure interaction problems such as explosion effects on structures. For the simulations performed in the scope of this study, Euler solver of Autodyn was used in order to model the main explosive material, the booster charges and the air around the test item. The copper casing used in the test item assembly, on the other hand, was modeled as a Lagrange part in Autodyn. The interactions between the Euler grid and Lagrange cells were solved by the Euler-Lagrange coupling feature of the software.

Autodyn utilizes material models that relate stress to deformation in a modelled part. The JWL formulation was used as the equation of state during modeling of the explosive materials, which are the main explosive material and the booster material. For the main explosive, the parameters found via the tests (see Table 5-6) were employed for constructing the JWL equation of state. For the booster material, the available material model parameters were utilized. The “Cu-OFHC material model” present in the Autodyn material library was used for modelling the case material. This material model employs a Shock equation of state and a Steinberg-Guinan strength model for modeling oxygen-free high conductivity copper. The parameters used in the modelling the copper casing and the booster charges are presented in Appendix C.

Simulations were performed in Autodyn with all the four explosive materials that have been used in the tests. In the models prepared in the simulation software, the booster charges and the copper cylinder were modelled with the dimensions of the real components used in test items. Gauge points are placed in the analyses at the positions where optical probes and ionization contact pins are positioned during cylinder expansion tests. Detonation of the explosive components is initiated at the center of the free surface of the booster charges, as in the case for the tests. The test items have been prepared as 2-D axysmmetrical models. The model used in the analysis of the setup with explosive P-1 is given as a sample in Figure 6-1.

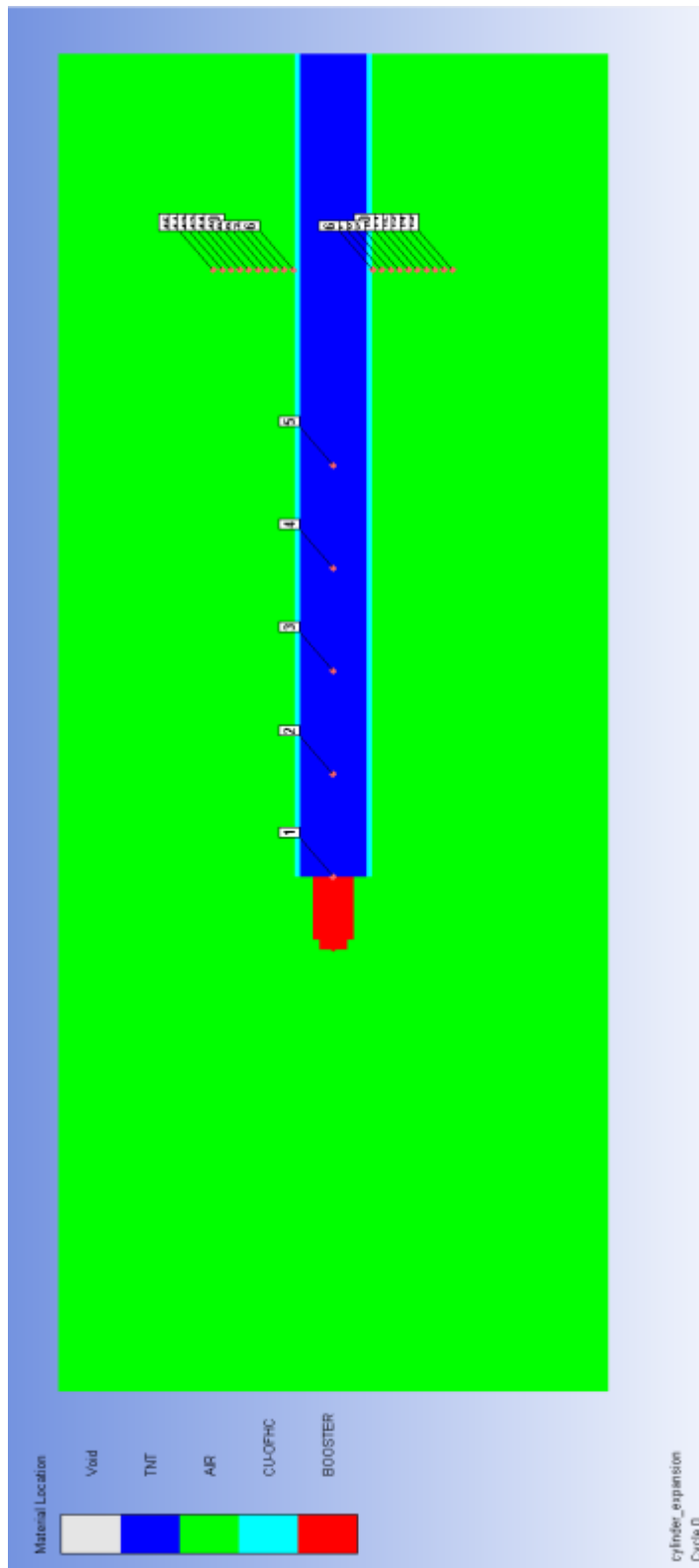


Figure 6-1 Autodyn Model of the Test Item Including P-1

In the analyses, the first gauge is placed at the interface between the booster charge and the main explosive charge. The next four gauges are used for simulating the optical probes that are used for measuring the detonation velocity in the cylinder expansion tests. After the termination of the analyses, the arrival times of the detonation front at the first four gauges are measured and the corresponding detonation velocity is calculated. The remaining gauge points used in the analyses are placed at the positions of the contact pins that are utilized for the radial expansion histogram in the tests. Similarly, the contact times of the expanding copper casing with these gauges have been found. The results found via the analyses have been compared with the ones measured during the tests. The gauges placed in the simulation environment and numbered from 1 to 15 can be seen in Figure 6-1. The gauges used for simulating the contact pins, which are numbered from 6 to 15, are shown in Figure 6-2 once again for better visualization. In Figure 6-2, the element size is 2 mm; therefore the distance between each consecutive gauge is 8 mm.

In Autodyn, several types of boundary conditions can be used in simulations. In the analyses conducted for simulating the cylinder expansion tests, flow out boundary condition was used at the edges of the environment. This boundary condition allows the material and the waves travelling outside the grid zone to pass through the edges. Although there are some reflected waves and energy at the boundary even if this boundary condition is applied, these are very small waves and do not have a significant effect on the general solution [10]. The lines where the flow out boundary condition has been applied are shown in Figure 6-3. No other boundary condition has been employed in the simulations performed.

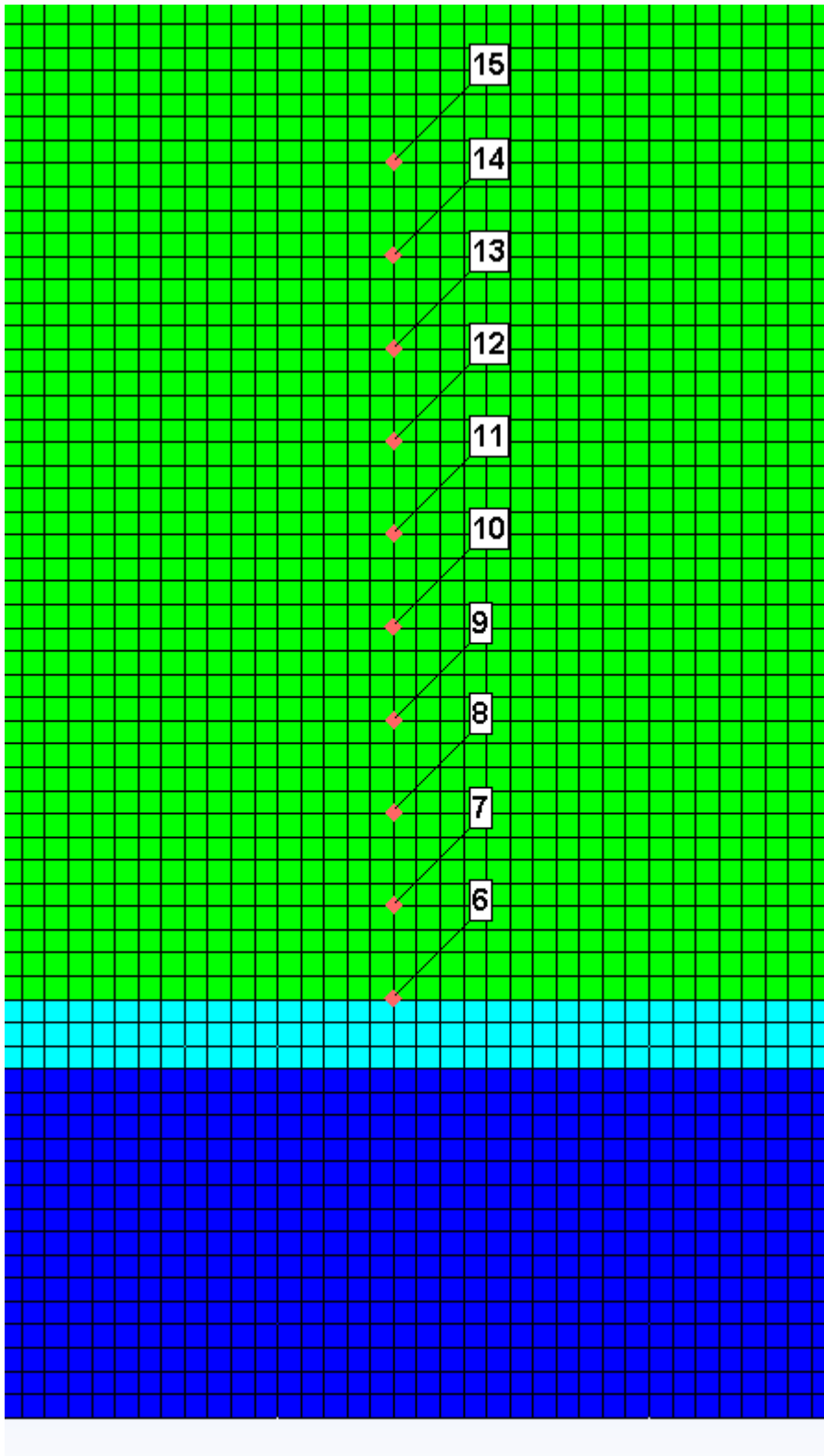


Figure 6-2 Gauges Used for Simulating the Contact Pins

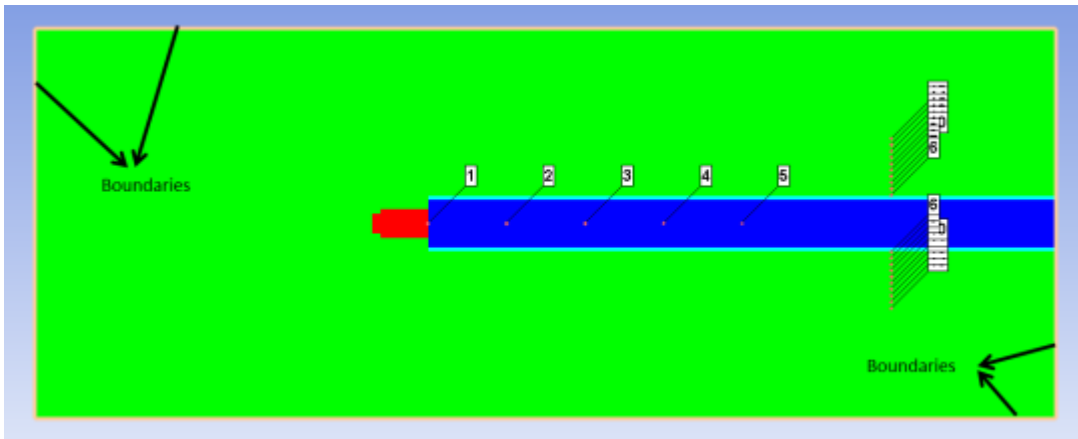


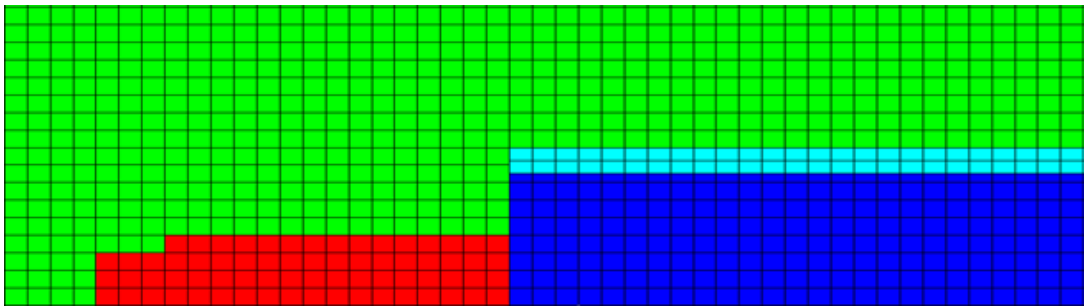
Figure 6-3 Boundaries where the Boundary Condition is Applied

Velocity can be defined for the parts as initial condition in Autodyn. Since the parts modelled are not in motion before the cylinder expansion test, initial velocity condition was not used in the analyses.

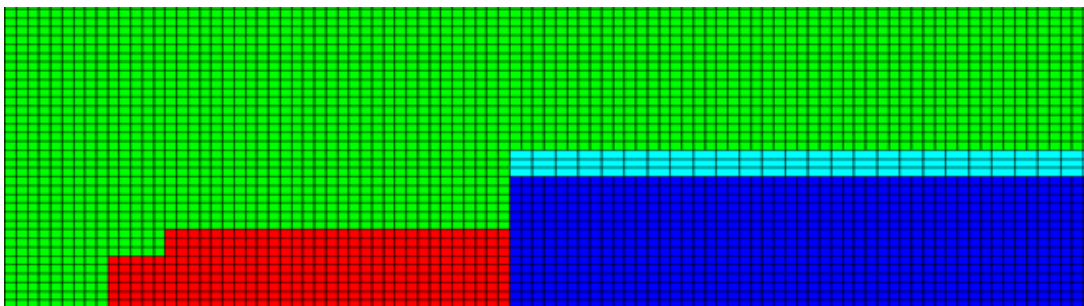
Structured square or rectangular cells were used for constructing the Euler grid and the Lagrange part. For examining the mesh independency of the results, a mesh sensitivity study has been performed by conducting analyses using different cell sizes for the Euler grid and the Lagrange part. The mesh sensitivity study has been performed for the model with explosive P-1. The mesh sizes and the corresponding number of elements for the models are given in Table 6-1. Since use of finer mesh than the ones selected increase the analyses time significantly, no finer mesh was used in the simulations. Other parameters such as material models, boundary conditions were the same for these models. The part dimensions were slightly different in the models which the part dimension is not a multitude of the cell size. For the remaining models the part dimensions were kept constant and equal to the actual sizes. The mesh grid for these six models are shown in Figure 6-4. A region with dimensions of 68 mm x 188 mm was shown rather than the whole models for achieving better illustration of the mesh.

Table 6-1 Cell Sizes Used in the Analyses

Model No	Euler Grid (mm x mm)	Lagrange Part (mm x mm)	Number of Euler Elements	Number of Lagrange Elements
#1	4x4	4x3	20475	400
#2	2x2	4x2	81250	600
#3	2x2	2x2	81250	1200
#4	1x1	2x2	325000	1200
#5	1x1	1x1	325000	4800
#6	0.5x0.5	1x1	1300000	4800



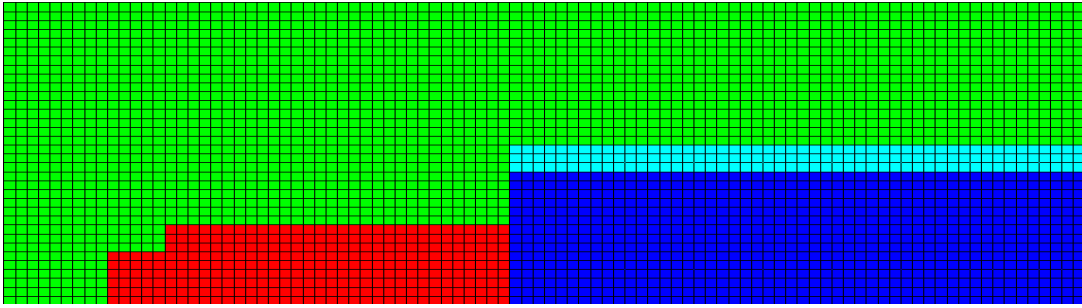
(a)



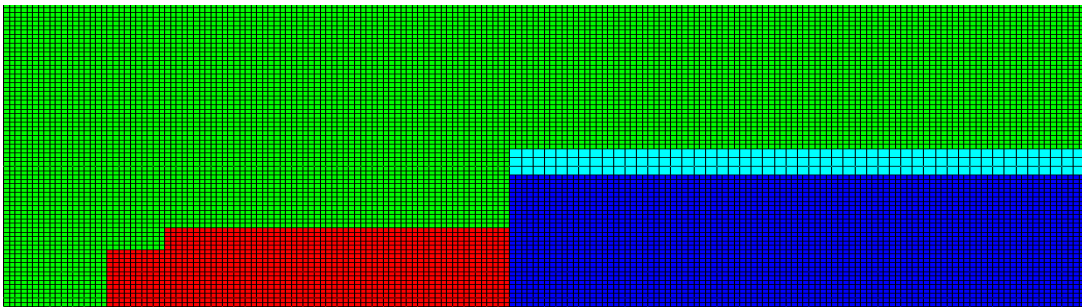
(b)

Figure 6-4 Models with Different Cell Sizes

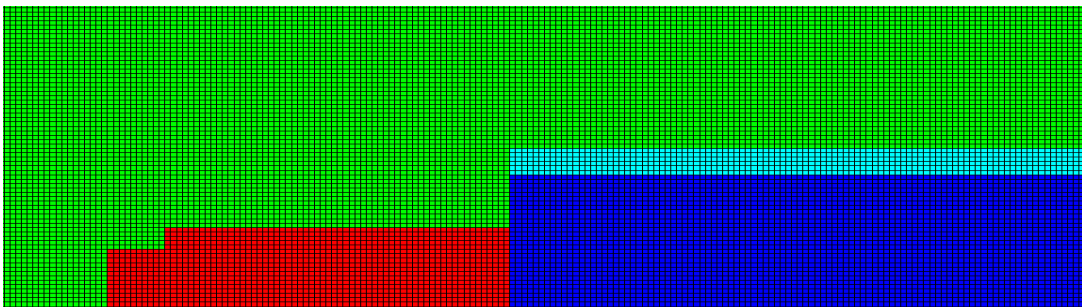
(a) Model #1 (b) Model #2 (c) Model #3
 (d) Model #4 (e) Model #4 (f) Model #6



(c)

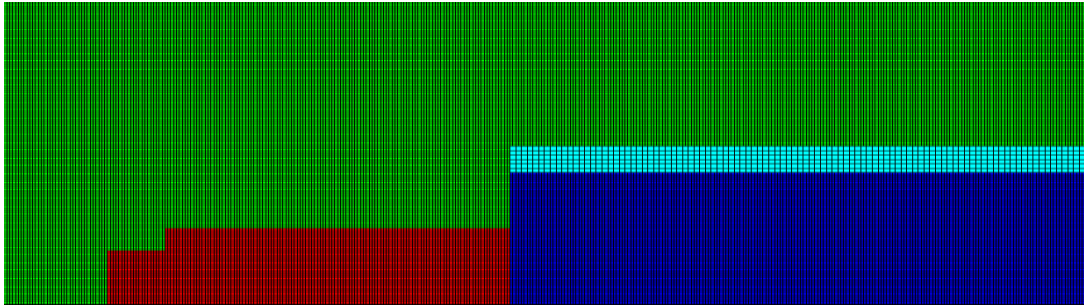


(d)



(e)

Figure 6-4 (continued)



(f)

Figure 6-4 (continued)

Several frames taken at different times during one of the analyses performed with P-1 are shown in Figure 6-5. The colors in Figure 6-5 are showing the materials occupying the corresponding grids. Red, blue, cyan and green colors represent the booster material, main explosive charge (P-1 for this case), copper (Cu-OFHC) and air, respectively. The expansion of the copper casing can be examined on these screen captures. The pressure variation in the parts modelled using Euler grid in the model during the propagation of the detonation wave and the expansion of the cylinder can also be examined with the analysis results. Sample frames showing the propagation of the detonation wave are presented in Figure 6-6. As discussed in Chapter 4, the propagation of the detonation wave is seen as one dimensional and the detonation front is linear. Therefore the design of the booster charges could be validated with the results of these analyses. However, it should be considered that the simulations are only approximations of the real case encountered in the test; therefore a stronger proof for the one dimensional propagation of the detonation front is the fact that the detonation velocity values calculated via measurements taken at four distinct points indicate to a fully developed propagation which propagated along the axis of the copper cylinder. Since the coefficient of determination values presented in Figure 5-1, Figure 5-2, Figure 5-3 and Figure 5-4

are very close to 1, it can be concluded that the detonation reaches to steady state and it propagates one dimensionally inside the copper casing during tests.

The arrival time values of the detonation wave at the four gages representing the four optical probes are presented in Table 6-2 for the six simulations performed with different cell sizes. Since the results obtained from different analyses are relatively close to each other, it can be concluded that the mesh used is fine enough to obtain accurate results. The results obtained with the finest mesh are compared with the values gathered during the tests performed with P-1 in Table 6-3. The detonation velocity values obtained from these detonation arrival time values are given in Table 6-4.

Similarly, the contact times obtained from the contact pins the analyses are given in Table 6-5 and the results from the analysis with the finest mesh are compared with the test results in Table 6-6. The charts comparing the propagation of the detonation wave in the axial dimension and the radial expansion histogram of the cylindrical copper casing are presented in Figure 6-7 and Figure 6-8, respectively. The results from the simulation with the finest mesh were used to obtain the analysis curves in these two figures. As in the presentation of the test results, the time values are normalized such that the time of arrival values at the first probe and the pin have been taken as zero.

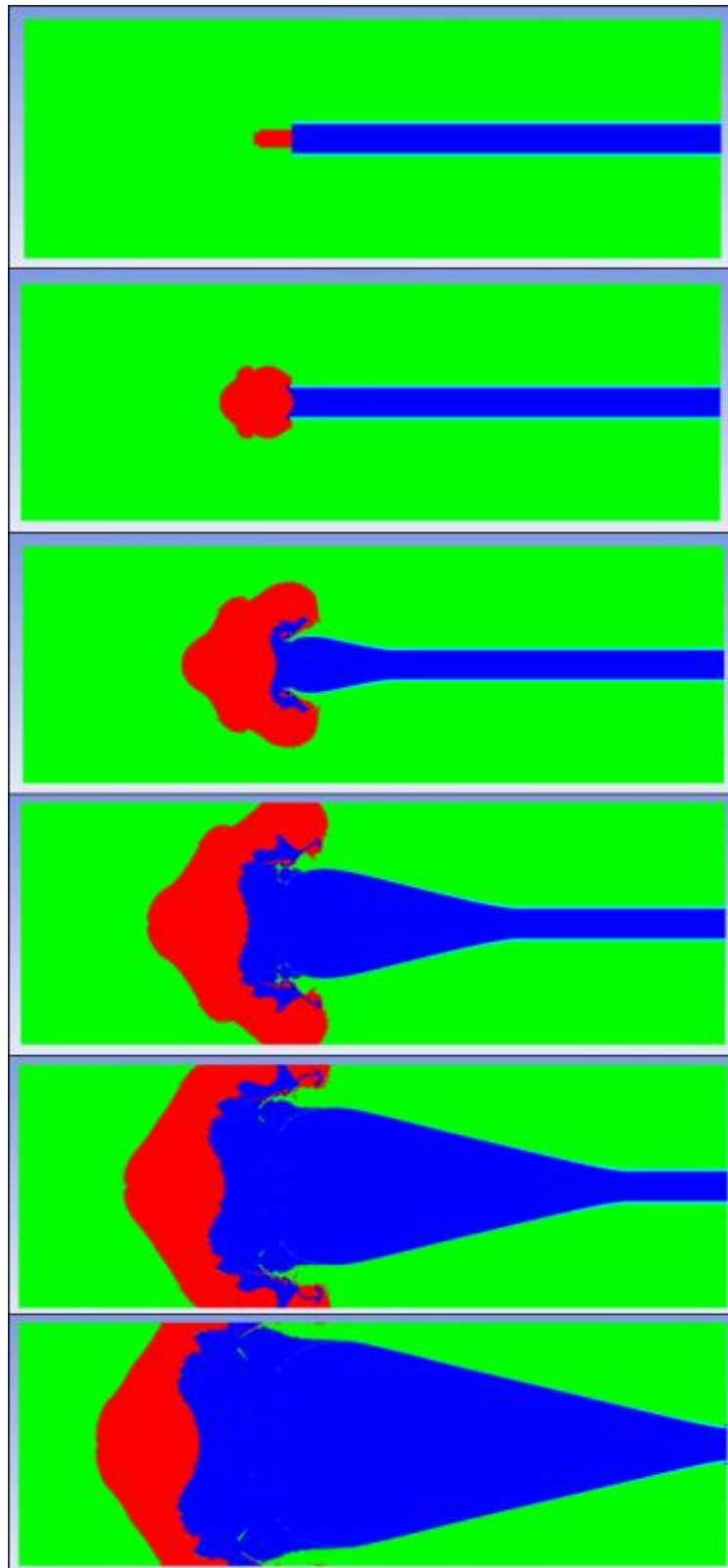


Figure 6-5 Sample Frames during the Analysis

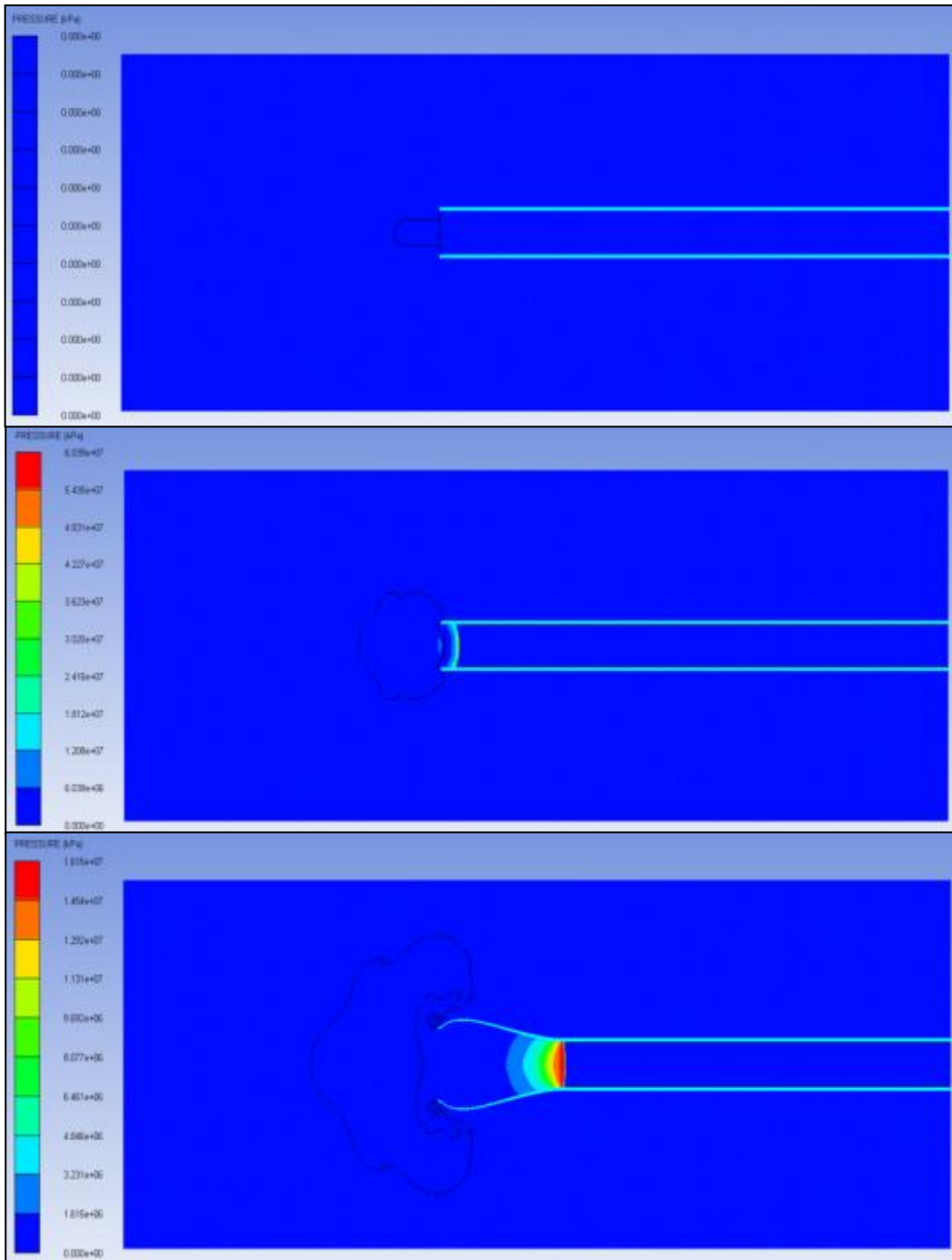


Figure 6-6 Propagation of Detonation Wave and Pressure Variation in the Analysis

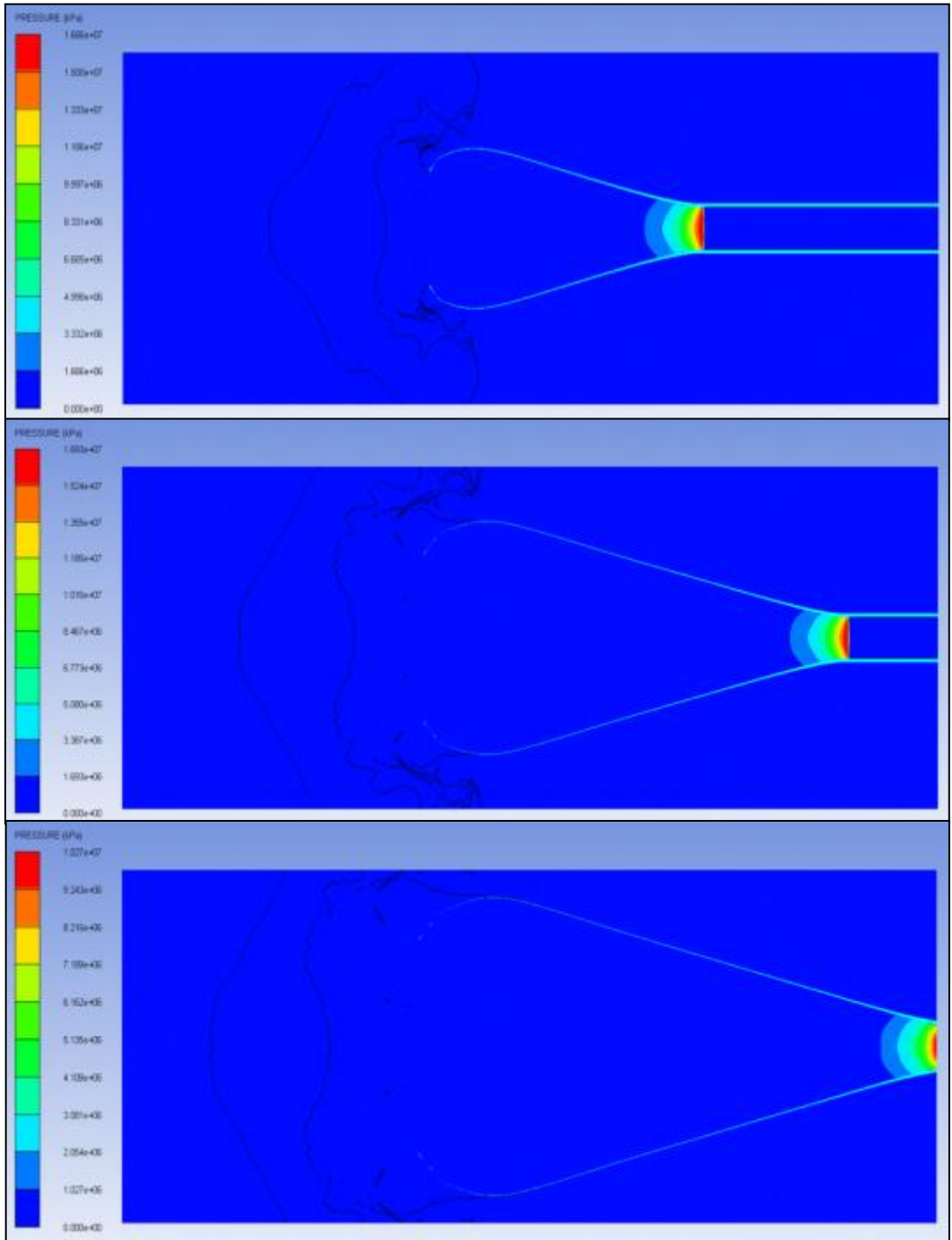


Figure 6-6 (continued)

Table 6-2 Detonation Front Arrival Times for P-1 Obtained from the Analyses

Detonation Front Arrival Times (μs)						
Gauge No	Analysis #1	Analysis #2	Analysis #3	Analysis #4	Analysis #5	Analysis #6
2	0.00	0.00	0.00	0.00	0.00	0.00
3	15.07	15.05	14.86	15.20	14.97	14.83
4	30.17	30.02	30.17	30.23	30.25	30.27
5	45.24	45.14	45.11	45.33	45.57	45.83

Table 6-3 Test and Analysis #6 Results for Detonation Front Arrival Times

Detonation Front Arrival Times (μs)				
Probe No	Gauge No	Test-1	Test-2	Analysis #6
1	2	0.00	0.00	0.00
2	3	15.05	15.01	14.83
3	4	30.15	30.08	30.27
4	5	45.24	45.17	45.83

Table 6-4 Detonation Velocity Values for P-1 Obtained via Tests and Analysis #6

Detonation Velocity (m/s)		
Test-1	Test-2	Analysis #6
6632	6641	6603

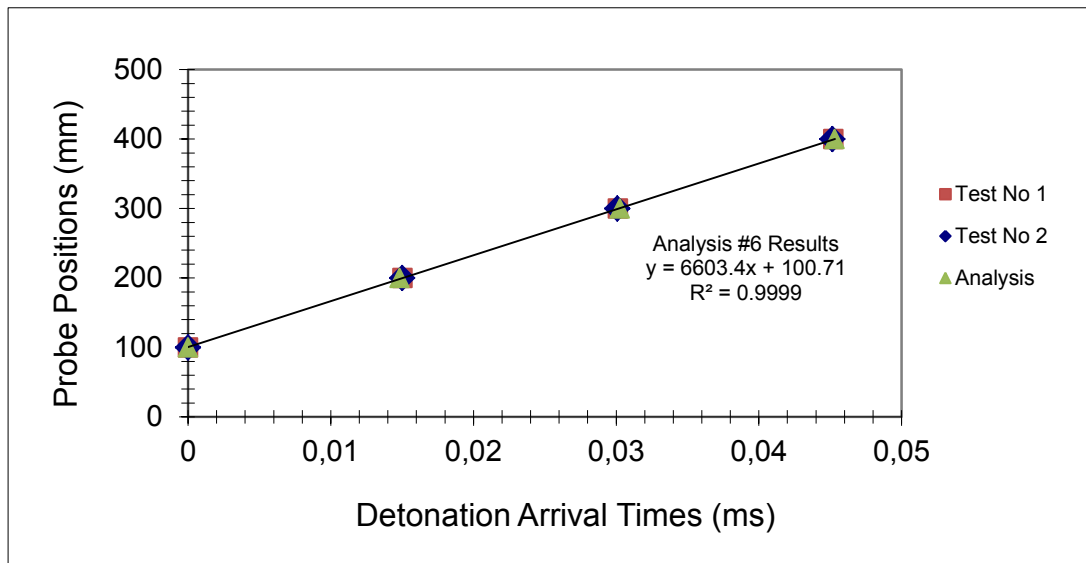


Figure 6-7 Comparison of Test Results and Analysis #6 Results for Velocity of Detonation

Table 6-5 Contact Pin Signal Times for P-1 Obtained from the Analyses

Gauge No	Radial Position (mm)	Pin Signal Times (μ s)					
		Analysis #1	Analysis #2	Analysis #3	Analysis #4	Analysis #5	Analysis #6
6	0.10	0.0	0.0	0.0	0.0	0.0	0.0
7	8.10	10.3	4.4	8.4	9.2	9.4	9.5
8	16.10	17.0	10.7	14.6	15.6	17.4	17.4
9	24.10	23.0	16.5	20.4	21.4	22.3	25.5
10	32.10	29.0	22.2	26.1	27.0	28.4	29.0
11	40.10	34.8	27.8	31.7	32.8	30.6	31.9
12	48.10	40.5	33.4	37.3	38.1	37.8	38.2
13	56.10	46.1	37.6	42.9	43.8	42.5	45.3
14	64.10	51.9	42.9	48.4	49.3	50.1	50.4
15	72.10	57.8	48.0	54.5	54.8	55.8	58.2

Table 6-6 Test and Analysis #6 Results for Contact Pin Signal Times

Pin No	Gauge No	Radial Position (mm)	Pin Signal Times (μs)		
			Test-1	Analysis #6	Relative Difference
1	6	0.10	0.0	0.0	-
2	7	8.10	9.3	9.5	2%
3	8	16.10	16.3	17.4	7%
4	9	24.10	23.1	25.5	10%
5	10	32.10	29.7	29.0	2%
6	11	40.10	35.2	31.9	9%
7	12	48.10	41.5	38.2	8%
8	13	56.10	47.5	45.3	5%
9	14	64.10	53.4	50.4	6%
10	15	72.10	-	58.2	-

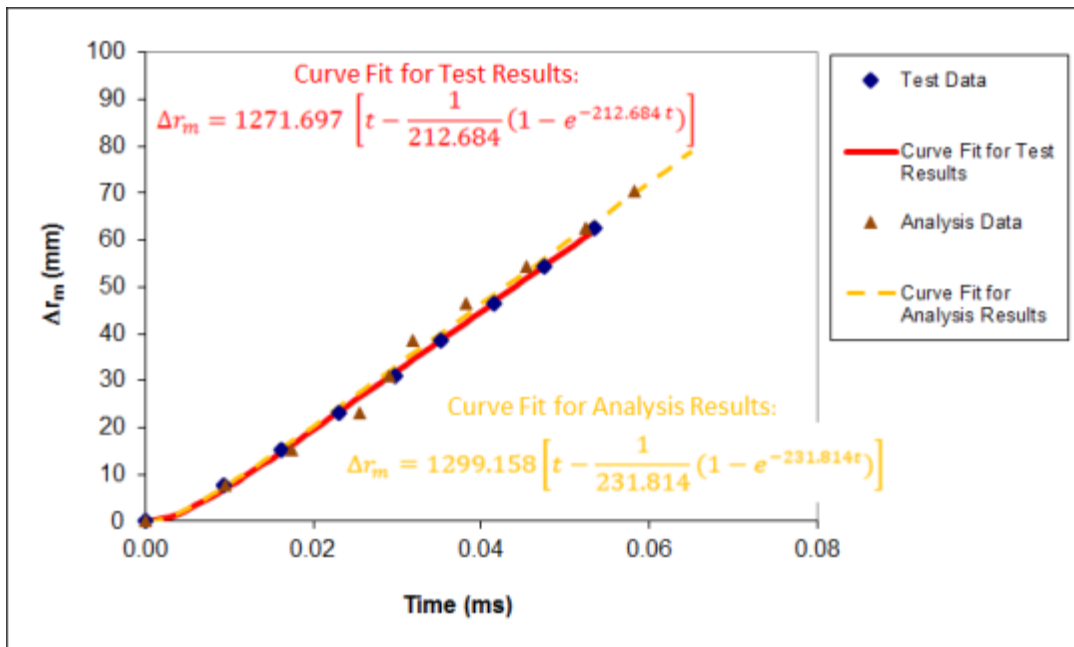


Figure 6-8 Comparison of Test Results and Analysis #6 Results for Radial Position of Cylinder Wall with Respect to Time

The comparison of values obtained from six different analyses with different mesh sizes has shown that the results between these analyses are fairly close. Therefore, it can be concluded that the dependency of the analysis results on the mesh size is very small for the finest mesh size used. There is no obvious tendency in the analysis results as the finite element mesh gets finer.

It should be noted that there are inputs to the analyses other than the cylinder expansion test results. Although the explosive used in each analysis has been modelled using the JWL formulation obtained from the tests, the copper casing and the booster charge were modeled utilizing the material models available in the Autodyn software. The analysis results are also affected by these parameters and one should take this into consideration when examining the analyses results. In this section, the results for P-1 have been presented for comparison purposes between test results and analysis results. When the measurement results obtained from the tests are compared with the gauge contact times observed in the analyses, it can be seen that the results are relatively close to each other, indicating well-constructed set of parameters for explosive P-1.

CHAPTER 7

CONCLUSION

7.1 Summary and Discussions

In the scope of this thesis study, a cylinder expansion test setup has been designed and developed considering the critical issues stated in the publications available in the literature. According to the knowledge of the author, such a test setup had never been developed and used in Turkey before. The designed setup has been used in 8 cylinder expansion tests totally with the use of 4 different explosive materials.

The main test item and other subcomponents of test setup assembly were designed in the scope of the study. The metallic components of the setup were manufactured and quality control measurements were done for these parts. Since strict tolerance requirements are present for the components, some of the components had to be rejected and replacement parts had been manufactured.

During the cylinder expansion tests, detonation velocity of the explosive and the radial expansion histogram of the copper cylinder housing were measured. For detonation velocity measurement, optical probes were utilized. The probes were placed along the longitudinal axis of the test item and data were obtained successfully. Off-the-shelf contact pins were employed for measuring the radial position of the cylinder wall at a single cross-section as a function of time. In one of the tests performed, signal could not be gathered from one of the contact pins. However the calculations could be performed from the data obtained via the other pins. Since the positions of the contact pins are critical for accurate measurement and these positions can be affected by the environmental effects due to the spindly

shape of the pins, it has been decided that it is advisable to protect the sides of the test setup using a covering material during the tests. For the last tests performed the sides of the table assembly were covered for protection against harsh effects.

The explosive compositions used in the tests are designated as P-1, P-2, P-3 and P-4. The explosive composition designated as P-1 is TNT, which is a conventional explosive composition and has been in use throughout the world for a long time. Detonation parameters including detonation velocity, Gurney velocity and JWL equation of state parameters were calculated for TNT using the test data. The results obtained for TNT were compared with the results presented in the literature. The detonation velocity and Gurney velocity values for TNT obtained from the test were somewhat lower than the values in the literature. It was concluded that the reason of this difference was the fact that the bulk density of the casted explosive used in the tests was lower than the value given in the literature. Pressure versus specific volume ratio curves were obtained based on both test results and literature data. P-3 was another explosive with equation of state parameters available in the literature. The results obtained for this explosive were also compared with the results based on the literature data. There were differences between the results obtained from the tests performed and the results calculated using the literature data. It was concluded that the differences were due to the variations in the percentages of the components in the chemical composition of the explosive, the bulk density of the explosive obtained and alterations in the manufacturing processes employed. The relative differences between the results were in acceptable margin.

Detonation velocity, Gurney velocity and JWL equation of state parameters were also obtained for P-2 and P-4. These two explosives are newly developed materials and hence data was not available on these explosives in the literature. The results obtained from two tests for each kind of explosive were fairly close and it was concluded that reproducible tests can be performed with the cylinder expansion test setup designed in the scope of this study.

Numerical simulations for the tests have been performed using Autodyn, which is a commercial explicit finite element analysis tool. The analyses results were in close proximity of the test results for gauge measurements. However, it has to be considered that components other than the main explosive charge were modelled in these simulations, too. Therefore, factors other than the JWL equation of state parameters contribute to the results obtained and errors encountered in these analyses. A mesh sensitivity analysis has been performed for the model containing explosive P-1. Although the analysis results did not show a clear tendency on the cell size, no significant dependency on the mesh has been encountered either.

The results obtained from the tests for the velocity of detonation have also shown that a fully developed and one dimensionally propagating detonation front could be obtained in the tests. This is also supported by simulation of the test setup conducted using Autodyn, which has shown that the detonation wave develops fully and its translation is one dimensional along the longitudinal axis of the test item.

When the pressure results obtained for the four explosive compositions are compared, it can be concluded that explosive P-1 results in lower pressure values than other explosives when the specific volume ratio is lower than 0.9 or higher than 7. However, this explosive gives the highest pressures if the specific volume ratio is around 2. For high and low values of the specific volume ratio, use of explosive P-4 results in the highest values of pressure when compared to the results of the other explosives. According to the results of this study, P-3 is the explosive with the highest detonation velocity among the four explosive compositions; whereas P-1 has the largest Gurney velocity value.

The JWL equation of state parameter sets obtained in this thesis study have been started to be used in various analyses performed in Roketsan by other colleagues. The results of those analyses employing the parameters are promising and in close agreement with test results.

7.2 Suggestions for Future Work

Future work is recommended about the improvement of the test setup in terms of cost and easy handling. Moreover, the measurement systems and equipment used in the setup can be improved. Different measurement techniques for the velocity of detonation and radial expansion histogram of the copper casing can be employed. Use of streak camera can be tried for obtaining the radial position and the radial velocity of the copper cylinder cross-section as a function of time.

Furthermore, the code used for calculating the JWL equation of state parameters can be developed further. Iteration methods different than the one employed in the current code can be tried and the results obtained via different methods can be compared. A more user friendly code can also be developed.

A more detailed study can be performed to examine the effects of variations in the design parameters and the test measurements on cylinder expansion test results and obtained JWL equation of state parameters as a future work. Moreover a detailed sensitivity analysis can be performed for examining the effect of each quantity on the JWL parameters independently as the other quantities remain constant. As an additional control method, radiographic inspection can be performed on the test items before the tests for checking the casting quality of the explosive, if x-ray equipment powerful enough to penetrate the walls of the copper cylinder is available.

The numerical simulations performed in the commercial software can also be improved in several ways. Other solvers available in Autodyn, as well as different computer tools can be used for simulations. Cell sizes other than the ones used in this study and various aspect ratios can be utilized for constructing the mesh grid and their effects on the analysis results can be studied. Analyses with three dimensional models can be performed as well as two dimensional ones. Results of different simulations can be compared among each other.

REFERENCES

- [1] Brown B.W., "Critical Review of Theories of Steady Non-Ideal Two-Dimensional Detonation of Condensed Explosives", UK, 2002.
- [2] Jones H. and Miller A. R., "The Detonation of Solid Explosives", Proc. Roy. Soc. London A, Vol.194, 1948.
- [3] Wilkins M.L., "The Equation of State of PBX 9404 and LXO4-01", Lawrence Radiation Laboratory Technical Report, UCRL-7797, 1964, Livermore, USA.
- [4] Lee E, Horning H.C and Kury J.W, "Adiabatic Expansion of High Explosive Detonation Products", Lawrence Radiation Laboratory Technical Report, UCRL-50422, 1968, Livermore, USA.
- [5] Esen S., Nyberg U., Arai H. and Ouchterlony F., "Determination of the Energetic Characteristics of Commercial Explosives with the Cylinder Expansion Test Technique", Swebrec, Sweden, 2005.
- [6] Elek P.M., Džingalašević V.V., Jaramaz S.S. and Micković D.M., "Determination of Detonation Products Equation of State from Cylinder Test: Analytical Model and Numerical Analysis", Thermal Science, OnLine-First Issue 00, 2013, pp. 138-138.
- [7] Ma G.W., Hao H. and Zhou Y.X., "Modeling of Wave Propagation Induced by Underground Explosion", Computers and Geotechnics, Vol.22, 1998, pp. 283-303.
- [8] Kerley G.I. and Christian-Frear T.L., "Prediction of Explosive Cylinder Tests Using Equations of State from the PANDA Code", Sandia National Laboratories Technical Report, 1993, USA.
- [9] Akbari Mousavi A.A., Burley S.J. and Al-Hassani S.T.S., "Simulation of Explosive Welding Using the Williamsburg Equation of State to Model Low Detonation Velocity Explosives", International Journal of Impact Engineering, Vol. 31, 2005, pp. 719–734.
- [10] ANSYS AUTODYN Theory Manual, Century Dynamics, Rev.4.3, 2005.

- [11] Feldgun V.R., Karinski Y.S. and Yankelevsky D.Z., “A Simplified Model with Lumped Parameters for Explosion Venting Simulation”, *International Journal of Impact Engineering*, Vol.38, 2011, pp. 964-975.
- [12] Yang Y., Liou W.W., Sheng J., Gorsich D. and Arepally S., “Shock Wave Impact Simulation of a Vehicle Occupant Using Fluid/Structure/Dynamics Interactions”, *International Journal of Impact Engineering*, Vol.52, 2013, pp. 11-22.
- [13] Carleone J., *Tactical Missile Warheads*, American Institute of Aeronautics and Astronautics, Inc., Ann Arbor, 1993.
- [14] Scilly N.F., "Measurement of the Explosive Performance of High Explosives", 1995.
- [15] Cook M.A., *The Science of High Explosive*, Robert E. Krieger Publishing, New York, 1971.
- [16] Catanach R., Hill L., Harry H., Aragon E. and Murk D., “Cylinder Test Specification”, Los Alamos National Laboratory, USA, 1999.
- [17] MIL-STD-1751, “Safety and Performance Tests for Qualification of Explosives”, Department of Defense Military Standard, USA.
- [18] Hansson H., "Determination of Properties of Emulsion Explosives Using Cylinder Expansion Tests and Numerical Simulation", Swebrec, Sweden, 2009.
- [19] Rumchik C. G., Nep R., Butler G.C., Breaux B. and Lindsay C. M., “The Miniaturization and Reproducibility of the Cylinder Expansion Test”, AIP Conference Proceedings, 1426:450, 2012.
- [20] Hodgson A.N. and Handley C.A., “DSD/WBL-Consistent JWL Equations of State for EDC35”, AIP Conference Proceedings 1426, 247 (2012); doi: 10.1063/1.3686265.
- [21] Souers P.C., "JWL Calculating", Lawrence Livermore National Laboratory, University of California, USA, 2005.
- [22] Renick J.D., Bell K., Olson D.B. and Bonner C.D., “Development and Characterization of a Cold-Cast Composite/Molecular Explosive”, Dyno Nobel Technical Report, 2013, USA.
- [23] Gold V.M., Baker E.L., Poulos W.J. and Fuchs B.E., “PAFRAG Modeling of Explosive Fragmentation Munitions Performance”, *International Journal of Impact Engineering*, Vol.33, 2006, pp. 294-304.

- [24] Goto D.M., Becker R. Orzechowski, T.J., Springer H.K., Sunwoo A.J. and Syn C.K., “Investigation of the Fracture and Fragmentation of Explosively Driven Rings and Cylinders”, *International Journal of Impact Engineering*, Vol.35, 2008, pp.1547-1556.
- [25] Chapra S.C. and Canale R.P., *Numerical Methods for Engineers*, McGraw Hill, New York, 2005.
- [26] Gerald C.F. and Wheatley P.O., *Applied Numerical Analysis*, Pearson-AddisonWesly, Boston, 2004.
- [27] Bocksteiner G, Wolfson M.G. and Whelan D.J. “The Critical Diameter, Detonation Velocity and Shock Sensitivity of Australian PBXW-115”, Defence Science and Technology Organization Aeronautical and Maritime Research Laboratory, Department of Defence, 1994, Commonwealth of Australia.
- [28] Suceska M., *Test Methods for Explosives*, Springer, New York, 1995.
- [29] Moser S., Nau S., Salk M. and Thoma K., “In Situ Flash X-Ray High-Speed Computed Tomography for the Quantitative Analysis of Highly Dynamic Processes”, *Measurement Science and Technology*, Vol.25-2, 2014.
- [30] Heindel T.J., “Review of X-Ray Flow Visualization with Applications to Multiphase Flows”, *Journal of Fluids Engineering*, Vol.133, 2011.
- [31] Swingala F.R., Hargather M.J. and Settles G.S., “Optical Techniques for Measuring the Shock Hugoniot Using Ballistic Projectile and High-Explosive Shock Initiation”, *International Journal of Impact Engineering*, Vol.50, 2012, pp.76-82.
- [32] Vogler T.J., Trott W.M., Reinhart W.D., Alexander C.S., Furnish M.D., Knudson M.D. and Chhabildas L.C., “Using the Line-VISAR to Study Multi-Dimensional and Mesoscale Impact Phenomena”, *International Journal of Impact Engineering*, Vol.35, 2008, pp.1844-1852.
- [33] MetroLaser, <http://www.metrolaserinc.com/pdvtempl.htm>, Last accessed on August 05, 2014.
- [34] Time of Arrival Detectors, <http://www.dynasen.com/html/pinintro.html>, Last accessed on May 15, 2014.
- [35] Cooper P.W., *Explosives Engineering*, Wiley-VCH, New York, 1996, pp. 385-394.

- [36] Forbes J.W., Tarver C.M., Urtiew P.A., Garcia F., Greenwood D.W. and Vandersall K.S., “Pressure Wave Measurements from Thermal Cook-Off of an HMX based High Explosive”, Lawrence Livermore National Laboratory, University of California, USA, 2000.
- [37] Chen Y., Hu H., Tang T., Ren G., Li q., Wang R. and Buttler W.T., “Experimental Study of Ejecta from Shock Melted Lead”, Journal of Applied Physics, Vol.111, 2012.
- [38] Jackson S.I., Kiyanda C.B. and Short M., “Experimental Observations of Detonation in Ammonium-Nitrate-Fuel-Oil (ANFO) Surrounded by a High-Sound-Speed, Shockless, Aluminum Confiner”.
- [39] Zhang F., Murray S.B., Yoshinaka A. and Higgins A., “Shock Initiation and Detonability of Isopropyl Nitrate”.
- [40] Zhang B., Mehrjoo N., Ng H.D., Lee H.S. and Bai C., “On the Dynamic Detonation Parameters in Acetylene-Oxygen Mixtures with Varying Amount of Argon Dilution”, Combustion and Flame, Vol.161, 2014, pp. 1390-1397.
- [41] Mehrjoo N., Portaro R. and Ng H.D., “A Technique for Promoting Detonation Transmission from a Confined Tube into Larger Area for Pulse Detonation Engine Applications”, Propulsion and Power Research, 3(1):9, 2014, pp. 9-14.
- [42] Pitts W.M., Yang J.C., Blais M. and Joyce A., “Dispersion and Burning Behavior of Hydrogen Released in a Full-Scale Residential Garage in the Presence and Absence of Conventional Automobiles”, International Journal of Hydrogen Energy, Vol.37, 2012, pp. 17457-17469.
- [43] Nagayama K., Mori Y. and Hidaka K., “Shock Compression Experiments on Several Polymers in the 1 GPa Stress Region”, Journal of Material Processing Technology, Vol.83, 1999, pp. 20-24.
- [44] Rosenberg Z., Ginzburg A. and Ashuach Y., “More on Commercial Carbon Resistors as Low Pressure Gauges”, International Journal of Impact Engineering, Vol.34, 2007, pp. 732-742.
- [45] Simple Optical Sensors for Firing Tests, <http://www.dtic.mil/ndia/2011fuze/SessionIIIACConnolly.pdf>, Last accessed on August 05, 2014.
- [46] Gurney R.W. “The Initial Velocities of Fragments from Bombs, Shells and Grenades”, U.S. Ballistics Research Laboratories Report 405, 1943.

- [47] Hiroe T., Fujiwara K., Hata H. and Takahashi H, “Deformation and Fragmentation Behaviour of Exploded Metal Cylinders and the Effects of Wall Materials, Configuration, Explosive Energy and Initiated Locations”, *International Journal of Impact Engineering*, Vol.35, 2008, pp. 1578–1586.
- [48] Hutchinson M.D., “The Escape of Blast from Fragmenting Munitions Casings”, *International Journal of Impact Engineering*, Vol.36, 2009, pp. 185–192.
- [49] Xiangshao K., Weiguo W., Jun L., Fang L., Pan C. and Ying L., “A Numerical Investigation on Explosive Fragmentation of Metal Casing Using Smoothed Particle Hydrodynamic Method”, *Materials and Design*, Vol.51, 2013, pp. 729–741.
- [50] Hutchinson M.D and Price D.W., “On the Continued Acceleration of Bomb Casing Fragments Following Casing Fracture”, *Defence Technology*, Vol.10, 2014, pp. 211-218.
- [51] Zhang F., *Shock Waves Science and Technology Reference Library, Volume 6, Detonation Dynamics*, Springer, 2012.
- [52] Lee E., Fingers M. and Colins W., “JWL Equations of State Coefficients for High Explosives”, Lawrence Livermore Laboratory Technical Report, UCID-16189, 1973, Livermore, USA.
- [53] Dobratz B.M. and Crawford P.C., *LLNL Explosives Handbook, Properties of Chemical Explosives and Explosive Simulants*, Lawrence Livermore Laboratory, Livermore, 1985.
- [54] Ortega J.M. and Rheinboldt W.C., *Iterative Solution of Nonlinear Equations in Several Variables*, Society for Industrial and Applied Mathematics, Philadelphia, 2000.

APPENDIX A

SAMPLE RESULTS OF CMM MEASUREMENTS

Table A-1 CMM Results for the Pin Gage Measurements





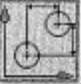

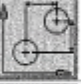


	Actual	Nominal	Upper Tol.	Lower Tol.	Deviation
 Overall Result					
All Characteristics:		20			
...In Tolerance:		20			
...Out of tolerance:		0			
...Over Warning Limit:		0			
...Not Calculated:		0			
Total Coord. systems:		1			
...Not Calculated:		0			
Total Text elements:		0			
 R36.1	36.0038	36.0000	0.0500	0.0000	---
 MESAFE 135	135.3406	135.0000	0.5000	-0.5000	---
 R 44.1	44.1100	44.1000	0.0500	-0.0500	-
 MESAFE 120	120.1759	120.0000	0.3000	-0.3000	---
 R 52.1	52.0994	52.1000	0.0500	-0.0500	-
 MESAFE 105	105.1725	105.0000	0.3000	-0.3000	---
 R 60.1	60.1024	60.1000	0.0500	-0.0500	-
 R 68.1	68.1015	68.1000	0.0500	-0.0500	-

Table A-1 (continued)













	Actual	Nominal	Upper Tol.	Lower Tol.	Deviation
 R 76.1	76.1008	76.1000	0.0500	-0.0500	- 0.0008
 R 84.1	84.1034	84.1000	0.0500	-0.0500	- 0.0034
 R 92.1	92.1036	92.1000	0.0500	-0.0500	- 0.0036
 R 100.1	100.1125	100.1000	0.0500	-0.0500	- 0.0125
 R 108.1	108.0985	108.1000	0.0500	-0.0500	- -0.0015
 Angle between Features 1	59°58'29"	60° 0' 0"	1° 0' 0"	-1° 0' 0"	- -0° 1'31"
 90	90.0910	90.0000	0.3000	-0.3000	- 0.0910
 75	75.0722	75.0000	0.3000	-0.3000	- 0.0722
 60	60.0560	60.0000	0.3000	-0.3000	- 0.0560
 45	45.0358	45.0000	0.3000	-0.3000	- 0.0358
 30	30.0185	30.0000	0.2000	-0.2000	- 0.0185
 15	15.0039	15.0000	0.2000	-0.2000	- 0.0039

Table A-2 CMM Results for the Pin Holder Measurements










	Actual	Nominal	Upper Tol.	Lower Tol.	Deviation
 Overall Result					
All Characteristics:		47			
...in Tolerance:		44			
...Out of tolerance:		3			
...Over Warning Limit:		0			
...Not Calculated:		0			
Total Coord. systems:		0			
...Not Calculated:		0			
Total Text elements:		0			
 Flatness1	0.0098	0.0000	0.2000		0.0098
 Radius170	170.0569	170.0000	1.0000	0.0000	0.0569
 Cylindricity1R170	0.0097	0.0000	0.2000		0.0097
 Radius150	150.0454	150.0000	0.5000	-0.5000	0.0454
 Radius190	193.0046	190.0000	1.0000	0.0000	3.0046
 Cartesian Distance130	130.0158	130.0000	0.5000	-0.5000	0.0158
 Cartesian Distance100	100.0086	100.0000	0.3000	-0.3000	0.0086
 Cartesian Distance150	149.9972	150.0000	0.5000	-0.5000	-0.0028

Table A-2 (continued)

	Actual	Nominal	Upper Tol.	Lower Tol.	Deviation
	Diameter_Circle1 6.0163	6.1000	0.1000	-0.1000	--- -0.0837
	Projection Angle One1 5° 4°57'36"	5° 0' 0"	0°30' 0"	-0°30' 0"	- -0° 2'24"
	Projection Angle One2 -5° -5° 2'50"	-5° 0' 0"	0°30' 0"	-0°30' 0"	- -0° 2'50"
	Angle between Features1 9°57'45"	9°57'51"	0°30' 0"	-0°30' 0"	- -0° 0' 7"
	Angle between Features2 9°59'37"	10° 5'45"	0°30' 0"	-0°30' 0"	- -0° 6' 8"
	Angle between Features3 9°58'20"	9°53'22"	0°30' 0"	-0°30' 0"	- 0° 4'59"
	Angle between Features4 10° 0'34"	9°59'18"	0°30' 0"	-0°30' 0"	- 0° 1'16"
	Angle between Features5 9°55' 4"	9°55' 0"	0°30' 0"	-0°30' 0"	- 0° 0' 4"
	Angle between Features6 9°59'57"	10° 0'29"	0°30' 0"	-0°30' 0"	- -0° 0'32"
	Angle between Features7 10° 4'16"	10° 4' 7"	0°30' 0"	-0°30' 0"	- 0° 0' 9"
	Angle between Features8 9°56'25"	9°56'12"	0°30' 0"	-0°30' 0"	- 0° 0'13"
	Angle between Features9 10° 0'27"	10° 1'23"	0°30' 0"	-0°30' 0"	- -0° 0'56"

Table A-2 (continued)





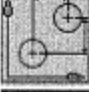







	Actual	Nominal	Upper Tol.	Lower Tol.	Deviation
	15°_ust 15° 3'50"	15° 0' 0"	0°30' 0"	-0°30' 0"	- 0° 3'50"
	15°_alt 15° 3'18"	15° 0' 0"	0°30' 0"	-0°30' 0"	- 0° 3'18"
	70°_ust 69°55' 5"	70° 0' 0"	0°20' 0"	-0°20' 0"	- -0° 4'55"
	70°_alt 69°56' 7"	70° 0' 0"	0°20' 0"	-0°20' 0"	- -0° 3'53"
	KONTROL 0.0000	0.0000	0.5000	-0.5000	 0.0000
	5°_1 5° 1' 5"	5° 0' 0"	0° 1' 0"	-0° 1' 0"	0° 0' 5" 0° 1' 5"
	10°_1 10° 0' 1"	10° 0' 0"	0°30' 0"	-0°30' 0"	- 0° 0' 1"
	5° -4°58'54"	-5° 0' 0"	0° 1' 0"	-0° 1' 0"	0° 0' 6" 0° 1' 6"
	15° -14°58'31"	-15° 0' 0"	0°30' 0"	-0°30' 0"	- 0° 1'29"
	25° -24°58' 8"	-25° 0' 0"	0°30' 0"	-0°30' 0"	- 0° 1'52"
	35° -34°57'24"	-35° 0' 0"	0°30' 0"	-0°30' 0"	- 0° 2'36"
	45° -44°58'54"	-45° 0' 0"	0°30' 0"	-0°30' 0"	- 0° 1' 6"

Table A-2 (continued)
















	Actual	Nominal	Upper Tol.	Lower Tol.	Deviation
 55°	54°58'40"	55° 0' 0"	0°20' 0"	-0°20' 0"	- -0° 1'20"
 65°	64°58'34"	65° 0' 0"	0°20' 0"	-0°20' 0"	- -0° 1'26"
 75°	74°59' 0"	75° 0' 0"	0°20' 0"	-0°20' 0"	- -0° 1' 0"
 85°	84°58'33"	85° 0' 0"	0°20' 0"	-0°20' 0"	- -0° 1'27"
 207.5	-207.4023	-207.5000	0.5000	-0.5000	 0.0977
 275.3	275.1648	275.3000	0.5000	-0.5000	- -0.1352
 48.5	48.4860	48.5000	0.3000	-0.3000	- -0.0140
 10°_2	9°59'48"	10° 0' 0"	0°30' 0"	-0°30' 0"	- -0° 0'12"
 10°_3	9°59'57"	10° 0' 0"	0°30' 0"	-0°30' 0"	- -0° 0' 3"
 10°_4	9°58'22"	10° 0' 0"	0°30' 0"	-0°30' 0"	- -0° 1'38"
 10°_5	10° 4'12"	10° 0' 0"	0°30' 0"	-0°30' 0"	 0° 4'12"
 10°_6	10° 0'29"	10° 0' 0"	0°30' 0"	-0°30' 0"	 0° 0'29"

Table A-2 (continued)

	Actual	Nominal	Upper Tol.	Lower Tol.	Deviation
	10°_7 9°57'36"	10° 0' 0"	0°30' 0"	-0°30' 0"	- -0° 2'24"
	10°_8 10° 1'51"	10° 0' 0"	0°30' 0"	-0°30' 0"	 0° 1'51"
	10°_9 10° 0'39"	10° 0' 0"	0°30' 0"	-0°30' 0"	 0° 0'39"

APPENDIX B

PARAMETERS CALCULATED VIA SIMPLE FIXED POINT ITERATION TECHNIQUE

The results obtained via the simple fixed-point iteration method for explosive P-1 is presented in this section. The parameter set obtained via this method is given in Table B-1. Results based on Souers' method are also presented in this table for comparison. The P-v curves obtained from the two methods and based on two different literature data set are given in Figure B-1. In this figure it can be seen that the results obtained from the fixed-point iteration method are significantly different than the values based on literature data. The relative differences between the pressure values obtained from the parameter set via the simple fixed point iteration method and the results based on literature data sets are presented in Table B-2. Such a comparison was given in Table 5-7 for the pressure values obtained via the Souers' method. The relative error values for the pressure at the Chapman Jouguet point and the detonation velocity were 4.87% and $1.02 \times 10^{-2}\%$, respectively. The error values encountered using the fixed point iteration method were significantly larger the ones encountered when the method suggested by Souers was employed; which led to inaccurate results for the fixed point iteration method.

Table B-1 JWL Parameter Sets for P-1 Obtained via Souers' Method and Simple-Fixed Point Iteration Method

Parameter/ Property	Unit	Souers' Method	Simple Fixed- Point Iteration
V_D	m/s	6632	6632
V_G	m/s	2348	2348
ρ	g/cm^3	1.59	1.59
E_0	kJ/m^3	5.675×10^6	5.561×10^6
P_{cj}	kPa	2.033×10^7	1.530×10^7
A	kPa	4.531×10^8	3.710×10^8
B	kPa	1.560×10^7	3.232×10^6
C	kPa	5.765×10^5	1.831×10^6
R_1	-	5.15	5.15
R_2	-	1.00	1.00
ω	-	0.334	0.665

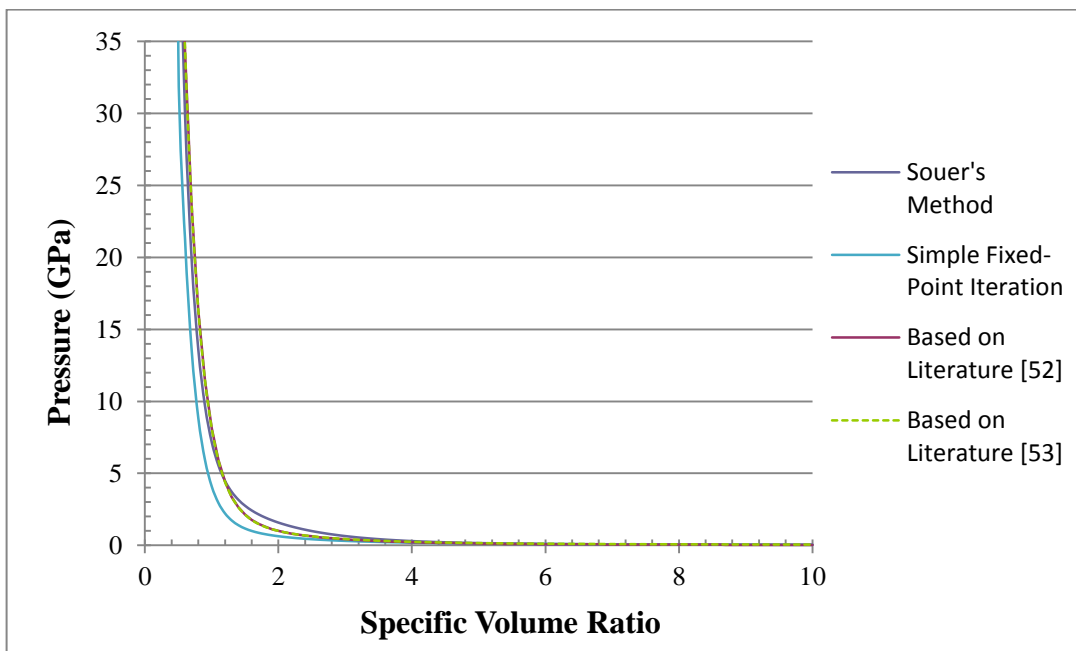


Figure B-1 P-v Curves for P-1

Table B-2 Comparison of Pressures at Selected Specific Volume Ratios for P-1
(Based on Simple Fixed-Point Iteration)

v	P (GPa) (based on Test-1)	P (GPa) (based on Ref. [52])	Relative Difference (Test-1 and Ref. [52])	P (GPa) (based on Ref. [53])	Relative Difference (Test-1 and Ref. [53])
0.2	306.959	174.453	76%	176.309	74%
0.4	34.262	77.789	56%	78.965	57%
0.8	8.828	17.426	49%	18.198	52%
1.2	2.217	5.181	57%	5.689	61%
1.6	1.000	2.299	57%	2.634	62%
2.0	0.633	1.373	54%	1.598	60%
2.4	0.457	0.935	51%	1.092	58%
3.2	0.277	0.490	52%	0.577	52%
4.0	0.188	0.277	32%	0.334	44%
6.0	0.089	0.093	1%	0.126	26%
8.0	0.040	0.057	17%	0.074	22%
10.0	0.027	0.039	18%	0.053	25%

APPENDIX C

PARAMETERS USED IN MODELLING OFHC COPPER AND BOOSTER

Table C-1 Parameters for the Equation of State Model of OFHC Copper [10]

Parameter	Value	Unit
Density	8.93	g/cm ³
Gruneisen Coefficient	2.02	-
Parameter C1	3940	m/s
Parameter S2	0	-
Reference Temperature	300.0	K
Specific Heat	383.0	J/kg-K

Table C-2 Parameters for the Strength Model of OFHC Copper [10]

Parameter	Value	Unit
Shear Modulus (G)	4.77×10^7	kPa
Yield Stress (Y)	1.20×10^5	kPa
Maximum Yield Stress	6.40×10^5	kPa
dG/dT	-1.798×10^4	kPa/K
Melting Temperature	1790	K

Table C-3 Parameters for the Model of Booster Material [10]

Parameter	Value	Unit
Reference Density	1.75	g/cm ³
Parameter A	8.26x10 ⁷	kPa
Parameter B	1.72x10 ⁷	kPa
Parameter R ₁	4.55	-
Parameter R ₂	1.32	-
Parameter ω	0.38	-
C-J Detonation Velocity	8500	m/s
C-J Energy per Unit Volume	1.02x10 ⁷	g/m ³
C-J Pressure	3.70x10 ⁷	kPa

APPENDIX D

CALCULATION OF JWL EOS PARAMETERS FOR P-1

In this Appendix, detailed calculation steps for obtaining the JWL EoS parameters of explosive P-1 using the data obtained from Test-1 are presented. The iterative method explained is essentially paraphrased from the work of Souers [25].

There are several parameters used as input in the iterative calculation steps. The bulk density of the explosive in solid state is obtained as dividing the explosive mass by the volume of the explosive before the tests. Density of P-1 was 1.59 g/cm^3 in Test-1. The initial inner and outer diameters of the copper cylinder were 60 mm and 72 mm, respectively. As discussed in Chapter 3, Chapter 4 and Chapter 5, the velocity of detonation of the explosive is measured during the test using the optical probes and the value of V_D for P-1 was found to be as 6632 m/s in Test-1.

The inner and outer radii for the copper cylinder, R_i and R_o , are 30 mm and 36 mm, respectively. The mean circle radius at the initial tube position, R_m , is then calculated from Equation (4.5) as 33.136 mm.

The radial position and radial velocity functions of the mean circle of the cylinder wall are obtained using the contact pin position and signal time values as discussed in Chapter 4. The constants a and b used in the expressions were found to be 1271.697 mm/ms and 212.683 1/ms, respectively, as presented in Chapter 5. Therefore the expressions for the radial position and radial velocity functions obtained via Test-1 are Equation (D.1) and Equation (D.2), respectively.

$$\Delta r_m(t) = 1271.697 \left(t - \frac{1}{212.683} \right) (1 - e^{-212.683t}) \quad (D.1)$$

$$V_r(t) = 1271.697 (1 - e^{-212.683t}) \quad (D.2)$$

Before the iterative calculations, initial guesses are assigned to A, B, ω and v_{cj} . The initial guesses should be close enough to the real values of the parameters in order that the iterative calculations converge to the real values. The initial guesses of A, B and ω have been taken as 3.71×10^8 , 3.23×10^6 and 0.3 for this case study.

The variable *bhe* is defined as;

$$bhe = \frac{1}{1-v_{cj}} s \quad (D.2)$$

For explosive materials, the value of *bhe* is around 3. Therefore the initial guess of v_{cj} is taken as 0.667.

Initially, the values of detonation energy E_d , at different values of specific volume ratio, v , are calculated using Equation (4.43). In this case study, the specific volume ratios at which the E_d values are calculated were taken as 2.2, 4.4, and 7.2. Moreover, E_d values at specific volume ratio of 7.0 is also computed in order to use in Equation (D.10) given below. The calculation steps for E_d at specific volume ratio of 2.2 is given below. Values of E_d at other specific volume ratios are calculated in a similar manner.

By combining Equation (4.6.b) and Equation (4.44), Δr_m can be written as a function of v as given in Equation (D.3).

$$\Delta r_m v = \sqrt{v \cdot R_i^2 + \frac{R_0^2 - R_i^2}{2}} - \frac{R_i^2 + R_0^2}{2} \quad (\text{D.3})$$

By substituting the value of the specific volume ratio in Equation (D.3), Equation (D.4) can be obtained.

$$\Delta r_m v = 2.2 = \sqrt{2.2 \cdot R_i^2 + \frac{R_0^2 - R_i^2}{2}} - \frac{R_i^2 + R_0^2}{2} \quad (\text{D.4})$$

Equation (4.7) can also be written for specific volume ratio of 2.2 as;

$$\Delta r_m v = 2.2 = a \cdot t v = 2.2 - \frac{1}{b} (1 - e^{-b \cdot t v = 2.2}) \quad (\text{D.5})$$

Equation (D.6) can be solved for the time at specific volume ratio of 2.2, by inserting the value of Δr_m which was obtained by Equation (D.5). The time value at specific volume ratio of 2.2 is found as 0.0152 milliseconds.

After obtaining $t v = 2.2$, the following computations can be performed by the obtained time value as the specific volume ratio in Equations (4.8), (4.14), (4.28) and (4.30).

$$V_r = a (1 - e^{-bt}) \quad (\text{D.6})$$

$$\theta = \tan^{-1} \frac{V_r}{V_D} \quad (\text{D.7})$$

$$V_w = 2 \cdot V_D \cdot \sin \frac{\theta}{2} \quad (D.8)$$

$$E_d = E_G = \frac{V_w^2}{2} \cdot \frac{M}{C} + \frac{1}{2} \quad (D.9)$$

For specific volume ratio of 2.2, the values of V_r , θ , V_w and E_d are found as 1221.06 m/s, 10.44°, 1205.87 and 3.526×10^6 kJ/m³, respectively.

The calculation steps given by Equations (D.4) to (D.9) can be also be performed to obtain the detonation energy, E_d , at other specific volume ratio values. The values E_d , at the other three specific volume ratios (i.e. 4.4., 7.0 and 7.2) were found to be 3.802×10^6 kJ/m³, 3.815×10^6 kJ/m³ and 3.816×10^6 kJ/m³.

To use in the rest of the calculations the chemical energy of the explosive, E_o , is calculated via Equation (D.10), which is an expression suggested by Souers. The constants in this equation are values obtained from chemical codes. The value of E_o is found to be 5.675×10^6 kJ/m³ from Equation (D.10)

$$E_o = 0.779 + 1.373 \cdot \frac{E_d(7)}{10^6} - 0.0236 \cdot \frac{E_d(7)}{10^6}^2 \cdot 10^6 \quad (D.10)$$

After this point, the iterative calculations begin. As the first step in the iterative calculations, the Chapman-Jouguet pressure, P_{cj} , is calculated using Equation (4.38). Then the value of parameter C is calculated using Equation (D.11). Equation (D.11) is obtained by leaving C at one side of the JWL equation, which was given as Equation (1.1).

$$C = v^{(\omega+1)} P - A \exp -R_1 v + B \exp -R_2 v \quad (D.11)$$

The values obtained for P_{cj} and C via Equation (4.38) and Equation (D.3) in the first iteration step are 1.624×10^8 kPa and 1.514×10^6 kPa, respectively.

After that, the new values of E_d at the three specific volume ratios of 2.2, 4.4 and 7.2 are calculated employing Equation (D.12), which is a modified version of Equation (4.43).

$$E_d(v) = E_0 - \frac{A}{R_1} \exp(-R_1 v) + \frac{B}{R_2} \exp(-R_2 v) + \frac{C}{\omega v^\omega} \quad (D.12)$$

Then Equation (4.41) is utilized to obtain the value of velocity of detonation, V_D , analytically. The first iterative value for this quantity is 6567.2 m/s. After calculating the detonation velocity analytically, the pressure at Chapman-Jouguet condition, P_{cj} , is obtained using two different equations, which are Equation (4.31) and the JWL equation given as Equation (1.1). For this case study, the values calculated from these two equations in the first iterative step are 2.286×10^7 and 1.624×10^7 . At this point, two different values for V_D and P_{cj} have been obtained. For V_D , one value has been obtained from equation (4.41) and the other value is the exact value which was measured during the cylinder expansion test. For P_{cj} , on the other hand, the values have been obtained from Equations (4.31) and (4.38), as stated above. Therefore the true error for V_D and the difference in P_{cj} values obtained from two different equations can be obtained by calculating the difference between the two different values for each of these two quantities. The true error for V_D at the first step is the numerical difference between 6632 and 6567.2, which is 64.8. Similarly, the difference between the two P_{cj} values, 0.662×10^7 , is calculated by subtracting 1.624×10^7 from 2.286×10^7 . As well as these two numerical differences, relative differences or errors for P_{cj} and V_D can be obtained from Equation (D.13) and Equation (D.14), respectively, as percentages.

$$Error_{V_D} = 100 \cdot \frac{V_{D_{II}} - V_{D_I}}{V_{D_I}} \quad (D.13)$$

$$Error_{P_{cj}} = 100 \cdot \frac{P_{cj_{II}} - P_{cj_I}}{P_{cj_I}} \quad (D.14)$$

In Equation (D.13), $V_{D_{II}}$ and V_{D_I} are the values of velocity of detonation obtained from Equation (4.41) and measured during the tests, respectively. In Equation (D.14), on the other hand, $P_{cj_{II}}$ and P_{cj_I} are the values for P_{cj} calculated from Equation (4.31) and Equation (4.38), respectively. The percentage relative errors for V_D and P_{cj} in the first iteration block were calculated to be -0.977 and 40.742, respectively.

After that, the new values for parameters A and B are computed using Equation (D.15) and Equation (D.16), respectively, as suggested by Souers [25]. In Equations (D.15) and (D.16), 0.003 and 0.005 are arbitrary values for calculating the new values of the parameters using the errors found by Equations (D.13) and (D.14). The values suggested by Souers were 0.03 and 0.05, respectively. However, one tenth of the suggested values were used in this thesis study in order to make smaller changes with each increment. Changing these two values do not make any difference in the results; however it helps to prevent obtaining divergent computations in several cases. Different values could also be used instead of 0.03 and 0.05.

$$A_{new} = A_{old} \cdot 1 - 0.003 \cdot Error_{V_D} \quad (D.15)$$

$$B_{new} = B_{old} \cdot 1 + 0.005 \cdot Error_{P_{cj}} \quad (D.16)$$

For obtaining the new value of v_{cj} , which will be used in the next iteration block, Equations (D.17) to (D.23) are employed.

$$\delta_{2.2} = 100 \cdot \frac{E_d(2.2)_{new} - E_d(2.2)_{initial}}{E_d(2.2)_{initial}} \quad (D.17)$$

$$\delta_{4.4} = 100 \cdot \frac{E_d(4.4)_{new} - E_d(4.4)_{initial}}{E_d(2.2)_{initial}} \quad (D.18)$$

$$\delta_{7.2} = 100 \cdot \frac{E_d(7.2)_{new} - E_d(7.2)_{initial}}{E_d(7.2)_{initial}} \quad (D.19)$$

$$\delta = \frac{\delta_{2.2} + \delta_{4.4} + \delta_{7.2}}{3} \quad (D.20)$$

$$bhe_{old} = \frac{1}{(1 - v_{cj_old})} \quad (D.21)$$

$$bhe_{new} = bhe_{old} \cdot 1 + 0.001 \cdot \delta \quad (D.22)$$

$$v_{cj_new} = \frac{1}{(1 - bhe_{new})} \quad (D.23)$$

The iterative calculations are performed until each of the absolute values of the percent errors calculated by Equations (D.13) and (D.14) reaches below a predetermined tolerance value. The tolerance value used in this case study was taken as 10^{-7} . If the errors do not get below the tolerance value, the next iterative computations are performed starting from the calculation of P_{cj} via Equation (4.38). If both errors reach below the predetermined tolerance value, the iterations are terminated.

After the iterations for parameters A and B are terminated, the final values for parameters ω and C should be obtained.

The relationship for the parameter ω is presented in Equation (D.24)

$$0.7^\omega = \frac{E_o - E_d(10)}{E_o - E_d(7)} \quad (\text{D.24})$$

Therefore, after calculating the values of $E_d(7)$ and $E_d(10)$ one again using Equation (D.12), the final value for parameter ω can be calculated via Equation (D.25). Similarly the final value of parameter C can be calculated from Equation (D.11).

$$\omega = \frac{\ln \frac{E_o E_d(10)}{E_o - E_d(7)}}{\ln(0.7)} \quad (\text{D.25})$$

For the quantities discussed above, the final values are tabulated in Table D-1.

It should be noted that the parameters R_1 and R_2 do not change in the iteration steps. Therefore, the parameter set is obtained for the initial values of these two parameters.

The iterative calculation method employed in this study may be improved in several ways. However, comparison of the results computed by the code with the literature data and the analysis results has shown that the parameters found are accurate enough to describe the behaviour of the explosives studied.

Table D-1 Final Values of the Quantities in the Code for the Sample Case

Quantity	Value	Unit
V_{D_II}	6632	m/s
P_{cj_I}	2.035×10^7	kPa
P_{cj_II}	2.035×10^7	kPa
$V_{D_II} - P_{D_I}$	-6.616×10^{-6}	m/s
$P_{cj_II} - P_{cj_I}$	-0.0187	kPa
tolerance	1×10^{-7}	
Error_ V_D	$-9.976 \times 10^{-8} \%$	-
Error_ P_{cj}	$-9.205 \times 10^{-8} \%$	-
bhe	3.436	-
v_{cj}	0.709	-
$E_d(v=2.2)$	2.410×10^6	kJ/m^3
$E_d(v=4.4)$	4.236×10^6	kJ/m^3
$E_d(v=7.0)$	4.576×10^6	kJ/m^3
$E_d(v=7.2)$	4.587×10^6	kJ/m^3
$E_d(v=10.0)$	4.699×10^6	kJ/m^3
delta	4.563×10^{-7}	
A	4.531×10^8	kPa
B	1.560×10^7	kPa
C	5.765×10^5	kPa
ω	0.334	-